THE UNIVERSITY
of EDINBURGH

Characterisation of five GH16 glycanase and transglycanase activities and of their hemicellulosic substrates

Thomas J. Simmons

Doctor of Philosophy – Cell and Molecular Biology

The University of Edinburgh

2013

DECLARATION

The thesis has been composed by me and the work, of which it is a record, has been carried out mostly by myself. Where substantial input has been made by others, acknowledgement is made. This work has not been submitted for any other degree or professional qualification.

ACKNOWLEDGEMENTS

I am heavily indebted to my primary supervisor Prof. Stephen Fry for offering me this PhD position, for allowing me the freedom to pursue my own interests as they arose and for consistent help and support throughout my time in Edinburgh. I am also in the debt of my secondary supervisor Prof. Andrew Hudson for support throughout, especially regarding the molecular aspect of this project. Both supervisors were hugely helpful and always prepared to sacrifice their time for me. For this, I am very grateful.

Numerous people have contributed significantly to the work presented here. Dr. Andrew Cronshaw was responsible for operation of much of the mass spectrometry equipment used during this study and was an invaluable source of guidance for the interpretation of the results and the writing of the corresponding text. Likewise, Prof. Ian Sadler, Dr. Dušan Uhrín and Dr. Lorna Murray of the Edinburgh Molecluar NMR unit were responsible for the operation of the NMR equipment used, for the interpretation of the spectra produced and again were instrumental in the the writing of the corresponding text. Mr. Timothy 'HPLC-man' Gregson was hugely helpful wherever needed but particularly with operation of the HPLC equipment; without his help significant portions of this work would not have been achieved. Miss Claire Holland was my partner in crime during the gruelling recombinant expression work and deserves credit for her contribution to its ultimate success. Janice Miller is an invaluable member of the group and provided constant support and friendship throughout. Employees of Genepool were responsible for operation of next generation sequencing equipment and annotation of bioinformatics data, and employees of the greenhouse and the teaching labs were all friendly faces who were able to help by supplying equipment/material for experiments whenever needed. I thank also Dr. Jimi-Carlo Bukowski-Wills for support in setting up the transcriptome database and Dr. Justin Goodrich and Dr. Stephen Spoel for guidance and suggestions which kept the project going when it reached difficult points. The BBSRC should also be acknowledged for funding this work.

I thank all past and present members of the Fry lab – Janice, Lenka, Dimitra, Aline, Christina, Clair, Cam Tu, Rebecca, Craig, Andrea, Shi, Airrianah, Kyle, David, Tayabba, Sandra – for making the lab such a friendly place to work. I thank my family: Mum, Dad, Dave and Mike for constant love and support. Finally I thank Inky, girlfriend and best friend, for her love and support throughout my time in Edinburgh and without whom I would have been unable to do so much.

ABSTRACT

Plant primary cell walls are hydrated extracellular complexes composed largely of polysaccharides: cellulose, hemicellulose and pectin. Cell wall constituents and composition vary in cell-, environment-, and species-dependent manners. For example, within land plant hemicelluloses xyloglucan is ubiquitous while mixed-linkage (1→3),(1→4)-β-D-glucan (MLG) is found only in the Poales and *Equisetum*. Glycosyl hydrolase 16 (GH16) enzyme family members include numerous enzymes with pertinence to the understanding of the 'lives' of cell wall hemicelluloses. However, despite this, the details of the interactions between GH16 enzymes and their substrates have often not been elucidated. Likewise, the true preferences of many of these enzymes and the range of substrates which they can utilise remain to be fully explored. By providing a greater wealth of information for the correlation of enzyme structure with reaction catalysed, such an understanding would enable better predictions of the activities of novel enzymes. Crucially, this would also allow better identification of roles performed by these enzymes *in planta* as well as of the potential applications of these enzymes.

This work sought to further our understanding of the interactions between GH16 enzymes and their substrates by the study of five activities exhibited by GH16 enzymes – xyloglucan endotransglucosylase (XET), xyloglucan endoglucanase/hydrolase (XEG/XEH), mixed-linkage glucan : xyloglucan endotransglucosylase (MXE), lichenase and cellulose : xyloglucan endotransglucosylase (CXE). All of the analysed activities act on xyloglucan and/or MLG. Of particular focus is the novel enzyme MXE from the evolutionarily isolated genus *Equisetum* (horsetail), which acts on both. Notable findings include: identification of MXE/CXE gene; determination of the substrate specificity of MXE; defining of the sites of attack of lichenase, XEG, XET and MXE; discovery of novel xyloglucan structures and discrepancies between the xyloglucan present in different barley organs.

LAY SUMMARY

Plant primary cell walls are hydrated extracellular complexes composed largely of three types of carbohydrate: cellulose, hemicellulose and pectin. Cell wall constituents and composition vary in cell-, environment-, and species-dependent manners. For example, within land plant hemicelluloses xyloglucan is ubiquitous while mixed-linkage (1→3),(1→4)-β-D-glucan (MLG) is found only in the crop plants and in horsetails. GH16 enzymes have particular pertinence to the 'lives' of cell wall hemicelluloses. Here, a collection of projects which study five activities exhibited by GH16 enzymes is described; all of the analysed activities act against xyloglucan and/or MLG. Of particular focus is a novel enzyme called MXE found in horsetails, which acts on both of these hemicelluloses. Notable findings include: identification of the DNA sequence which codes for MXE; determination of the preferences that MXE exhibits for different substrates; defining of the sites of attack of two gycanases and two transglycanases (including MXE); discovery of novel xyloglucan structures; and discovery of discrepancies between the xyloglucan present in different barley organs.

ABBREVIATIONS AND ACRONYMS

BAW	Chromatography solvent: butan-1-ol : acetic acid : water (2:1:1)
BMLG	Barley mixed-linkage (1→3),(1→4)-β-D-glucan
CXE	Enzyme activity: cellulose : xyloglucan endotransglycosylase
DP	Degree of polymerisation; the number of glycosyl residues in a carbohydrate molecule.
EAW	Chromatography solvent: ethyl acetate : acetic acid : water (10:5:6)
EMLG	*Equisetum* mixed-linkage (1→3),(1→4)-β-D-glucan
EPW	Chromatography solvent: ethyl acetate : pyridine : water (8:2:1)
GH	Glycosyl hydrolase (class of carbohydrate-active enzymes defined in CAZy database)
IMMLG	Iceland moss mixed-linkage (1→3),(1→4)-β-D-glucan (aka lichenan)
LC-MS/MS	Analytical technique: liquid chromatography-mass spectrometry
MLG	Type of hemicellulose: mixed-linkage(1→3),(1→4)-β-D-glucan (see 1.3.1 for description)
MLGO	Mixed-linkage (1→3),(1→4)-β-D-glucan oligosaccharide
MXE	Enzyme activity: mixed-linkage (1→3),(1→4)-β-D-glucan : xyloglucan endotransglucos-ylase
PNW	Chromatography solvent: propan-1-ol : nitromethane : water (5:2:3)
PyAW	Buffer: pyridine : acetic acid : 0.5 % (w/v) aqueous chlorobutanol (1:1:98, pH 4.7, unless otherwise stated)
SEC	Size-exclusion chromatography
SEPs	Sloughed extracellular polysaccharides; yielded from a cell culture medium.
TLC	Analytical technique: thin-layer chromatography
TXyG	Tamarind xyloglucan
U-^{14}C	Universally ^{14}C-labelled; ^{14}C-labelled compounds in which all constituent carbons have equal specific activity.
XEG	Enzyme activity: xyloglucan endoglucanase
XEH	Enzyme activity: xyloglucan endohydrolase
XET	Enzyme activity: xyloglucan endotransglycosylase
XGO	Xyloglucan oligosaccharide
XGO-ol	Reduced xyloglucan oligosaccharide
XTH	Xyloglucan endotransglycosylase/hydrolase (enzyme/gene family)
XXXG	A specific xyloglucan oligosaccharide. For a guide to xyloglucan oligosaccharide nomenclature, see Fry (1993)

XXXGol	A specific reduced xyloglucan oligosaccharide. For a guide to xyloglucan oligosaccharide nomenclature, see Fry (1993)
XyG	Type of hemicellulose: xyloglucan (see 1.3.1. for description)

CONTENTS

1. INTRODUCTION

1.1. The plant cell wall

A defining feature of plant-life as distinct from other life forms is the presence of unique extracellular matrices which encases virtually all plant cells – plant cell walls. Plant cell walls (from hereon referred to as cell walls) are dynamic hydrated structures composed largely of complexed polysaccharides and other less predominant polymers (e.g. proteins and polyphenolics). The first recognised description of cell walls was by Grew (1682), who described plant organs as being composed of compartments with rigid walls, akin to the way that a house is made from bricks. It wasn't until the 19th century however, that Julius von Sachs first recognised the cell wall as a dynamic structure with a pivotal role in cell growth and differentiation (Sachs, 1887). Contemporary science also recognises roles in pest and pathogen defence (Hückelhoven, 2007), cell signalling, cell-to-cell adhesion, the determination of cell morphology (Albersheim *et al.*, 2011) and as a source of biologically-active signalling molecules (Fry, 1994; Creelman & Mullet, 1997). In addition, cell walls are an invaluable resource of raw materials for medicinal and pharmaceutical products (Guo *et al.*, 1998; Jackson *et al.*, 2007; Smelcerovic *et al.*, 2008; Laurienzo *et al.*, 2010; Dilbaghi *et al.*, 2013), food additives (Geshi *et al.*, 2010), novel materials (Travan *et al.*, 2012; Kochumalayil *et al.*, 2013; de Souza *et al.*, 2013) as well as conventional materials (such as paper and wood), and are a source of bioenergy (Perlack *et al.*, 2005; Sticklen, 2008; Carroll & Somerville, 2009). For all these applications, the potential of plant cell wall material is far from exhausted (Persin *et al.*, 2011).

It was comparatively recently that the apoplastic enzymes responsible for cell wall dynamism and physiology were first elucidated. Now a plethora of apoplastically-active enzymes are known to exist. Indeed, it is estimated that 10% of the *Arabidopsis thaliana* genome (~2,500 genes) is devoted to cell wall construction, sensing functions, dynamic architecture and metabolism (Carpita, 2011). A widely accepted model of the plant cell wall stems largely from work pioneered by Albersheim's school in the 1970s, having studied sycamore cell walls (Keegstra *et*

al., 1973). Despite various significant counter-evidences (e.g. Cavalier *et al.*, 2008), this model has thus far largely withstood the test of time. The polysaccharide components of the cell wall can generally be categorised into three groups (cellulose, hemicellulose and pectin) based on their structures and chemistries and, within this model, members of each group perform distinct roles (Cosgrove, 2005):-

1) **Cellulose microfibrils** are the major strength-giving components of the cell wall. They are composed of multiple chains of β-D-(1→4)-linked glucopyranosyl residues hydrogen-bonded together in a semi-crystalline structure. A cross-section at any point along the microfibril contains ~ 36 such chains.
2) **Hemicelluloses** hydrogen bond to cellulose microfibrils, coat them and perform a tethering role between adjacent ones. The result is a supermolecular structure in which each microfibril is linked to every other through a complex network of polysaccharides. A consistent feature of hemicelluloses is a structure which restricts the attractive forces that cause individual cellulose chains to crystallise together to form microfibrils. This can be caused by a variation in backbone structure (e.g. mixed-linkage glucan) or by sidechain decoration (e.g. xyloglucan).
3) This cellulose : hemicellulose network is embedded in a **pectic polysaccharide** 'gel'. There is some evidence of hemicellulose : pectin covalent linkage (Popper and Fry 2008), though typically pectins are isolated from cell walls without breaking such bonds. A classical structural characteristic of pectic polysaccharides is a high galacturonic acid (GalA) composition, to which they owe a negative charge.

There further exist two developmentally and structurally distinct types of cell wall: the primary and the secondary. The primary cell wall surrounds plant cells throughout their lives, and it is the ability of it to yield to, or to resist, Turgor pressure which the plant controls to regulate the direction and rate of cell expansion (Cosgrove, 2005). The secondary cell wall is deposited following/during growth cessation and provides a structural role only. In comparison to the primary cell wall, the secondary cell wall is more rigid, having a distinct polymeric constitution

(Scheller & Ulvskov, 2010). It is deposited between the primary cell wall and the cell membrane of some cells during and/or following the cessation of growth (Taylor, 2000).

1.1.1. Cell wall evolution and phylogeny

The occurrence, prevalence and structure of cell wall components often exhibit phylogenic, cell-type and stimulus-dependent variation, the result of the different evolutionary pressures and the differing characteristics granted to cell walls by each component. Despite this diversity, the cell walls of many land plants can be categorised in one of two ways, based on similarities in occurrence, prevalence and structure of cell wall components (Scheller & Ulvskov, 2010). Consistent with the crucial role the cell wall appears to have played in plant evolution, these two groups are compatible with an important distinction in land plant phylogeny: type I cell walls, characterised by a large amount of xyloglucan and pectin, are found in eudicots and some monocots; while type II cell walls, characterised by low amounts of xyloglucan (levels in barley are extremely low or absent: 2–5% (w/w), Scheller & Ulvskov, 2010) and pectin with large amounts of glucuronoarabinoxylans and MLG, are found in all Poaceae and and a small number of related Poales (Smith & Harris 1999; Popper & Fry 2004). However, while generally applicable to a wide array of plants, (typically angiosperms) this classification system is not broad enough to encapsulate the whole range of cell wall architectures observed in nature; many species, those in the primitive and/or evolutionarily isolated taxa (for example *Equisetum*) in particular, often contain cell walls which cannot be made to fit comfortably into either group.

1.2. Glycosyl Hydrolase Family 16 (GH16)

Members of the Glycosyl Hydrolase 16 (GH16) enzyme family are found throughout the eukaryotic and prokaryotic taxa. Despite significant sequence variation, they share a conserved catalytic machinery and structure: a β-jelly-roll fold in which two anti-parallel β-sheets align and fold around a substrate binding cleft orientated perpendicular to the β-strands (Summary in Strohmeier *et al.*, 2004). Almost all GH16 enzymes catalyse endo-hydrolysis of β-(1→3) and β-(1→4) glycosidic bonds and they utilise a canonical retaining catalytic mechanism to do this; a group of non-

enzymically active invertebrate GH16 proteins involved in Toll pathway immune response activation are the only exception (Lee *et al.*, 2009). GH16 and GH12 families together comprise GH clan-B, indicating their distant homology (Michel *et al.*, 2001).

The Carbohydrate Active enZyme (CAZy) database (http://www.cazy.org; Cantarel *et al.*, 2009) shows the fundamental importance of the GH16 family to the study of the plant cell wall; GH16 contains enzymes involved in backbone hydrolysis of various cell wall polysaccharides: xyloglucan (EC 3.2.1.151), laminarin/callose (EC 3.2.1.39), mixed-linkage (1→3)(1→4)-β-D-glucan (MLG) (EC 3.2.1.6; EC 3.2.1.73), and the algae-specific polysaccharides κ-carrageenan (EC 2.4.1.207); as well as the *in situ* remodelling of xyloglucans through xyloglucan endotransaglucosylase activity (XET; EC 2.4.1.207). The scope of GH16 activity extends beyond the cell wall however, also catalysing endo-cleavage of the glycosaminoglycans among others (See http://www.cazy.org).

Barbeyron *et al.* (1998) showed that, using sequence homology, GH16 family members cluster in accordance with their substrate specificities, regardless of their pro/eukaryotic phylogeny, suggesting their having arisen through gene duplication. The authors suggest that common GH16 ancestor proteins which existed before the separation of archaea, bacteria, and eukaryotes, were laminarinases. This is akin to a proposal previously made of GH17s (Høj & Fincher 2003); it is interesting to note that both of these families now share lichenase activity. Those GH16 clusters pertinent here are the XTHs and the mixed-linkage (1→3)(1→4)-β-D-endoglucanases (lichenases; for relationship between these enzyme groups see Eklöf *et al.*, 2013) which, together with Crh enzymes – which catalyse chitin : laminarin endotransglycosylation in yeast (Cabib *et al.*, 2007; Cabib *et al.*, 2008; Cabib, 2009) – comprise the subfamily GH16b, all members of which contain active site residues on a regular β-strand. Other GH16 enzymes (those in subfamily GH16a) contain active site residues on a β-bulge, a feature they share in common with GH7 β-(1→4)-D-glucanases. This work investigates five inter-related enzyme activities catalysed by GH16b family members, all of which are active against plant cell wall polysaccharides: xyloglucan endotransglycosylase (XET, xyloglucan endohydrolase/endoglucanase (XEG/XEH), mixed-linkage glucan : xyloglucan

ednotransglycosylase (MXE), lichenase and cellulose : xyloglucan endotransglycosylase (CXE); the first four of these activities are schematised in Fig. 3b.

1.3. Pertinent hemicelluloses and corresponding hydrolases

Of all hemicelluloses, xyloglucan and mixed-linkage (1→3)(1→4)-β-D-glucan (MLG) are those most pertinent to the present work. Hydrolytic activities against both of these polysaccharides are found in the GH16 family.

1.3.1. Xyloglucan

Xyloglucan comprises a (1→4)-linked β-D-glucopyranosyl backbone with taxonomically dependent substitution patterns. Typically the first two or three of every four consecutive glucosyl residues are α-D-xylosylated at position six (hence XXGG, XXXG; Vincken *et al.*, 1997; see Fry *et al.*, 1993 for a description of xyloglucan nomenclature). Poacean xyloglucan differs markedly from those of many other species, as they exhibit exceptional variation in subunit length: $XX(G)_n$, where n = 1–4 (Hsieh and Harris 2009). Gibeaut *et al.* (2005) identified XXGG and XXGGG as the major repeat units of the xyloglucan of 3-day old barley coleoptiles with slightly more of the latter, but the presence of XXGGGG and XXGGGGG was also significant; they were unable to confirm the presence of L structures there.

These xyloglucan 'base units' are then further decorated by other residues, providing a wide scope for final xyloglucan structure (Fry 1989). Xyloglucan side chain structures can also vary widely in different plant tissues and species (Vincken *et al.*, 1997). An easily accessible xyloglucan is Tamarind (*Tamarindus indica*) seed xyloglucan whose physiological role is as a storage polysaccharide. Tamarind xyloglucan is commonly used in research; its most common subunits are XXXG, XXLG, XLXG and XLLG. Consistent with the observed variation in xyloglucan structure across the plant taxa and *Equisetum's* evolutionary isolation, the oligosaccharides produced by enzymatic degradation of *Equisetum hyemale* xyloglucan have been shown to differ considerably from those of most other plants (Fry *et al.*, 2008; Peña *et al.*, 2008; current work). Notably, *Equisetum* xyloglucan

contains D and E groups (Fig. 1) α-L-Ara*p* residues only known elsewhere in the lycopodiphytes (Peña *et al.*, 2008).

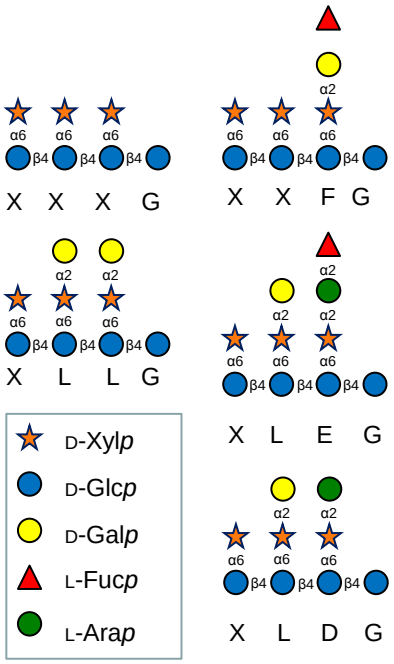

Fig. 1. Xyloglucan subunit structures and nomenclature. Structures of various xyloglucan subunits observed in different species. The α-L-Ara*p*-containing side chains D and E are highly uncommon, being found in only *Equisetum* and related taxa (Peña *et al.*, 2008). Following carbohydrate symbol scheme described by Varki *et al.* (2009) and xyloglucan nomenclature scheme described by Fry *et al.* (1993).

The phylogenic distribution of xyloglucan is a case in point for the significance of changes in cell wall content to plant evolution and adaptation. Xyloglucan appears ubiquitous in the embryophytes and absent elsewhere (Popper & Fry 2003; Popper & Fry 2004; Popper 2008), suggesting a pivotal role in the transition from water to the colonisation of land. A comparative genomic approach lends support to this hypothesis suggesting the acquisition of the synthetic machinery for a primordial xyloglucan-like polymer by streptophytic algae was a pre-adaptation that subsequently allowed the colonisation of the land (Del Bem & Vincentz 2010). The assumption that xyloglucan-containing cell walls are a prerequisite for survival on land was challenged more recently by the discovery of Cavalier *et al.* (2008) that an *Arabidopsis* mutant deficient in two xylosyltransferase genes and lacking detectable

xyloglucan, exhibited no gross morphological phenotype. Despite this, xyloglucan continues to play a central role in the standard model of the cell wall and remains crucial to the story of plant evolution. The proper understanding of spatio-temporal distributions of distinct xyloglucan moiteties within individual plants (Gibeaut *et al.*, 2005; Peña *et al.*, 2012) may be crucial to fully comprehending the role(s) of xyloglucan *in planta*, but the scope of these variations are yet to be fully assessed.

1.3.1.1. Xyloglucan endoglucanase (XEG)

Xyloglucan endoglucanase (XEG; also called endo-xyloglucanase or xyloglucan endo-hydrolase; EC 3.2.1.151) activity resides in six glycosyl hydrolase enzyme families: GH5, GH7, GH12, GH16, GH44 and GH 74 (Gilbert *et al.*, 2008; Gilbert 2010), two of which (GH7 and GH16) are members of GH clan B (Henrissat & Bairoch 1996; Eklöf and Brumer 2010). By cleaving xyloglucan's β-D-glucosyl backbone at specific points, XEG can liberate xyloglucan subunits (now xyloglucan oligosaccharides) greatly facilitating structural studies of the polysaccharide. Despite this, the exact site of attack and mode of recognition of different XEGs is poorly, if at all, understood. Gloster *et al.* (2007; using GH5 and GH12 enzymes), Martinez-Flietes *et al.* (2006; GH74 enzyme) and Warner *et al.* (2011; GH44 enzyme) all demonstrate XEG activity against tamarind xyloglucan. Further, Gloster *et al.* (2007) and Martinez-Flietes *et al.* (2006) characterise the oligosaccharides produced: XXXG, XXLG/XLXG and XLLG. Importantly, these enzymes are not routinely used to characterise xyloglucans; because these studies are performed using tamarind xyloglucan alone, detailed accounts of the substrate specificity of these enzymes cannot be attained.

Structural characterisation of different xyloglucans has largely been the preserve of a single fungal GH12 XEG (Pauly *et al.*, 1998) and, because of this, this XEG is by far the best understood. This XEG typically (e.g. in the 'XXXG' repeat unit structure of dicot xyloglucan) cleaves the bond ---GX--- in the xyloglucan backbone. However, the oligosaccharides produced by digestion of some more exotic xyloglucans (e.g. GGXXG-based subunits; Peña *et al.*, 2008) shows this understanding to be far too simplistic. By observing XEG digestion of tomato (*Solanum lycopersicum*) xyloglucan, Jia *et al.* (2003) were able to determine some more specific requirements

for XEG digestion, though the task of characterising the enzyme is far from complete.

1.3.2. Mixed-linkage (1→3)(1→4)-β-D-glucan (MLG)

Mixed-linkage (1→3)(1→4)-β-D-glucan (MLG) (Fig. 2) is an unbranched β-D-glucopyranosyl homopolysaccharide in which cellosyl (1→4)-linked regions – of variable length, but typically 3-4 residues – are connected by single (1→3) bonds; (1→3) bonds are never found consecutively (Peat *et al.*, 1957; Parish *et al.*, 1960). Owing to their structural similarity to cellulose, these (1→4)-bonded regions are commonly referred to as cellobiose, cellotriose, cellotetraose etc. A small proportion of considerably longer subunits, e.g. of DP 12, also occur in some species (Wood *et al.*, 1994; Izydorczyk *et al.*, 1998; Papageorgiou *et al.*, 2005; Sørenson *et al.*, 2007; Liu & White, 2010). The cello units are rigid while the (1→3) bonds connecting them tend to be flexible, giving mixed-linkage glucan molecules a kinked appearance, but with overall flexibility (Burton & Fincher 2009).

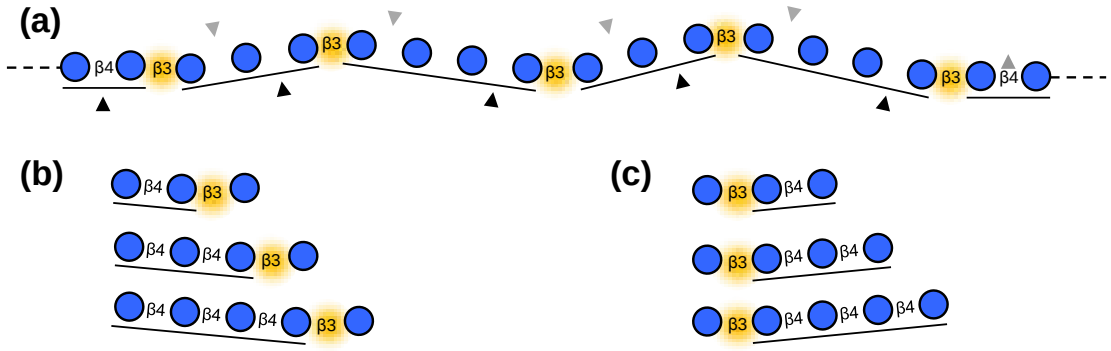

Fig. 2. Mixed-linkage (1→3)(1→4)-β-D-glucan (MLG) and sites of attack of a *Bacillus subtilis* lichenase and an *Aspergillus japonicus* cellulase (a) MLG polymer structure showing kinks caused by β-(1→3) bonds as well as distinct sites of enzymic attack: a *Bacillus subtilis* lichenase cleaves β-(1→4) bonds after β-(1→3) bonds (gray downward arrowheads; Planas, 2000), an *Aspergillus japonicus* cellulase cleaves β-(1→4) bonds before β-(1→3) bonds (black upward arrowheads; Grishutin *et al.*, 2006). DP 3–5 products of lichenase (b) and cellulase (c) activity on MLG. Reducing termini on right; blue circles, D-Glc residues; β3, β-(1→3)-linkage (highlighted in orange); β4, β-(1→4)-linkage; cello-like β-(1→4)-linked regions underlined

In contrast to the wide phylogenic distribution of xyloglucan, MLG is known only in three widely separated lineages: the Poales (grasses, cereals, reeds and their relatives; Smith & Harris, 1999; Popper & Fry, 2004), *Equisetum* (horsetails; an evolutionaily isolated genus of non-flowering vascular plants), and some lichens, e.g. *Cetraria islandica* (Iceland 'moss', whose MLG is known as lichenan; Perlin & Suzuki 1962); MLG does not occur in the majority of plants, algae or fungi. Its presence in *Equisetum* was an unexpected recent discovery (Fry *et al.*, 2008; Sørensen *et al.*, 2008; Xue and Fry, 2012); the Poales had long been assumed to be the only vascular plants possessing it (Stone & Clark 1992), though an MLG-related polysaccharide was found in the leafy liverwort *Lophocolea bidentata* (Popper & Fry, 2003).

The phylogenetic distance between these species indicates that the acquisition of MLG is most probably an example of convergent evolution. In both Poales and *Equisetum*, MLG is regarded as a hemicellulose because it is extractable from cell walls with alkali, and because MLG chains are thought to hydrogen-bond to cellulosic surfaces, possibly tethering adjacent microfibrils and contributing to wall architecture. Further, MLG's observed ability to (cause) silica formation from silicilic acid (Law & Exley, 2011), may be a shared role of MLG between these two embryophyte taxa, both of which maintain high levels of silica. As far as I am aware, the presence of silica in MLG-possessing lichens (e.g. *C. islandica*) has yet to be assessed. However, there is evidence to suggest that MLG can play distinct roles within these distinct taxa. For example, in the Poales MLG is often metabolically labile, being hydrolysed to glucose after germination and thus serving as a carbohydrate reserve (Inouhe & Nevins 1991; Hatfield & Nevins 1987); there is no evidence for this in *Equisetum*, whose MLG tends to be abundant in both young and senescing tissues (Sorenson *et al.*, 2008). Further, the presence of MXE (See 1.3.2.3) in *Equisetum*, but not in members of the Poaceae (Fry *et al.*, 2008; Mohler *et al.*, 2012), suggests another distinct functional role.

Given the likelihood of MLG's independent evolution in the Poales, *Equisetum* and lichens, their wide phylogenetic separation, and MLG's possible independent roles therein, it is understandable that their MLGO subunit ratios differ. The MLG3 : MLG4 ratio of MLG is typically >24 in *C. islandica* (Lazaridou *et al.*, 2004, Tosh *et*

al., 2004a), ~1.5–4.5 in various species of the Poales (Lazaridou & Biliaderis, 2007; Fry *et al.*, 2008b), and <0.25 in *Equisetum* (Fry *et al.*, 2008; Sørensen *et al.*, 2008; Xue & Fry, 2012). As well as being documented in the literature, a comparison of the structure of these three polysaccharides appears in the current work. Even slight structural variations with MLGs have been shown to cause dramatic variations in physical and chemical attributes such as viscocity etc. (see 1.3.2.3.). Because of this, the functions of MLG *in vivo* could be entirely different within these different taxa.

While MLG2 (aka laminaribiose) is a clearly established constituent of *Equisetum* MLG (Fry *et al.*, 2008; Sørensen *et al.*, 2008; Xue & Fry, 2012) and some have reported its presence in poalean MLG (e.g. Roubroeks *et al.*, 2000), many investigators have failed to report it in the latter and in Iceland moss MLG (Wood *et al.*, 1994; Izydorczyk *et al.*, 1998; Wood *et al.*, 2003; Lazaridou *et al.*, 2004; Tosh *et al.*, 2004; Vaikousia *et al.*, 2004; Papageorgioua *et al.*, 2005; Liu & White, 2011).

1.3.2.1. Lichenase: an MLG-specific endohydrolase

Lichenase (EC 3.2.1.73) is an MLG-specific endohydrolase which resides in the GH16 and GH17 families in the microbial and plant kingdoms respectively (Planas, 2000). It is often used analytically to characterise the subunit composition of MLG (e.g. Fry *et al.*, 2008; Sorenson *et al.*, 2008; Xue & Fry, 2012), its target site classically understood as being all (1→4) bonds immediately following a (1→3) bond (in the non-reducing to reducing terminal direction; Fig ANa,b); it does not hydrolyse pure (1→3)-β-D-glucans or (1→4)-β-D-glucans (Planas, 2000). The result of such classical lichenase activity on MLG would be a range of oligosaccharides in which the reducing end is always G3G and any other G residues are 4-linked as extensions at the non-reducing end. Such oligosaccharides are described here as MLGOs, or specifically MLG2, MLG3, MLG4 etc. according to their DP. MLG2/3/4 etc. are used interchangeably here to refer to these oligosaccharides and the units within the polysaccharide from which they are created. Thus, although lichenase-generated MLGOs are not themselves cello-oligosaccharides, they indicate the presence of differently sized cello-oligosaccharide subunits in the original polysaccharide. For example, the yield of MLG3 in a lichenase digest is taken to indicate the abundance of cellotriosyl units in the polysaccharide prior to digestion.

Cellulase can also be used for analytical hydrolysis of MLGs in a manner analogous to the use of lichenase (Fig. 2a,c). However, cellulases can exhibit sites-of-attack distinct to that of lichenase: they can target (1→4) bonds immediately before a (1→3) bond (Grishutin *et al.*, 2006). Thus the result of cellulase activity on MLG is believed to be solely a range of oligosaccharides in which the non-reducing end is always G3G and any other G residues are 4-linked as extensions at the reducing end.

1.3.2.3. The technological significance of MLG

The technologically exploitable properties of MLGs are thought to be a product of their concentration, molecular weight and subunit composition. To better understand this, numerous studies have been aimed at characterising MLGs from different (usually poalean) sources, particularly with respect to the ratio of the two most common subunits: MLG3 and MLG4. For example, Tosh *et al.* (2004) showed that differences in the MLG3 : MLG4 ratio affect the gelation characteristics and elasticity of MLG systems, lichen MLG (high DP3:DP4 ratios) forming gels at a quicker rate and with a higher 'melting' point than cereal MLGs. Likewise, cereal MLGs with the highest MLG3 : MLG4 subunit ratios form gels the quickest (Lazaridou & Biliaderis, 2007).

MLGs are also important components of the human diet. MLG consumption can affect blood glucose and cholesterol concentrations (Battilana *et al.*, 2001; Bell *et al.*, 1999; Bourdon *et al.*, 1999; Dikeman & Fahey, 2006; Kahlon *et al.*, 1993; Lazaridou & Biliaderis, 2007; Wood, 1994; Wood, 2007), alleviate constipation by increasing faecal bulk (Malkki & Virtanen, 2001; Lazaridou & Biliaderis, 2007), and can also have beneficial effects on the immune system (Porter *et al.*, 2006). For these reasons, a better understanding of MLGs, and the enzymes that act on them, is desirable.

1.2.2.4. Subunit arrangements of MLGs

Few studies have attempted to characterise the distribution of MLGO subunits along the intact MLG chain, probably because of the lack of suitable techniques for doing so. Despite this, subunit distribution would presumably have a dramatic effect on the physical properties of MLG solutions. Staudt *et al.* (1983) attempted this by mathematically modelling the production of the four main penultimate products of

lichenase digestion, i.e. DP6–8 oligosaccharides with two (1→3) linkages, namely G4G3G4G4G3G, G4G3G4G4G4G3G, G4G4G3G4G4G3G and G4G4G3G4G4G4G3G. They concluded that cellotriose and cellotetraose subunits are distributed randomly throughout the polysaccharide, but did not discuss the distribution of other, less predominant, units. Any observed pattern in the distribution of MLG subunits must be explained by any scheme seeking to model MLG synthesis.

1.4. Endotransglycosylases

Plants make use of many different mechanisms to modulate the extensibility of their cell walls (Cosgrove, 2005), a common mechanism being the covalent modification of hemicelluloses by apoplastic endotransglycosylases (Fry *et al.*, 1992, Nishitani & Tominaga, 1992; Schroder *et al.*, 2004; Fry *et al.*, 2008; Franková & Fry, 2011; Johnston *et al.*, 2013). The need for such a group of enzymes – that are able to cleave and reform intermicrofibrillar hemicellulosic tethers – was proposed more than thirty years ago (Albersheim, 1974/) to enable controlled loosening of intermicrofibrillar hemicellulosic tethers during Turgor-driven growth without ever compromising the strength of the wall. A similar proposal was made for yeast cell walls over twenty years ago (Cabib *et al.*, 1988).

All sequenced endotransglycosylases are members of the glycosyl hydrolase (GH) CAZy enzyme class (Okazawa *et al.*, 1993; Schröder *et al.*, 2006; Johnston *et al.*, 2013) and catalyse a two-step reaction utilising a retaining mechanism: the first step involves the endo-cleavage of the donor polysaccharide after which an enzyme-substrate intermediate exists; the second step involves formation of a glycosidic bond between the new potentially-reducing terminus and the non-reducing terminus of a nascent oligo/polysaccharide (the acceptor substrate; Fig. 3a), thereby liberating both enzyme and product (Fig 3a; e.g. Saura-valls *et al.*, 2008). Because the difference between endohydrolysis and endotransglycosylasation is a competition between glycans and water for the place as acceptor substrate, all retaining hydrolases can, given sufficient substrate, catalyse endotransglycosylation. However, this is typically far above natural substrate concentrations and thus is not considered physiologically significant. In this work, the term endotransglycosylase is reserved for those enzymes

which catalyse these reactions at physiologically significant (in μM range) substrate concentrations. While endotransglycosylases are thought *in vivo* to catalyse endotransglycosylation between polysaccharides, *in vitro* assays are typically performed using a polysaccharides donor and a labelled oligosaccharide acceptor (Fig. 3). There is however evidence that polysaccharide-to-polysaccharide endotransglycosylation does occur (Purugganan *et al.*, 1997; Fry *et al.*, 2008).

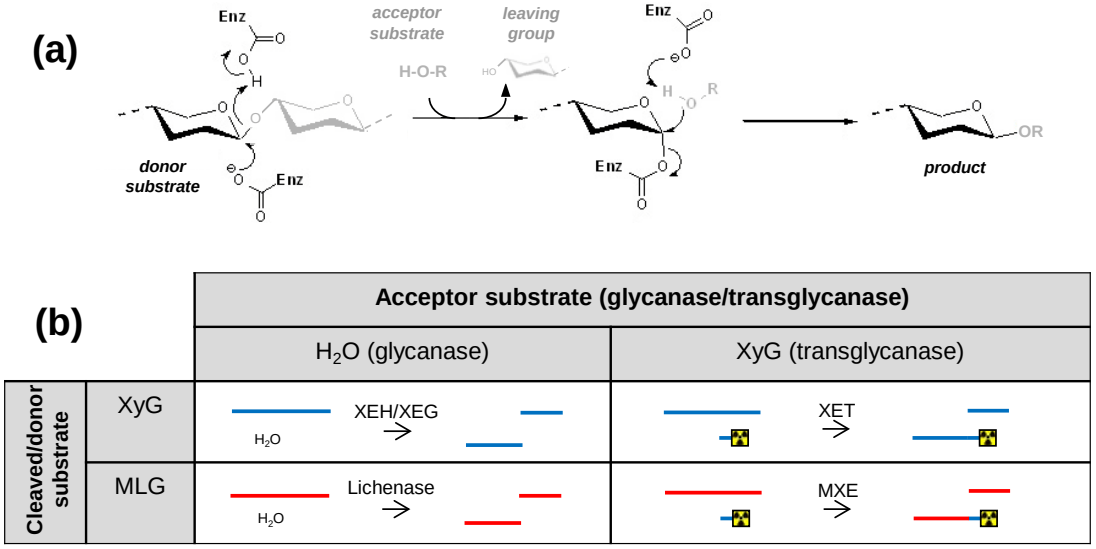

Fig. 3. Glycanase and transglycanase reaction mechanisms and four inter-related activities studied in this work (a) Canonical retaining glycanase/transglycanase mechanism. Where R = H, glycanase (endo-hydrolase) activity occurs; where R = part of a glycan, transglycanase (endo-transglycosidase) activity occurs. (b) Four of the activities studied in this work. Blue lines, xyloglucan; red lines, mixed-linkage glucan (MLG).

1.4.1. The XTH subfamily and the XET:XEH distinction

Xyloglucan endotransglucosylase (XET; Fry *et al.*, 1992; Nishitani & Tominaga, 1992; Fig. 3b) – which uses xyloglucan both as donor and acceptor – is catalysed by members of GH16, appears ubiquitous in the land plants and is believed to play crucial roles in cell wall physiology. As well as containing XET-active enzymes, GH16 also contains xyloglucan endohydrolase (XEH)-active enzymes (aka XEG), a reaction, biochemically similar to XET (Fig 3a), which, unlike XET, is exhibited by members of six different GH families (see 1.2.1.1.). In acknowledgement of the

biochemical similarity of the XET and XEH reactions (Fig. 3a), and because the structural (primary and tertiary) similarity of the GH16 enzymes exhibiting them suggests a distinct phylogenetic clade, nomenclature recognises xyloglucan endotransglucosylase/hydrolase (XTH) as a subfamily which encompases all XET- and XEH-active GH16 enzymes (Rose *et al.*, 2002). This is also highly fitting given that many XTHs exhibit both activities to varying degrees and that our ability to accurately predict enzyme function is not sufficiently advanced.

Despite the biochemical and structural similarity between XET- and XEH-active GH16 enzymes, they have significant potential for functional disparity *in vivo*: XEH would presumably be unable to produce the controlled wall-loosening that XET could. The fact that XEH activity appears entirely dispensible while XET holds an apparently crucial role in cell expansion (Kaewthai *et al.*, 2013) underlines the physiological significance of these activities' relatively minor biochemical distinction. The XTH distinctions previously identified (I, II and III; Rose *et al.*, 2002) have since been redefined – in accordance with the more detailed biochemical study and the deeper collection of genes now available – as I/II, which contains the majority of XTHs, III-A and III-B (Baumann *et al.*, 2007; Eflöf & Brumer, 2010). The phylogenetic distinction between clade III-A and the rest appears functionally significant, with this clade containing the only predominantly hydrolytic members (Eflöf & Brumer, 2010). Such phylogenic analyses suggest that XTHs share a common endotransglycosylase ancestor, from which endohydrolysis activity evolved (Baumann *et al.*, 2007), an evolutionary path which is presumably distinct from that of XEHs from other GH families. There is currently no firm experimental evidence that other clades within XTH (e.g. within I/II) exhibit any functional disparity (Eflöf & Brumer, 2010).

Baumann *et al.* (2007) show that a loop around that active site of a GH16 XEH is a major, though not the sole, contributing factor to defining the XET:XEH distinction. The loop 2 extension is missing from *Tm*NXG1 and *Tm*NXG2, both strict hydrolases, but present in *Ptt*XET16-34, a strict transglycosylase. It also represents an important distinction between XTH clade III-A and all other clades (of XET is the sole known activity), being present only in the former. The three dimensional

structure of *Tm*NXG1 shows the extension of loop 2 is capable of interacting with substrates when bound in the positive subsites of the enzyme; this might confer the ability to modulate the binding of xylogluco-oligosaccharide acceptor substrates. As proof of concept, a hybrid Ptt-XET16-34–like enzyme with a truncated loop 2 has a slightly boosted rate of transglycosylation and diminished hydrolytic activity. However, their inability to generate a strict transglycosylase from a predominant hydrolase indicates that this is not the only determinant. In support of this contention, a different group analysed XTHs by homology modelling and suggested that clade III-B members, though containing a truncated loop 2, might be XEHs rather than XETs (Xu *et al.*, 2010).

Just as xyloglucans have varying structural decoration of their backbones, XET activities exhibit varying substrate specificities. For example, Maris *et al.* (2009) and Maris *et al.* (2011) showed that seven recombinant XTHs from *A. thaliana* display distinct acceptor substrate specificity profiles using various purified [^{3}H]XGO-ols (as well as distinct pH optima), but were unable to efficiently use xyloglucan like substrates as acceptor or donor substrates. Campbell & Braam (1999) showed that four Arabidopsis XTHs exhibit distyinct pH and temperature optima as well as distinct substrate specificities. Also, although XETs clearly prefer xyloglucan, they can often display significant promiscuity with regard to their substrates outside of this particular glycan (see 1.4.2.). This physiological significance of this is also unknown.

Much effort has been invested in the identification of the structural determinants of XTH substrate specificity. XTH active sites contain seven subsites (-4, -3, -2, -1, +1, +2, +3), each binding a xyloglucan backbone residue and/or its substitutions; donor cleavage occurs between subsites -1 and +1, before the acceptor substrate occupies the positive subsites. It is also possible that glucoses at a putative +4 position (i.e. the reducing terminal residue in XXXG; Mark *et al.*, 2009) and those behind subsite -4 (Saura-Valls *et al.*, 2008) can exhibit some interactions with XTHs. Three loops around the active site (1, 2 and 3) may interact with the substrate and influence substrate specificity (Mark et al., 2009). In addition, XETs contain an N-glycan, removal of which often destroys XET activity (Campbell & Braam, 1998; Campbell

& Braam, 1999). This glycan interacts closely with the polypeptide chain and is unlikely to play a direct role in catalysis, perhaps instead merely promoting enzyme stability (Johansson *et al.*, 2004). Because of this, eukaryotic recombinant expression systems such as the yeast *Pichia pastoris* provide the greatest promise for XTH expression (Bollock *et al.*, 2005; Kaewthai *et al.*, 2010).

There is also evidence that XET activities can exhibit distinct preferences with regard to the length of their substrates. For example, *Va*XTH1 only acted efficiently using donor xyloglucans of over 10 kDa (Nishitani & Tominaga, 1992). Tabuchi *et al.* (1997) characterised an XTH from azuki bean epicotyls which transferred 50 kDa portions from high-Mr xyloglucans to labelled XGOs and separately hydrolysed the high-Mr xyloglucans to 50 kDa products; xyloglucans of 60 kDa were not hydrolyzed at all. In contrast, other work (Fanutti *et al.*, 1993; Fanutti *et al.*, 1996; Schröder *et al.*, 1998; Baumann *et al.*, 2007; Saura-Valls *et al.*, 2008) has shown that (for some enzymes) oligosaccharides can function as efficient donor substrates. With regard to acceptor substrate, *Va*XTH1 acted equally regardless of differences in size (Nishitani and Tominaga 1992), whereas recombinant *At*XTH22 protein had a much higher affinity for xyloglucan polysaccharides (Km = 0.3 μM) than for XLLGol (Km = 73 μM; Purugganan *et al.*, 1997). It remains conjectural how XTHs appear able to 'measure' glycans of far greater size than them; one possibility is that the xyloglucan used exhibits some structural pattern which the enzyme recognised, though there is currently no evidence for this. Such abilities to measure xyloglucan length may have dramatic effects on XET roles *in situ*. Nonetheless it appears that most XTHs exhibit a random cleavage mechanism (Nishitani & Tominaga, 1992; Steele *et al.*, 2001).

1.3.1.1. Situation and roles of XET

XTHs are apoplastic enzymes which can be found bound ionically – to charged cell wall components – from which they can be extracted using high salt solutions (Nguyen Phan & Fry, unpublished results) – or, because XTHs can form stable enzyme-substrate intermediates (Sulová *et al.*, 1998; Piens *et al.*, 2008), covalently bound in a 'primed state' to cell wall xyloglucans (Sulová *et al.*, 2001) – from which they can be extracted by application of xyloglucan oligosaccharides (or presumably by interaction with endogenous xyloglucan polysaccharides), which act as acceptor

substrates allowing endotransglycosylation to occur. This remarkable stability has also been exploited for purification of XETs, based either on the intermediate's high molecular weight (Steele & Fry, 1999) or its increased affinity for cellulose (Sulová & Farkaš, 1999), or by the use of conjugated XGO-columns (Baumann *et al.*, 2007). It is not known whether this intermediate stability is a feature of all endotransglycosylase reactions.

Despite over twenty years of study the precise role/s of XETs remain conjectural. An observed negative correlation between XET activity and cell age, led Fry *et al.* (1992) to speculate that XETs may indeed be performing the hypothesised role of endotransglycosylases in controlled wall-loosening during cell expansion; it was also suggested that XETs might participate in cell wall assembly. More recent reports have further implicated XETs in regulated cell expansion (Van Sandt *et al*., 2007; Lee *et al*., 2010; Sasidharan *et al*., 2010; Harada *et al*., 2011; Miedes *et al*., 2011). However, various counter-evidences for the role of XETs in the promotion of cell expansion have appeared. McQueen-Mason *et al.* (1993) suggested that XET activity does not enhance wall extension in *in vitro* assays, though the fact that they used boiled plant material limits the conclusions that can be drawn here (Rose *et al.*, 2002). Also Miedes *et al.* (2010) suggest XTHs from group I are probably involved in the restructuring of the cell wall during growth and development, and are not the limiting factor for plant growth.

It has become apparent in addition, that XTHs may be implicated in other physiological phenomena, such as cell wall restructuring (Thompson & Fry, 2001), the development of vascular tissues (Hernández-Nistal *et al.*, 2010) and, by allowing the integration of newly secreted xyloglucans into the pre-existing cell wall architecture, cell wall assembly (Thompson *et al.*, 1997; suggested previously by Fry *et al.*, 1992). Some evidence supports the hypothesis that XTHs may exhibit functional disparity in response to varying conditions. Vissenberg *et al.* (2005b), for example, showed that XTH localisation can vary with the mechanical properties of the cell wall. They showed two patterns of XET localisation: fibrillar and uniform – the fibrillar pattern (transverse to the long axis of the cell) appeared to correlate with the diffuse growth – which suggests distinct roles of XTHs. Further, it appears that

some XTHs may also, in some situations, be implicated in the cessation of cell expansion. Mellerowicz *et al.*, (2008) suggest XTH proteins produced during wood secondary cell wall development are involved in the strengthening of xylem tissues. Nishikubo *et al.*, (2011) propose that the ratio of newly synthesised xyloglucan to XTH within Golgi vesicles can dictate whether XET action strengthens or loosens the cell wall. Maris *et al.*, (2009) showed that application of *At*XTH14 or *At*XTH26 to onion epidermal peels during constant-load extensiometry actually decreased wall extensibility.

Finally, various authors have reported presumed relationships between XTHs and phenomena not directly-related to cell wall structure; some of these are possibly pleitropic effects (Miedes & Lorences, 2007; Choi *et al.*, 2011; Singh *et al.*, 2011). Because of their effects on a multitude of plant characteristics, XTHs represent a sensible target of genetic modifications and/or breeding. For example it has been shown that decreasing XTH activity (antisense RNA) can increase the shelf-life of lettuce (Wagstaff *et al.*, 2010).

Such a range of apparent roles for XETs should not however appear too surprising. The fact that all higher plants maintain large XTH families (20–60 genes; Eklöf & Brumer, 2010) whose members are actively transcribed in spatio-, temporal- and stimulus-dependent manners (Rose *et al.*, 2002; Yokoyama *et al.*, 2004; Becnel *et al.*, 2006; Mellerowicz & Sundberg, 2008; Miedes & Lorences, 2009), and exhibit varying substrate specificities, pH optima and expression patterns, supports the hypothesis that each might perform a distinct function (Nishitani & Vissenberg, 2006). This line of reasoning is countered however, by the observation that bryophytes, which contain significantly fewer cell-types than tracheophytes, maintain similar numbers of XTHs (Yokoyama et al., 2010).

1.4.2. Other endotransglycosylase activities

With the prevalence of XET activity throughout the plant kingdom, its' proposed fundamental role(s) in the regulation of plant growth and development, and the vast diversity displayed by cell wall hemicelluloses, the relative recentness of the discovery of other endotransglycosylases is perhaps surprising. There now exists

evidence for endotransglycosylases which utilise three of the four main hemicelluloses as both donor and acceptor: XET, mannan endotransglycosylase (Schröder *et al.*, 2004; Schröder *et al.*, 2006; Schröder *et al.*, 2009) and xylan endotransglycosylase/trans-β-xylanase (Franková & Fry, 2011; Johnston *et al.*, 2013). At the ouset this project there existed no evidence for endotransglycosylases using MLG as both donor and acceptor.

In spite of the dearth of direct evidence for any further endotransglycosylase activities, other lines of inquiry provide tantalising indications. Firstly, Carpita & McCann (2010) observed an increase in the molecular mass of a portion of the MLG from maize (*Zea mays*) seedlings upon deposition into the cell wall from the Golgi. Secondly, Thompson & Fry (2000) and Popper & Fry (2005) provide evidence for a covalent linkage between xyloglucan and pectin fractions of suspension-cultured angiosperm cells; despite their attempts to identify an appropriate endotransglycosylase they were also unable to. The previous observation of Kerr and Fry (2003) that the molecular mass of xylans in walls of suspension-cultured maize cells dramatically increases in the first few hours after wall-deposition might now be attributed to xylan endotransglycosylase/trans-β-xylanase.

However, as well as from undiscovered endotransglycosylase activities, these phenomena could also arise as the product of XTH side-reactions. Indeed, as well as exhibiting the xyloglucan specificity to which they owe their name, XTHs often exhibit further promiscuity with respect to the substrates they utilise (e.g. Mohand & Farkaš, 2006; Garajová *et al.*, 2008; Hrmova *et al.*, 2007; Hrmova *et al.*, 2009; Maris *et al.*, 2009; Kosík et al., 2010; Stratilová *et al.*, 2010; Maris *et al.*, 2011). This promiscuity might also reconcile the apparent incongruity between the abundance of XET throughout the plant kingdom and xyloglucan's chequered albeit ubiquitous distribution (Fincher, 2009). One notable case is the Poaceae, whose cell walls possess low xyloglucan content (Scheller & Ulvskov, 2010; Capita & Gibeaut, 1993) despite the large number of putative XTH genes they maintain (Yokoyama, 2004; e.g. 30 and 32 in rice and maize respectively, Eklöf & Brumer, 2010). Indeed, Hrmova *et al.* (2007) suggested that the 44.2% and 0.2% activity (compared to the XET reaction), of a barley XTH, when hydroxyethylcellulose and MLG respectively

are used as donor substrates, could translate *in situ* into a physiologically-meaningful activity against the more prevalent polysaccharide members of the barley cell wall. The evolutionary and structural relationship between XTHs, GH16 lichenases and GH11 xylan endohydrolases provides a potential mechanism as to how such an evolution in specificity to more prevalent components of type II cell walls might occur (Strohmeier *et al.*, 2004). Until 2007, while numerous accounts of these promiscuous XTHs had been described, their ability to catalyse XET activity always exceeded their ability to catalyse other activities. This favouring of xyloglucan is typically so stark that physiological significance of the side-reactions is dubious.

In addition, the scope of endotransglycosytion – which could, in theory utlise any substrate combination imaginable – is further revealed when searching outside of the plant kingdom. Fungal GH16 enzymes are capable of catalysing the formation of a glycosidic bond between chitin and the β-(1→6)-D-glucan side chains of laminarin (Cabib *et al.*, 2007; Cabib *et al.*, 2008; Cabib, 2009). A fungal GH17 enzyme is capable of laminarin endotransglycosylation by cleavage of the donor substrate two residues from the reducing terminus and formation of a β-(1→6) bond between the non-reducing terminal portion and the non-reducing terminus of anoth laminarin (Mouyna *et al.*, 1998).

1.5. *Equisetum*: an extremely evolutionarily-isolated genus

The order Equisetales (for *Equisetum* taxonomy see taxonomic classifications Table 1) is one of the most ancient and distinctive clades of extant tracheophytes, whose rich fossil record (Brown, 1975; McIver & Basinger, 1989; Stewart & Rothwell, 1993; Taylor & Taylor, 1993) can be used to trace the evolutionary path that led to its single extant genus – *Equisetum* (aka horsetails). Today, species of the genus *Equisetum*, together with the ferns, form a monophyletic group and are together the closest extant relatives of seed plants (Pryer *et al.*, 2001). Despite this, *Equisetum* is a highly evolutionarily isolated genus, whose ancestors are thought to have diverged from its closest extant relatives ~ 370 Mya (Bell & Hemsley, 2000; Smith *et al.*, 2006). Molecular dating (Des Marias *et al.*, 2003) suggests that the probable divergence of the extant crown group of the genus *Equisetum* was approximately 65 million years ago in the Paleogene. However, paeleobotanical findings (Stanich *et*

al., 2009; Channing *et al.*, 2011) indicate that that the characteristic synapomorphies of *Equisetum* had already evolved by the Lower Cretaceous (136 Ma) and the extant crown group may have originated far earlier in the Mesozoic. This would probably make *Equsietum* the oldest extant vascular plant genera in the world (Arnold, 1947).

Kingdom:	Plantae
Division:	Pteridophyta
Class:	Equisetopsida (aka Sphenopsida)
Order:	Equisetales
Family:	Equisetaceae
Genus:	Equisetum
Subgenera:	Equisetum and Hippochaete

Table 1. *Equisetum* taxonomy

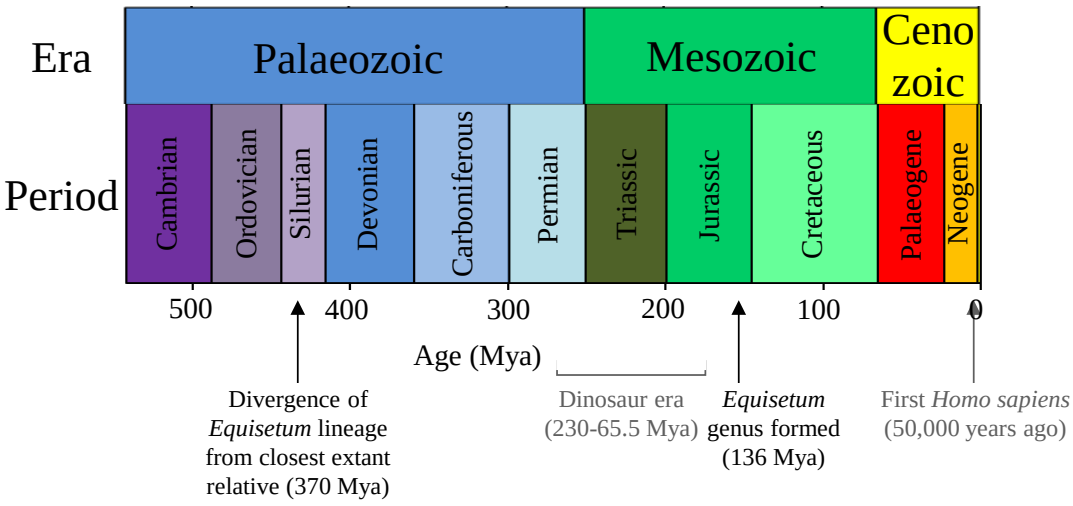

Fig. 4. Geological eras and periods of the Phanaerozoic eon and notable points in *Equisetum* evolution Divergence of *Equisetum* ancestors, formation of the genus itself and other notable phenomena are shown.

Comparisons between extinct and extant members of the Equisetales show clear transformational series of both morphology and anatomy documenting a monophyletic group that has developed over an exceptionally long time scale with

relatively few character state changes (Brown, 1975; McIver & Basinger, 1989; Stewart & Rothwell, 1993; Taylor & Taylor, 1993). This has lead researchers in the field to call the *Equisetum* body plan one of the most successful body plans ever (Rothwell, 1996). Morphologically, species within the genus *Equisetum* are non-flowering vascular plants with unique upright jointed aerial stems which arise from an extensive underground rhizome system. All species are herbaceous perennials, the aerial stems of some species die back seasonally. Small microphyllous leaves are arranged in true whorls and are fused together to form a cylindrical sheath around each node. Some, but not all, species (e.g. *E. arvense* but not *E. fluviatile*) form whorls of lateral branches at the nodes of the aerial stems (Golub & Wetmore, 1948). The stobilus is the specialised reproductive structure of *Equisetum*, consisting of a stem with short internodes and sporangium-bearing appendages, generally modified leaves called sporophylls, attached in a spiral pattern. A cross-section of an *Equisetum* internode shows an alternating sub-epidermal pattern of chollenchyma strengthening tissue and chlorenchyma, with the former present at ridges and the latter at furrows. Internally, vallecular canals are found in the cortex opposite furrows, and carinal canals, together with vascular bundles, opposite ridges; all of this surrounds a large central cavity (Leroux *et al.*, 2011 and references therein).

It is now widely recognised that *Equisetum* contains 15 extant species, as is the presence of two distinct subgenera (Des Marais *et al.*, 2003; Guillon, 2004; Guillon, 2007): *Equisetum* (*E. arvense*, *E. bogotense*, *E. diffusum*, *E. fluviatile*, *E. palustre*, *E. pratense*, *E. sylvaticum* and *E. telmateia*) and *Hippochaete* (*E. gigateum*, *E. hyemale*, *E. laevigatum*, *E. myriochaetum*, *E. ramosissimum*, *E. scirpoides* and *E. variegatum*). These subgenera can be readily distinguished by characteristics such as stomatal position, among others. In addition to these 15 species many interspecific hybrids are readily found in the wild, most of which have also been experimentally synthesised using controlled crosses (Guillon, 2004). These hybrids are considered to be sterile, relying on vegetative growth for survival. In agreement with the subgenera distinction described here, hybridisation appears strictly confined within the two subgenera with none occurring between them (Duckett, 1979).

1.5.1. *Equisetum* cell walls

Fittingly, in light of the evolutionary isolation in which *Equisetum* is found and the distinctiveness of its general morphology, *Equisetum* cell walls are equally unique, being comprised of a distinct complement of polymers that transcends the typical type I : type II cell wall classification. While containing high levels of mixed-linkage glucan – characteristic of type II cell walls – they lack type II levels of (glucurono)xylans and contain high levels of cellulose and pectin – features characteristic of type I walls (Popper & Fry, 2004; Fry *et al.*, 2007; Nothnagel & Nothnagel, 2007; Sorenson *et al.*, 2007). *Equisetum* species also contain unusual lignins. For example, Espiñeira *et al.* (2010) showed that *Equisetum telmateia* contains lignin composed purely of guaiacyl (coniferyl) monomer, *Equisetum fluviatile* however contains significant proportions of syringyl monomers (Logan & Thomas, 1985).

At least two studies have attempted to characterise the spatial distribution of polysaccharides within the *Equisetum* cell wall, both using an immunological approach; Leroux *et al.* (2011) use *E. ramosissimum* while Sørensen *et al.* (2007) use *E. arvense* and their findings are not entirely compatible. In Leroux *et al.* (2011), an anti-MLG antibody was shown to bind to the inner wall regions of the cells of the sclerenchymic strengthening tissue found in internodal ridges and far less intensely to the walls of some cortical parenchyma cells between the chlorenchyma and the vallecular canals. In Sørensen *et al.* (2007) the same antibody again bound to the sclerenchymic strengthening tissues, but here the labelling was found throughout the thickness of the cell walls and extended into the middle lamella, though it was less prevalent here. However, in Sørensen *et al.* (2007) the signal was much more widespread, occurring also in the epidermis, pith parenchyma and throughout the cortical parenchyma. In both studies labelling was weak or absent in vascular tissues and, except for sclerenchymic tissue, in the middle lamella. The significant discrepancies in the results in these two studies are unlikely to be explained by species differentiation alone and are possibly the result of epitope masking (Marcus *et al.*, 2008; Marcus *et al.*, 2010) and/or developmental regulation of MLG incorporation into cell walls.

1.5.1.2. *Equisetum* cell walls have high levels of deposited silica

One of the most distinguishing features of *Equisetum* cell walls, in addition to their unusual polymer complement, is the abnormally high level of deposited silica (up to 25% dry weight; Timell, 1964): an oxide of silicon with the chemical formula SiO_2. Despite silicon being a mineral constituent of all terrestrial plants, it is not considered an essential element for general plant life (Epstein, 1994), endowing plants with merely beneficial effects such as increased drought and heavy metal tolerance, and pest and pathogen resistance. In *Equisetum* however, silicon is considered essential and is speculated to play various roles in the life cycle (Chen & Lewin, 1969; Hoffman & Hilson, 1979; Epstein, 1994).

As well as MLG, *Equisetum* also share this unusually high silica content with the type II cell walls of the Poaceae. Indeed, recognition of this led Fry *et al.* (2008b) to propose that MLG may play a role in silica deposition *in planta*. The prior observation of Perry *et al.* (1987), that a large increase in MLG biosynthesis during the development of Phalaris (canary grass) trichomes correlated with a shift from sheet-like to globular silica deposition, provides further support for this. Law & Exley (2011) later demonstrated the ability of barley MLG to stimulate the production of silica from a solution of silicic acid *in vitro*. Various anatomical correlations support the contention that MLG stimulates silica formation in *Equisetum*. For example, the observations of Perry & Fraser (1991) that silica is absent from the middle lamella and found exclusively in the secondary cell wall is consistent with the localisations of MLG by Leroux *et al.* (2011) and Sørensen *et al.* (2007). Sapei *et al.* (2007) report that, silica is found in the epidermal cell walls of *E. hyemale* hydrogen-bonded to polysaccharides, but also that amorphous, colloidal silica which is associated with little organic matter is concentrated in ‘knobs’ on the ridges of stems

1.5.1.3. Mixed-linkage glucan : xyloglucan endotransglucosylase

A recent kingdom-wide screen for novel endotransglycosylases made the surprise finding of the first apparently predominant hetero-endotransglycosylase within crude extracts of all *Equisetum* species tested. The novel activity: mixed-linkage glucan : xyloglucan endotransglucosylase (MXE), catalyses a reaction identical to that of

XET activity, but uses mixed-linkage glucan as a donor substrate instead of xyloglucan (Fry *et al.*, 2008a) (Fig. 3b). This makes MXE particularly important as it is the first known example of an apparently predominant hetero-endotransglycosylase. While MLG may perform some shared function in the cell walls of all species in which it is present, because MXE activity has not been found in any other of these species (Fry *et al.*, 2008), it seems feasible that MLG may also perform a unique function in *Equisetum*.

MXE activity has thus far only been assayed using non-natural substrates – barley (*Hordeum vulgare*) and Iceland moss (*Cetraria islandica*) mixed-linkage glucan as the donor substrate and tamarind (*Tamarindus indica*) xyloglucan-derived oligosaccharides as the acceptor substrate (Fry et al., 2008a). These were used owing to their low cost and high availability but also because *Equisetum* mixed-linkage glucan and [^{3}H]XGO-ols had yet to be prepared. Fry *et al.* (2008a) showed that MXE activity is higher against MLG from barley than against that of Iceland moss lichen. This increase in activity correlates with an increase in the predominance of cellotetraose units within the mixed-linkage glucan of barley, suggesting that MXE may exhibit specificity toward cellotetraose units. This positive correlation between MXE activity and cellotetraose content has led to the hypothesis that MXE would favour *Equisetum* MLG over BMLG as the former contains an even higher cellotetraose content. No such correlation between the activity of MXE against different [^{3}H]XGO-ols is known that could be extrapolated to aid such a prediction of the suitability of the *Equisetum* xyloglucan structures for MXE activity. However one could predict that MXE, an enzyme only known to occur within higher plants in *Equisetum*, might favour those xyloglucan structures (see Fig. 1) also native to *Equisetum* and while not genus-unique, nonetheless rare within the kingdom.

1.5.1.4. Cellulose:xyloglucan endotransglucosylase

In addition to MXE activity, crude enzyme extracts from *Equisetum* are able to catalyse a further novel endotransglucosylase reaction – cellulose:xyloglucan endotransglucosylase (CXE); CXE has yet to be identified in any other species (unpublished data). The structural similarities between MLG, cellulose and xyloglucan, as well as the co-occurrence of MXE and CXE in *Equisetum* alone,

suggest that these activities could be catalysed by the same enzyme, which displays a somewhat promiscuous ability to utilise different donor substrates.

1.6. Scheme of work

While many GH16 enzyme family members are known to play crucial roles in plant cell wall metabolism and breakdown, there are fundamental gaps in our knowledge of how their structure is able to impart on them their substrate specificities and reaction preferences (e.g. transglycosylation vs. hydrolysis, specificity for xyloglucan vs. for mixed-linkage glucan). Further, in many cases the specific functions of these enzymes are unknown; elucidation of the enzymic preferences will be invaluable in reliably inferring function.

This work sought to aid the identification of structural motifs which confer enzyme: carbohydrate recognition, and the determination of enzyme function(s) by investigating the range of substrate specificities exhibited by GH16 members and the sites of cleavage and mode of recognition of substrates by GH16 members and related enzymes. This work investigated five distinct, but related, enzymes: xyloglucan endotransglucosylase (XET); xyloglucan endoglucanase/endohydrolase (XEG/XEH); lichenase; mixed-linkage glucan : xyloglucan endotransglucosylase (MXE); and, cellulose : xyloglucan endotransglucosylase. This involved numerous related, but not reliant, areas of work, all investigating GH16 enzyme family members, their activities and/or their hemicellulosic substrates. Accordingly, this thesis is divided into 7 distinct research areas: (1) Identification of MXE gene in *Equisetum fluviatile* – this section sought further to compare the identified MXE gene with related enzymes (XTHs and lichenases) in an attempt to elucidatedifferences which might account for MXE's novel substrate specificities; (2) MXE substrate specificity – this section sought to probe the substrate specificity of the MXE enzyme, a necessary step for the understanding of how its structure relates to its novel specificity; (3) Identification of the nature and location of the bonds broken and formed during the MXE reaction – this section sought to identify the mechanism of recognition of MLG by MXE as determined by the location of cleavage of the MLG polysaccharide; (4) Presence of MXE in other species and tissues – this section sought to investigate the prevalence of MXE actuivity in other

members of the plant kingdom and in other *Equisetum* tissues; (5) Analysis of cellulose : xyloglucan endotransglucosylase (CXE) activity – this section sought to determine whether the activity CXE was catalysed by the same enzymes as MXE; (6) An unexpectedly lichenase-stable hexasaccharide yields new information on MLG subunit composition and distribution – this section sought to better understand the substrate specificity of a commonly used GH16 lichenase by the biochemical characterisation of its oligosaccharide products; and (7) The mode of recognition and site of attack of xyloglucan-cleaving enzymes – this section sought to better understand the site of attack and mode of recognition of GH16 XTHs and a commponly used GH12 XEG.

2. MATERIALS AND METHODS

2.1. General materials

Barley mixed-linkage glucan (beta glucan, medium viscosity) and Iceland moss mixed-linkage glucan (lichenan) were from Megazyme (Bray, Republic of Ireland). Tamarind seed xyloglucan was a generous gift from Dr K. Yamatoya, Dainippon Pharmaceutical Co. (http://www.ds-pharma.co.jp). Dialysis tubing (12–14-kDa cut-off) was purchased from Medicell International, Ltd. (London, UK). Miracloth was from Calbiochem (http://www.emdbiosciences.com). Solvents and scintillant were from Fisher Scientific (Loughborough, UK). Whatman papers (No. 1, 3 MM; http://www.whatman.com) were purchased from VWR (Lutterworth, UK). Other general chemicals came from Sigma-Aldrich (UK).

2.2. Plant sources

Early (Apr–May) and late (Sep–Nov) season *E. fluviatile* lateral shoots were taken from the King's buildings pond in Edinburgh. Lateral *E. arvense* shoots (Sep–Nov) and strobuli (Apr–May) were taken from a roadside in Edinburgh. Yorkshire fog grass (*Holcus lanatus*) was taken from the King's buildings campus in Edinburgh. Mung bean (*Vigna radiata*) was purchased from Sainsbury's (UK). Winter barley (*Hordeum vulgare L.*) cultivar Pearl was grown from seed in a glasshouse under natural light for up to 12 wk. Barley seedlings were germinated on wet tissue paper at 25°C for 3 days.

Maize (*Zea mays* L., Black Mexican sweetcorn) cell-suspension cultures were grown under constant light on an orbital shaker at 25°C. Cells were sub-cultured fortnightly into 200 ml fresh medium [0.47% (w/v) Murashige and Skoog basal inorganic medium (Sigma, M5519), 2% (w/v) sucrose and 2 mg l^{-1} (w/v) 2,4-dichlorophenoxyacetic acid, pH 4.6–4.8], in 500-ml conical flasks. Maize cells and cell media were extracted from 4-day old cultures.

2.3. Enzyme preparations

All enzyme extraction procedures were carried out at 5°C, and samples were aliquotted and stored at -80°C. Before use aliquots were allowed to thaw completely in an ice bucket.

2.3.1. *Equisetum* crude extract

Equisetum tissues (lateral shoots, strobili, strobili stalk) were homogenised in a pestle and mortar with extractant buffer (10 mM $CaCl_2$, 165 mM Na:citrate, 20 mM ascorbate 3% (w/v) polyvinylpyrrolidone at pH 6.1; 4 ml g^{-1} plant material) and a pinch of sand. The homogenate created was incubated for 1–2 hours to facilitate desorption of ionically-bound enzyme and filtered through miracloth. The homogenate was the centrifuged at 12000 *g* for 5 mins. The supernatant was retained as the enzyme sample.

2.3.2. Yorkshire fog grass (*Holcus lanatus*) crude extract

Yorkshire fog grass was homogenised in a pestle and mortar with extractant buffer (0.2 M Na:succinate, pH 5.5, 10 mM $CaCl_2$; 4 ml g^{-1} plant material) and a pinch of sand. Polyvinylpolypyrrolidone (PVPP; 2% w/v) was suspended in all extractants. The homogenate was stirred slowly with a magnetic stirrer for 3 h at 5°C. After filtration through two layers of Miracloth, the extract was centrifuged at 12 000 *g* for 40 min. The supernatant was retained as the enzyme sample.

2.3.3. Mung bean (*Vigna radiata*) crude extract

Fresh mung beans were homogenised in a benchtop blender in extractant buffer (200 mM Na:citrate, pH 5, 10 mM $CaCl_2$; 2 ml g^{-1} plant material). Suspension was agitated for 4 h at before it was filtered using a miracloth. Filtrate was centrifuged at 4000 rpm at and supernatant was precipitated in 75% (v/v) saturated ammonium sulphate. Ammonium sulphate was resuspended in 75% (v/v) saturated ammonium sulphate three times before finally being resuspended in 100 ml 200 mM pH 5.5 10 mM $CaCl_2$. The supernatant was retained as the enzyme sample.

2.3.4. MXE purification

All purification steps were performed at 5°C. 100 ml crude *E. fluviatile* extract was precipitated in 10% 'cuts' from 10–60% (v/v) saturated ammonium sulphate by adding dry ammonium sulphate with constant stirring followed by centrifugation. Each 'cut' was then redissolved in 25 ml 10 mM Na:citrate 0.05% triton X-100 pH 6.1. The majority of MXE precipitated in the 30–40% fraction, 6 ml of which was fractionated by SEC (Biogel P100). MXE-rich (~ 30 kDa) SEC fractions 30–33 were then further fractionated using a 1.8 ml bed-volume Concanavalin A column; MXE activity eluted from the column in the presence of 640 mM methyl-α-mannopyranoside (MeMan*p*). MXE-rich Concanavalin A fractions 26–31 were fractionated by isoelectric focusing after which MXE was found in a region of pH ~ 4.0.

2.4. Polysaccharide extractions

2.4.1. Alcohol-insoluble residue (AIR) creation

In general: plant material was homogenised either with a food blender/pestle and mortar in 75% (v/v) ethanol or in a bead mill after drying *in vacuo*, before suspending in 75% (v/v) ethanol. Alcohol-insoluble material (AIR) was extracted either by centrifugation or by collection on miracloth and this step was repeated numerous times with 75% (v/v) ethanol.

For *Equisetum arvense* batch AIR creation: 437 g of late season *E. arvense* lateral shoots were vigorously blended in 75% (v/v) ethanol (~ 8 ml g^{-1}). The suspension was then stirred at 70°C for 4 hours. AIR was then collected on Miracloth and washed with 75% (v/v) ethanol again while still in the Miracloth before being squeezed dry. The AIR was stirred overnight (~16 hours) at room temperature in 2 l 0.5% (w/v) SDS before again being collected on miracloth and squeezed dry. The AIR was then stirred over two nights (~55 hours) at room temperature in 3.5 l 0.5% (w/v) SDS before being heated to 60°C while stirring for 6 hours, collected on miracloth and squeezed dry to remove any excess SDS. The AIR was then stirred in successive 5 l portions of distilled water allowing at least 4 hours to stir until water ran without froth (~8 times). The remaining AIR was squeezed dry in miracloth. AIR

was then stirred at room temperature in ~ 1.5 l acetone for ~ 4 hours before being filtered through a miracloth and squeezed dry. AIR was then left to dry in an open container for ~ 2.5 days. The final dry weight of AIR recovered was 42.12g (96 mg g^{-1} fresh plant material).

2.4.2. Hemicellulose extractions

2.4.2.1. General hemicellulose extraction from AIR

AIR was stirred in 0.5 M NaOH, 0.1% (w/v) $NaBH_4$ at room temperature for 16 hours (hemicellulose fraction 1) or in 6.0 M NaOH, 0.1% (w/v) $NaBH_4$ at 37°C for 16 hours (hemicellulose fractions 1 and 2).

2.4.2.2. *E. arvense* hemicellulose extractions (For *Ea*MLG and *Ea*XGO purification)

Hemicellulose fraction 1 was solubilised by stirring 5 g *E. arvense* AIR in 250 ml 0.5 M NaOH, 0.1% (w/v) $NaBH_4$ at room temperature for 16 h. Insoluble hemicellulose was pelleted by centrifugation. The pellet (AIR minus hemicellulose 1) was then resuspended in 250 ml 6 M NaOH, 0.1% (w/v) $NaBH_4$ and stirred at 37°C for 16 hours, thereby solubilising hemicellulose fraction 2. Hemicellulose 2 was also collected in the supernatant following bench centrifugation of the suspension; the pellet was rejected. Both supernatants were slightly acidified (pH 5−6) with acetic acid and dialysed at 5°C against several changes of deionised water in a 12 kDa cut-off sac, before being centrifuged and rejecting pellets.

2.4.2.2.1. *E. arvense* MLG purification

To hemicellulose fraction 1, 0.025 volumes of 10% (w/v) aqueous ammonium formate were added, followed by ethanol (added with vigorous shaking) to a final concentration of 45% (v/v). The suspension was stood overnight without stirring before being centrifuged. The supernatant was rejected and the inside of the tube was lightly blotted with tissue paper to remove as much ammonium formate as possible without allowing the pellet to dry out. The pellet was then thoroughly resuspended in 70% (v/v) ethanol and after incubating for 2 hours at room temperature centrifuged again. The supernatant was again rejected and the inside of the tube lightly without

drying. The pellet was redissolved 14 ml water by boiling and prolonged agitation before any remaining insoluble matter was pelleted by centrifugation. Saturated aqueous ammonium sulphate was added to the isolated supernatant to a concentration of 47% (v/v) with vigorous shaking before incubation at 4°C for ~ 16 hours. The suspension formed was centrifuged, the supernatant rejected and the inside of the tube again lightly blotted without drying. The pellet was redissolved in 20 ml water and dialysed for 3 hours at 5°C against deionised water in a 12 kDa cut-off sac. Post dialysis, insoluble material was then pelleted by bench centrifugation and the supernatant was extracted. Using the anthrone procedure the total hexose mass of the supernatant sample was shown to be ~ 27.0 mg. Concentrating, where necessary, was achieved by heating in a stream of cool air (up to 5.7 mg ml^{-1}).

For batch purification of 6x: hemicellulose was solubilised by stirring 5 g *Equisetum arvense* alcohol-insoluble residue (AIR) in 250 ml 6 M NaOH 0.1% (w/v) $NaBH_4$ at 37°C for 16 hours before being centrifuged, acidified, dialysed and centrifuged again as above. This hemicellulose solution was then digested with lichenase, after which ethanol was added to 75% (v/v) and undigested polysaccharides were pelleted by centrifugation.

2.4.2.2.2. *E. arvense* XGO purification

To hemicellulose fraction 2, saturated aqueous ammonium sulphate was added with vigorous shaking to give a final conc of 47% (v/v). The solution was then stood at 4°C for ~ 16 h before being centrifuged. 50 ml of the supernatant was then dialysed at 5°C against several changes of deionised water in a 12 kDa cut-off sac. 0.025 volumes 10% (w/v) ammonium formate was then added to the solution post dialysis to which ethanol was added to a final conc. of 75% (v/v). The solution was then stood at 4°C for ~ 16 hours before being centrifuged. The pellet was collected and thoroughly resuspended in 75% (v/v) ethanol before being centrifuged again. The pellet was digested with XEG before being dried *in vacuo*, redissolved in water and centrifuged. The supernatant was fractionated by SEC (Biogel P-2 column 1) from which XGO-containing fractions (determined by TLC) were pooled. The total hexose mass of the solution was shown to be 0.9 mg anthrone Glc equivalent.

2.4.2.3. Maize (*Zea mays*) soluble extracellular polysaccharide isolation and deacetylation of one half

A 4-day old 200-ml maize (*Zea mays*) cell culture suspension was filtered through miracloth, after which cloth-bound material was rejected. The filtrate was centrifuged and the supernatant was boiled for 30 mins before being centrifuged again. The remaining supernatant was split into two halves. One half was incubated in 0.1 M NaOH at room temperature for 2 h before being slightly acidified with acetic acid. An equimolar (~pH 5) solution of sodium acetate was added to the second half. Both solutions were dialysed with numerous changes of water and concentrated (without drying) to 300 µl by boiling in a constant flow of air.

2.4.2.4. Creation of comparable maize cell wall and SEP xyloglucan-containing samples

A 4-day old maize suspension culture was centrifuged and the cell-containing pellet was separated from the SEPs-containing supernatant. The supernatant was filtered through miracloth and cloth-bound material was rejected. AIR of both pellet and filtered supernatant was created and hemicellulose fractions 1 and 2 were extracted together. Both were concentrated to 2.5 ml by boiling in a constant flow of air.

2.5. Enzyme and chemical treatments

2.5.1. Enzyme treatments

2.5.1.1. General soluble-donor endotranglycosylase reactions

General soluble-donor endotransglycosylase (e.g. XET and MXE) reactions were performed by incubating buffered enzymes with 0–0.7% (w/v) donor substrate and ≤3 µM acceptor substrate in the case of MXE or ≤80 µM acceptor substrate in the case of XET. Reactions were stopped by the addition of 0.5 reaction volumes of 50% (v/v) formic acid. Unless otherwise stated reaction mixtures were dried onto 4 x 4 cm squares of Whatman 3 MM paper and washed for 24–48 hours in running tap water. Incorporated radioactivity was then assayed by scintillation counting using 1 ml paper scintillant. Alternatively, products were precipitated by the use of 75% (v/v) ethanol, before being redissolved and quantified by scintillation counting.

2.5.1.2. Cellulose : xyloglucan endotransglucosylase (CXE)

2.5.1.2.1. NaOH pre-treatment of Whatman No. 1 chromatography paper

Whatman No. 1 paper was incubated overnight at 37°C in 45 ml 6.0 M NaOH. The paper was then subjected to numerous washing steps with water, until the washings had a pH of 7.2, before being washed with a solution of pyridine : acetic acid : water (ratio 33:1:300, pH 6.5). The paper was then washed again after which the water was pH ~6.8. Finally, the paper was lyophilised, and aliquotted by mass.

2.5.1.2.2. CXE reaction

Reaction mixtures (110 µl) containing 18% (v/v) rotofor enzyme fraction, 0.1 µM (1 kBq) [^{3}H]XXXGol, 0.05% (w/v) chlorobutanol, 140 mM Na:citrate buffer pH 6.1 were applied to 35 mg 'aliquots' of NaOH-treated paper, such that the paper was totally soaked without excess liquid. Reactions were then incubated in a sealed environment for 24 h at 25°C before addition of 50 µl 50% (v/v) formic acid directly to the paper. Paper was washed 0.5% (w/v) chlorobutanol for 6–16 hours with gentle agitation in successive 15 ml portions, after which the liquid was removed from the paper following centrifugation. This washing was performed 6 times after which no enzyme controls gave a background reading. Paper-incorporated radioactivity was detected by incubating the paper with 2 ml dH_2O and 20 ml aqueous scintillant and counting for 10 minutes twice

2.5.1.3. *In vivo* endotransglycosylase action assay

Unless otherwise stated, razor blade-cut cross-sections (~0.5 mm thick; total 50 mg) of various barley organs (Fig. 29) were immediately immersed in 250 µl water containing 1 µM (25 kBq) [^{3}H]XXLGol in a 1.5-ml tube and incubated with constant agitation for 16 h at 20°C. AIR was then prepared, by shaking in a bead mill before hemicellulose 1 and 2 were extracted together (6 M NaOH). Total extracted hemicelluloses were then digested with XEG, lichenase, or neither. Reaction products were subjected to incubation in 75% (v/v) ethanol and centrifugation before supernatants (oligosaccharide products) were analysed by TLC.

2.5.1.4. Xyloglucan endoglucanase (XEG) digestion

Samples were incubated in 20% (v/v) PyAW/CB 10^{-3}% (w/v) xyloglucan endoglucanase (XEG; a generous gift from Novo Nordisk A/S, Bagsværd, Denmark; Pauly et al., 1999) at 25°C for 1 h.

2.5.1.6. Lichenase digestion

Lichenase (from *Bacillus subtilis*; 330 U mg^{-1}; Megazyme, Inc.) was pelleted from ammonium sulphate by centrifugation after which the supernatant was rejected. The pellet was redissolved at 2 U ml^{-1} in PyAW/CB and stored at –20°C. For digestion, 1 volume of lichenase solution was added to 1 volume of sample solution and incubated at 20°C for 4 h, unless otherwise stated.

2.5.1.7. Driselase digestion

One volume of 0.5% (w/v) purified driselase (partially purified as described by Fry, 2000) in PyAW/CB was added to 1 volume of carbohydrate sample and incubated at 37°C for 48 h with constant agitation.

2.5.1.8. β-glucosidase digestion

β-D-glucosidase (from *Aspergillus niger*; 52 U mg^{-1}) from Megazyme, Inc. (Bray, Ireland) was pelleted from ammonium sulphate and redissolved at 0.25 U ml^{-1} in PyAW/CB. 1 volume sample solution was mixed with one volume enzyme solution and incubated at 20°C.

2.5.1.9. Cellobiohydrolase digestion

Cellobiohydrolase (CBH1 from *Trichoderma longibrachiatum*; 0.07 U mg^{-1}) from Megazyme, Inc. was pelleted from ammonium sulphate and redissolved at 0.5 U ml^{-1} in PyAW/CB. 1 volume sample solution was mixed with one volume enzyme solution and incubated at 20°C for 2 h unless otherwise stated.

2.5.1.10. Cellulase digestion

Cellulase*a* (from *Aspergillus niger*; 86 U mg^{-1}; incapable of digesting xyloglucan) from Megazyme, Inc. was pelleted from ammonium sulphate and redissolved at 10 U ml^{-1} in PyAW/CB. 1 volume sample solution was mixed with one volume enzyme solution and incubated at 20°C for 2 h unless otherwise stated.

Cellulase*b* (endo-1,4-β-D-glucanase from *Trichoderma longibrachiatum*; capable of digesting xyloglucan; a GH7 family member from E.C: 3.2.1.4) from Megazyme, Inc. was pelleted from ammonium sulphate and redissolved at 10 U ml^{-1} in PyAW/CB. 1 volume sample solution was mixed with one volume enzyme solution and incubated at 20°C for 2 h unless otherwise stated.

2.5.1.11. α-xylosidase digestion

Thermostable α-xylosidase (specific activity 2.6 U g^{-1}) was from CPC Biotech, Agrate Brianza, Milan, Italy. Reaction mixtures contained (10 µl) containing 1% (w/v) enzyme and trace amounts of radiolabelled oligosaccharitol was incubated in 0.15% (v/v) acetic acid, 0.55% (v/v) pyridine (pH 5.5), 0.5% (w/v) chlorobutanol at 65ºC. The reaction was stopped on ice and products were purified by PC or TLC.

2.5.1.12. Stopping enzyme reactions

Unless stated otherwise, all reactions stopped by the addition of 0.5 reaction volumes of 50% (v/v) formic acid or by boiling thoroughly.

2.5.2. Chemical treatments

2.5.2.1. TFA hydrolysis

Samples were incubated in 2 M trifluoroacetic acid for 1 h at 120°C.

2.5.2.2. Sodium borohydride ($NaBH_4$) reduction

Samples were incubated at room temperature for 16 h in 0.5 M $NaBH_4$ in 1 M NH_3; before NH_3 was allowed to evaporate in moving air. The sample was then slightly acidified with acetic acid and applied to a cation exchange column. The eluted sample was dried *in vacuo* before being redissolved and dried in a methanol : acetic acid (9:1 by volume) solution. This redissolving and drying was repeated at least six times.

2.6. Chromatographic and electrophoretic methods

2.6.1. Thin layer silica-gel chromatography (TLC)

Merck silica-gel 60 TLC plates (VWR, Lutterworth, UK) were either used from the box, or were pre-washed by incubating in a flat-bottomed plastic box with 4-5

changes of acetone : acetic acid : water (1:1:1) solution with constant agitation before drying. Samples were applied along a pencil line drawn 20 mm from the bottom of the sheet. A malto-oligosaccharide ladder (produced by degraded starch) plus glucose was routinely used as a marker mixture. After drying, sheets were typically developed in butan-1-ol : acetic acid : water (BAW; 2:1:1) with two ~ 8 h ascents or propan-1-ol : nitromethane : water (PNW; 5:2:3) with one 6 h ascent. When used preparatively, the desired oligosaccharides were extracted from pre-run TLCs by cutting the TLC region containing the oligosaccharide (identified by fluorography, autoradiography, or by partial thymol-staining) from the rest of the gel, and incubating with constant agitation in 0.05% (v/v) chlorobutanol for 8–16 h before drying *in vacuo*. This was done once or twice, in which case solutions were pooled.

2.6.2. Paper chromatography

Samples were pipetted as spots or streaks onto a pencil line drawn 90 mm from one end of a sheet of Whatman No. 1 or Whatman 3 MM chromatography paper. A marker mix containing ~ 75 μg GalA, Gal, Glc, Man, Ara, Xyl, Rib and Rha was often separately pipetted onto each chromatogram. The paper was folded 20 and 70 mm from that same end. The opposite end was serrated. Paper chromatograms were developed in one of two chromatography solvents:

EPW (for monosaccharide analysis): developed for 16 h in ethyl acetate/pyridine/water (8:2:1 by volume).

BAW (for purification of [^{3}H]XGO-ols): developed for 16 h in ethyl acetate/pyridine/water (8:2:1 by volume)

2.6.3. Size-exclusion chromatography (SEC)

Five different size-exclusion chromatography (SEC) columns were used during the present work. The void volume (K_{av} 0) and the whole included volume (K_{av} 1) of each column was determined using 5–40 MDa Dextran and [^{3}H]H_2O/glucose respectively.

Three different Biogel P2 columns (Bio-Rad, Inc.):

P2 column 1: internal diameter 75 mm, column bed volume 166 cm^3.

P2 column 2: internal diameter 1.4 mm, column bed volume 69 cm^3.

P2 column 3: internal diameter 9 mm, column bed volume 19 cm^3.

Biogel P100 (Bio-Rad, Inc.): column diameter 14 mm, column bed volume 82 cm^3.

Sepharose Sephadex CL-6B (column bed volume ~ 250 ml, internal diameter ~ 1.4 mm) equilibrated with PyAW (1:1:23), from which 80 ~ 3.6 ml fractions were collected.

2.6.4. SDS-PAGE

SDS-PAGE was performed using a Bio-Rad Mini PROTEAN Tetra Cell system. Protocols followed Laemmli (1970). Gels were composed of a 5% stacking gel above a 12% resolving gel. Gels were run at 75 V for ~15 mins then at 100 V for ~ 75 mins.

2.6.5. Isoelectric focusing

A Rotofor isoelectric focusing kit (BioRad) was assembled and used according to the manufacturer's instructions. Prior to focusing, the inside of the equipment was washed with 0.25% (w/v) triton X-100. Ampholytes (address) 3–5 or 3–10 were added to protein-containing solutions. Focusing was performed at 10 W until voltage and current stabilised. Recovered fractions were immediately assayed using pH meter before storing at -80°C.

2.6.6. Concanavalin A lectin-affinity chromatography

Concanavalin A (from jack bean)-Sepharose 4B beads (1 ml) were packed in a Poly-Prep (Bio-Rad) column and washed with excess 50 mM citrate (pH 6.3) containing $CaCl_2$, $MnCl_2$, $MgCl_2$ (1 mM each). The protein-containing solutions was applied to the column and eluted in wash buffer containing increasing concentrations of methyl-α-mannopyranoside (MeMan*p*).

2.6.7. Muniscus agarose gel electrophoresis

Agarose powder (0.75–1.5% (w/v)) was solubilised in TBE (89 mM Tris:boric acid, 2mM disodium EDTA) by heating. The solution was allowed to cool slightly before ethydium bromide was added to 2 x 10^{-3}% (v/v). 25 ml was applied to a glass sheet

with well-comb positioned before being allowed to cool. After immersing in TBE, PCR products were applied to wells and the gel was developed at ~ 150 V for 1–2 h.

2.6.8. Cation exchange chromatography

A 1–2 ml bed-volume of Dowex-5 (H+ form; Sigma–Aldrich) resin column was incubated for > 1 h in 1M HCl before being washed thoroughly with distilled water until no salt (determined using a conductivity meter) eluted. Sample was then applied to the column before being eluted in dH_2O.

2.6.9. HPLC

HPLC was performed on a CarboPac PA1 column (high-performance anion-exchange chromatography, HPAEC; Dionex, Camberley, UK) with elution at 1 ml min–1. For oligosaccharide analysis the elution profile was 0.1 M NaOH which also contained: 0–30 min, 0→0.3 M sodium acetate (linear gradient); 30–36 min, 1 M sodium acetate; 36–42 min, 0 M sodium acetate. For TFA hydrolysate analysis the elution profile was: 0–3 min, 20 mM NaOH (isocratic); 3–44.5 min, H2O (isocratic); 44.5–75 min, 0→800 mM NaOH (concave gradient); 75–81 min, 800 mM NaOH (isocratic); 81–82 min 800→20 mM NaOH (linear gradient); 20 mM NaOH (isocratic). A pulsed amperometric detector (PAD) with a gold electrode was used. PAD response was calibrated by use of known weights of malto-oligosaccharides. For preparative HPLC, collected fractions were slightly acidified with acetic acid (to pH<6) immediately, then desalted by cation-exchange on Dowex-5.

2.6.10. Immobilised metal ion affinity chromatography (IMAC)

IMAC was performed on a Chelating Sepharose Fast Flow (2 ml bed vol.) column. The column was charged beforehand with 0.2 M nickel sulphate. The binding buffer was 0.02 M sodium phosphate, 0.75 M NaCl, pH 7.0. The elution buffer was 0.02 M sodium phosphate, 0.5–1.0 M NaCl, 0.05 M imidazole, pH 7.0. Following elution, the desired protein fraction was further purified using a PD-10 desalting column. Proteins were eluted in 0.1 M sodium citrate, 0.025 % (w/v) triton X-100, 0.5 % (w/v) chlorobutanol, pH 6.3.

2.7. Staining and quantification methods

2.7.1. Silver nitrate staining

For paper chromatograms (PCs): PCs were dipped through three solutions consecutively, allowing 15 mins to dry in between: Dip1, 5 mM silver nitrate in acetone (dH_2O used to dissolve any precipitate); Dip 2, 124 μM NaOH in 96% (v/v) ethanol; Dip 3, 10% (w/v) sodium thiosulphate in dH_2O. Dip 2 was sometimes used up to three times to increase staining. The paper was immediately washed in running water and left for up to 24 hours before being allowed to dry.

For SDS-PAGE gels: Gels were fixed by incubating in a solution of 50% (v/v) ethanol, 12% (v/v) acetic acid, 1.875% (v/v) formaldehyde for half an hour. Gels were washed briefly in 50% (v/v) ethanol three times before being incubated in 0.01% sodium thiosulphate for 60 sec. After washing them three times in distilled water, I stained the gels by incubating in 0.1% (w/v) silver nitrate, 2.77% (v/v) formaldehyde for 20 min. Gels were washed three times in distilled water and then developed in 3% (w/v) sodium carbonate , 18.75% (v/v) formaldehyde, 10^{-4}% (w/v) sodium thiosulphate until staining became apparent. Staining was stopped by incubation of gels in 4% (w/v) Tris, 2% (v/v) acetic acid.

2.7.2. Thymol staining

Thin layer chromatograms (TLCs) were dipped through 5% (v/v) sulphuric acid, 0.5% (w/v) thymol in ethanol. TLCs were left to dry before being baked at 105°C for ~ 5 minutes (Jork et al., 1994).

2.7.3. Anthrone assay

To one volume of sample (containing < 10^{-2}% (w/v) hexose sugars) two volumes 0.2% (w/v) anthrone in conc. sulphuric acid were added. Mixtures were thoroughly mixed by vortexing before boiling for 5 minutes. Samples were cooled slightly in an ice bucket before being measured by A_{620}.

2.7.4. Coomassie blue staining

SDS-PAGE gels were incubated with water for 5 min three times before being incubated for 1 h with agitation in GelCode Blue stain (Pierce). After staining, destaining was performed by incubating numerous times in water until background gel was clear.

2.7.5. Bradford assay

Bio-Rad Protein Assay Dye (0.2 ml) was added to a protein-containing solution (0.8 ml) and mixed thoroughly by inversion. A_{595} was measured immediately and calibrated using known concentrations of BSA.

2.8. Radioactive labelling, detection and analysis

2.8.1. Autoradiography and fluorography

Autoradiography was performed by incubating paper chromatograms or TLCs containing ^{14}C-labelled moieties with Kodak BioMax MR film at room temperature. Fluorography was performed by dipping TLCs containing ^{3}H-labelled moieties through a solution of 7% (w/v) poly(vinylpolypyrrolidone) (PPO) in (diethyl)ether before allowing to dry. Plates were then incubated with preflashed Kodak BioMax MR film in a cassette at -80°C.

2.8.2. NaB^3H_4 oligosaccharide reductive radiolabelling

To 50 MBq of 4.33 MBq μmol^{-1} NaB^3H_4 (8 μmol), 100 μl 2M NH_3 followed immediately by ~ 0.3 mg (Glc equivalent by anthrone) of purified *Equisetum* XGOs in 330 μl water was added. Mixture was left un-capped overnight to allow evaporation of ammonia. The solution was then purified by cation exchange chromatography. The sample was dried *in vacuo* and resuspended in 100 μl methanol/acetic acid (10:1) before being redried *in vacuo* again. This step was preformed 8 times before the sample was finally redissolved in H_2O. Four distinct radioactive bands were subsequently isolated by preparative paper chromatography (BPW; fluorography) and preparative TLC (BAW; fluorography).

2.8.3. Radioisotope plate reader

TLC plates were quantitatively profiled by counting on a LabLogic AR2000 radioactivity scanner (http://www.lablogic.com/).

2.9. Mass spectrometry

After coomasie blue-staining an SDS-PAGE gel, protein bands were tightly cut from the minigel with the minimum amount of surrounding acrylamide. Gel pieces were stored at –20^{o}C. Gel pieces were incubated twice in 300 µl 200mM ammonium bicarbonate (ABC) in 50% (v/v) acetonitrile (ACN) at room temp for 30min before decanting solvent – to remove SDS. Pieces were then incubated in 300 µl 20 mM dithiothreitol, 200 mM ABC, 50% (v/v) ACN at room temp for 1h – to reduce protein. Pieces were washed three times in 300 µl 200 mM ABC, 50% (v/v) ACN for ~ 30 sec. Protein cysteines were alkylated in 100 µl 50 mM iodoacetamide, 200mM ABC, 50% ACN (made fresh) at room temperature in the dark for 20 min. Pieces were washed three times in 500 µl 20mM ABC, 50% (v/v) ACN for ~ 30 sec. Gel pieces were then carefully cut into 2 x 1mm pieces, centrifuged and covered with ACN for 5 min until they turned white. ACN was decanted and gel pieces were allowed to dry.

Stock solution of trypsin was prepared by adding 50 µl 50 mM ABC to a new vial of trypsin (Promega) at 4^{o}C. Gel pieces were incubated in 29 µl 50 mM ABC containing 1 µl trypsin at 4^{o}C. This solution was stored at 4^{o}C until the gel swelled, after which the solution was incubated at 32^{o}C for 16–24 h. Internal calibration peaks were created by setting up a trypsin digest blank. Samples were then sonicated for 10 min after which peptide fragments were observed in the solution. Digests were stored long term at –80^{o}C.

For MALDI-TOF analysis, aliquots of 0.5 µl digests were mixed with 0.5 µl α-cyano-4-hydroxycinnamic acid (Sigma) matrix on a MALDI sample plate and allowed to dry. The samples were then analysed on a Voyager DE-STR MALDI-TOF MS (Applied Biosystems).

For LC-MS analysis, the 5 µl desalted sample was loaded onto a HTC PAL autosampler (CTC Analytics, Switzerland) in series with an Agilent 1200 Series HPLC with a PicoTip Emitter (FS 360-100-8-N-20-C12, New Objective). The PicoTip Emitter was packed with Reprosil-Pur C18-AQ 3um (Dr Maisch GmbH) to a length of 6.5-7.5cm. The PicoTip column was equilibrated with solvent A (0.5% acetic acid in 5% acetonitrile) and eluted with a linear gradient, from 0%B over 8min; from 0 to 60%B over 8 to 38 min; from 60 to 80% B over 38 to 45min; solvent B (0.5% acetic acid in 99.5% acetonitrile), over 70 min at a flow rate of 0.7 µl/min for the first 8min and 0.3ul/min thereafter. Data dependent acquisition was controlled by Xcalibur software (ThermoScientific).

Processed spectra were searched against the NCBI non-redundant database and an *E. fluviatile* transcriptome database using in-house licensed MASCOT software.

2.10. Molecular biology

2.10.1. RNA extraction

Approximately 500 mg lateral shoot of a single *E. fluviatile* individual were finely ground in liquid N_2 using a pestle and mortar and was allowed to dry before being thoroughly mixed with 3 ml Trizol (Invitrogen). The suspension was then centrifuged (12,000 *g*, 4ºC for 5 min) and 200 µl chloroform was added per ml of the extracted supernatant and mixed by shaking. The mixture was then centrifuged (12,000 g, 4ºC for 15 min) and the upper phase was removed to which 0.54 volumes of ethanol was added. The solution was then applied to a Purelink spin cartridge and purified as described (Invitrogen). Nanodrop analysis showed total yield was ~ 34.6 µg.

2.10.2. Reverse transcription

5’ RACE templates were created using the SMART oligo system (Clontech) 1 µl (30 µM) oligo dT, 1 µl (10mM) dNTP, 1 µl (30 µM) SMART II oligo and 600 µg RNA were made up to 11.5 µl with water and heated at 65ºC for 5 min before chilling on ice. 4 µl 5 x RT buffer, 2 µl (0.1 M) dithiothreitol.

2.10.3. 454 sequencing

The transcriptome of a single late season *E. fluviatile* individual was sequenced using 454 sequencing technology (Roche). Raw data was assembled using Roche Newbler assembler version 2.5.

Sequencing stats:	No. of raw reads	268,000
	Mean read length	248.73
	S Dev of read length	111.19
	N50 read length	311
	No. of reads in N50	91,568

2.10.3. PCR

Unless otherwise stated: Primers were designed to have a salt-adjusted annealing temperature of ~ 60ºC using OligoCalc (Kibbe 2007); standard PCR reaction mixtures contained 7.4 µl dH_2O, 1 µl yellow buffer, 0.2 µl primer 1 (10 µM), 0.2 µl primer 2 (10 µM), 0.2 µl dNTPs (10 mM) and 0.4 µl 5-fold diluted T*aq* (diluted from concentrate in storage buffer; PCR reaction cycles consisted of 1 min 94 ºC, 35 cycles of (10 sec 94ºC, 15 sec 55ºC, 30 sec 72ºC), 2 min 72 ºC. High fidelity PCR was performed by use of Phusion® High-Fidelity DNA Polymerase (New England Biolabs, USA) according to the manufacturer's instruction.

2.10.4. Primers used

UpstreamFw MXE:pPICZαA (*Eco*RI-incorporating): GAA TTC GGT TTC TAT GGG GAC TTT CAG
DownstreamRv MXE:pPICZαA (*Xba*I-incorporating): TCT AGA TAG AAA CCA CGG TTT GAG CAT T

2.10.2. Gene cloning

Gene cloning was performed using the pJET1.2 vector system (Fermentas) in *E. coli* (DH5α). In brief: amplicons (0.5 µl) were blunted by incubating with 5 µl 2x buffer, 3 µl dH_2O and 0.5 µl blunting enzyme at 70°C for 5 mins before resting on ice. 0.5 µl pJET1.2 vector and 0.5 µl ligase were then added and thoroughly mixed before incubating at room temp for 5-10 mins. 5 µl ligation mixture was added gently to 100

µl thawed competent *E. coli* cells and incubated for 15 mins on ice. Cells were heat-shocked at 42°C for 90 sec before returning to ice. 750 µl L-broth was added and cells were incubated at 37°C with constant agitation for 1 hour. Cells were pelleted by centrifugation at 6000 RPM, resuspended in ~100 µl of their L-broth solution, spread onto ampicillin Petri dishes (100 µg ampicillin/ml) and grown overnight at 37°C. Isolated colonies were screened by applying to a PCR mix (extra 1 µl dH_2O added) with appropriate primers. Plasmids were extracted using a QiaQuick Miniprep kit (QiaGen, UK).

Primers were designed to amplify putative mature proteins (i.e. coding region without signal peptides) and incorporate *Eco*RI and *Xba*I restriction sites upstream and downstream respectively. A high fidelity amplicon was then cloned and after screening, four colonies were selected. Cloning vectors were extracted from these and inserts were extracted using *Eco*RI and *Xba*I before ligation into a pPICZαA vector pre-cut with the same restriction enzymes. The consensus sequence was created by site-directed mutagenesis by use of the QuikChange (Quickchange, UK) method.

2.10.4. Recombinant protein expression (*Pichia pastoris* system)

Inserts were ligated into the pPICZαA expression vector by *Eco*RI, *Xba*I forced ligation. pPICZαA:insert vectors were cloned in *E. coli* using low salt L-B (10 g tryptone, 5 g NaCl, 5 g yeast extract, pH 7.5 with NaOH in 1 l. For agar, 15 g l^{-1} added before autoclaving) with 40 µg ml^{-1} Zeocin (Invitrogen). Plasmids were extracted from positive colonies by the use of the QuiaQuik kit (Quiagen) and linearised by the use of *SacI*. 0.1 vol. 10% (w/v) 3 M sodium acetate pH 5.2 and 2.5 vol. ethanol was then added to the sample and the sample was incubated at -20°C for 1 h before centrifugation. The pellet was washed with 70% (v/v) ethanol before being redissolved in H_2O). Plasmids 0.2–2 µg were applied to *Pichia pastoris* strain SMD1168H (pep4; pre-washed, as described in pPICZαA manual; Invitrogen) and electroporation was performed in 1 mm cuvettes at 1.6 kV with time constants of 4.6–5 ms. Cells were streaked on plates (10 g tryptone, 5 g NaCl, 5 g yeast extract, 15 g agar, 20 g glucose, pH 7.5 with NaOH in 1 l, 100 µg ml^{-1} Zeocin). Positive colonies were selected and grown in liquid growth media (90% (v/v) low salt LB, 1%

(w/v) glycerol, 0.00004% (w/v) biotin, 100 μg ml^{-1} zeocin). Expression was stimulated by centrifugation and resuspention of the culture in expression medium (identical to growth medium but with glycerol replaced with 10% (v/v) methanol). After 24 h the culture media was harvested and assayed for endotransglycosylase activity.

2.11. Nuclear magnetic resonance spectroscopy (NMR)

Samples were initially dried *in vacuo*, redissolved in $^{2}H_2O$ and dried again before redissolving $^{2}H_2O$. 1D CSSF–TOCSY spectra were acquired with the pulse sequences described by Robinson et al. (2004). The anomeric protons were inverted by the use of a 40-ms Gaussian pulse, while the protons of the Glcol were inverted with an 80-ms Gaussian pulse. The CSSF was set to yield zero excitation 60 Hz (residues **a**, **e**), 6.2 Hz (residues **b**-**d**), 25 Hz (Glcol(1–3)) and 15 Hz (Glcol(4–6)) from the chemical shift of the inverted resonance. Ten increments of the CSSF were acquired with 8 scans each (80 scans in total). The DIPSI-2 mixing times of 20, 40, 80 (data not shown) and 160 ms were used. A 20-ms adiabatic pulse was applied concurrently with an 11% PFG (Thrippleton & Keeler 2003). Acquisition and relaxation times were 2.7 and 3 s, respectively, yielding the total acquisition time of 8.5 min per spectrum. 1D CSSF–NOESY spectra (Robinson et al. 2004) were acquired with identical CSSF parameters as used for 1D TOCSY–CSSF spectra. A 200-ms mixing time was used and 64 scans were accumulated in each CSSF increment resulting in total acquisition time of 1 h per spectrum.

A sensitivity-enhanced multiplicity-edited echo–antiecho ^{1}H–^{13}C HSQC spectrum with adiabatic pulses (Bruker pulse program hsqcedetgpsisp2.3) was acquired with standard Bruker parameters. Relaxation time was 2 s, and acquisition times 160 and 25 ms in t_2 and t_1, respectively, were used. Eight scans were accumulated into each of 1024 complex points in t_1 resulting in the total acquisition time of 5 h. Identical parameters were used to acquire a 2D ^{1}H–^{13}C HSQC–TOCSY spectrum with a HH mixing time of 20 ms (Bruker pulse program hsqcdietgpsisp). A constant-time 2D HMBC experiment (Claridge & Perez-Victoria 2003; Cicero et al. 2001) with adiabatic pulses and two-stage low-pass *J*-filter (Bruker pulse program hmbcctetgpl2nd) was used for mapping the long-range proton–carbon correlations.

The spectrum was acquired with standard Bruker parameters. The low-pass filter was optimised for 140 and 160 Hz, the long-range correlation interval was set to 83 ms. Relaxation time was 1.5 s, and acquisition times 286 and 16 ms in t_2 and t_1, respectively, were used. 44 scans were accumulated into each of 768 complex points in t_1, resulting in the total acquisition time of 18 h.

3. RESULTS AND DISCUSSION

3.1. Identification of MXE/CXE gene in *Equisetum fluviatile*

3.1.1. MXE purification

MXE activity was discovered previously in crude extracts of *Equisetum* species (Fry *et al.*, 2008a) but the identity of the enzyme which catalyses MXE was not then determined. Identification of this enzyme is crucial to allowing elucidation of the structural features which confer on it its novel substrate specificity. The stratregy I used to identify MXE was purification and MS/MS analysis of the native MXE protein from *E. fluviatile* coupled with concomitant transcriptomic analysis of a late season *E. fluviatile* individual. Transcriptomic analysis was necessary owing to the adsence of a sequenced *Equisetum* genome. Late seaon *E. fluviatile* was used owing to the correlation of MXE activity prevalence with tissue age (Fry *et al.*, 2008a).

MXE was purified from a crude *E. fluviatile* extract by four sequential techniques: differential ammonium sulphate precipitation, SEC, lectin affinity-chromatography and isoelectric focusing (Table 2). Preliminary analyses had showed MXE to have an unusually low pI of ~ 4, indicating that isoelectric focusing is a particularly useful purification strategy. The resultant sample was analysed by SDS-PAGE showing a single predominant ~ 30 kDa coomassie blue-stained protein (Fig. 5).

Purification strategy	Protein (mg)	Total MXE activity (cpm)	Specific activity (cpm mg^{-1} protein)	Yield (%)	Purification
n/a (crude extract)	75.3	5685500	75505	100	1
$(NH_4)_2SO_4$ precipitation	20.0	3326063	166303	59	2
Biogel P100 SEC	2.4	1110259	462608	20	6
Lectin affinity chromatography	0.7	849348	1249041	15	16
Isoelectric focusing	0.1	572631	5205732	10	69

Table 2. Four step strategy for MXE purification MXE activity assayed by incubating reaction mixtures (10 µl containing 0.5% (w/v) BMLG and 50% (v/v) enzyme) at 25ºC for 4 h. Protein concentration was determined by use of the Bradford assay.

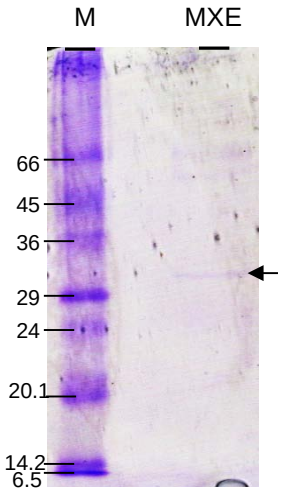

Fig. 5. SDS-PAGE gel analysis of purified MXE protein. Gel stained using Coomassie blue. M, marker ladder (sizes in kDa); MXE, purified MXE sample from rotofor. Arrow indicates putative MXE protein.

3.1.2. Mass spectrometric/transcriptomic identification of MXE

A coomassie blue-stained band was cut and subjected to in-gel trypsin digestion. Digestion fragments were analysed by MALDI-ToF (Fig. 6) and LC-MS (Fig. 7). Because there is currently no sequenced genome for an Equsietum species, the transcriptome of a late season *E. fluviatile* individual – chosen owing to the correlation of MXE activity with age – was sequenced by the use of 454 technology (Database statistics in materials and methods) and MS data was used to search the transcriptome for candidate genes. The two highest scoring putative partial gene products from the transcriptome database were partial gene sequences for XTH homologous proteins; collectively four fragmentation spectra matched predicted fragmentation spectra of in silico digestion products – three fragmentation spectra matched the putative partial gene product and one spectrum matched the second. Further, two of the ions identified as matching these genes (doubly charged m/z: 482.3 and 774.9; corresponding to expected Mr = 962.5 and 1547.8 respectively) are very similar to major ions identified in the MALDI spectrum (m/z: 964.5 and 1549.7; Fig. 6; MS/MS fragmentation spectra shown in Fig. 7). No candidate glycan-acting proteins were identified by searching public databases.

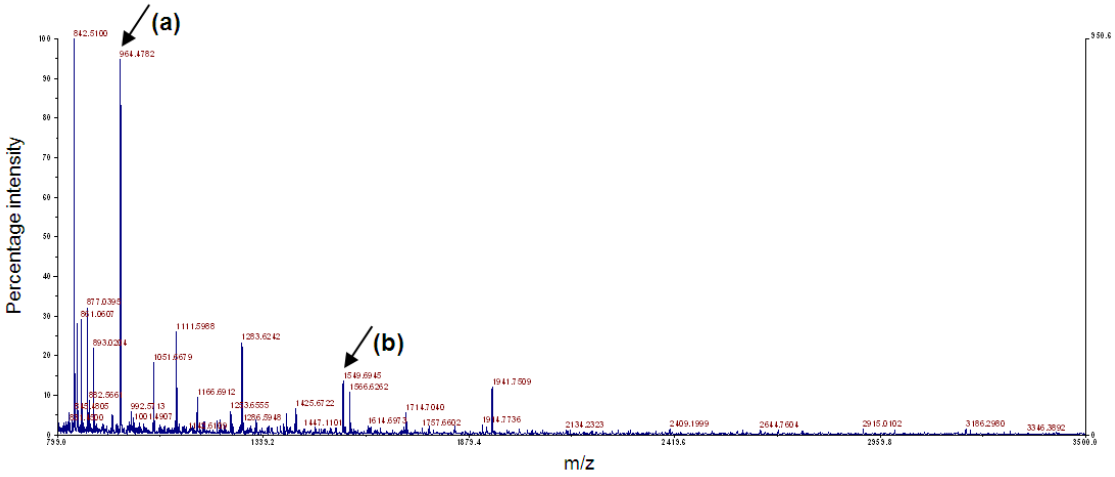

Fig. 6. MALDI-ToF spectrum of purified putative MXE The two ions with apparent masses matching those of LC-MS ions in Fig. 7 are indicated by arrows.

The full length sequence of the two candidate genes were identified by the use of 5' and 3' RACE from late season *E. fluviatile* cDNA, results showed that these were two parts of the same full-length gene. Having identified the gene, new primers were designed to enable the amplification of the DNA coding for the putative mature protein (i.e. total protein without signal peptide) by use of high fidelity RT-PCR and incorporation of EcoRI and XbaI restriction site upstream and downstream respectively. Following cloning of PCR products, genes A, C, F and G were identified as distinct MXE candidates. The consensus sequence of these genes was created by site-directed mutagenesis of G (Fig. 8); *E. fluviatile* transcriptome analysis provided no evidence that mutations which distinguish A, C, F and G from the consensus are real.

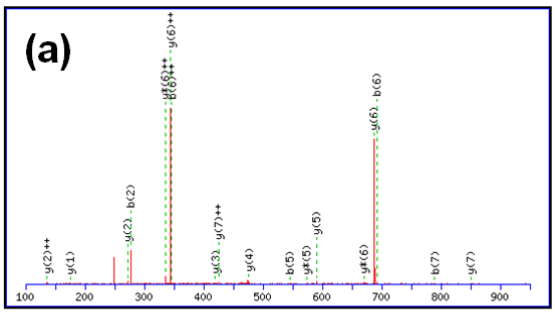

Monoisotopic mass of neutral peptide Mr(calc): 962.4974
Fixed modifications: Carbamidomethyl (C)
Ions Score: 45 Expect: 0.011
Matches (Bold Red): 18/50 fragment ions using 44 most intense peaks

#	b	b^{++}	b^*	b^{*++}	Seq.	y	y^{++}	y^*	y^{*++}	#
1	114.0913	57.5493			L					8
2	**277.1547**	139.0810			Y	**850.4206**	**425.7139**	833.3941	417.2007	7
3	374.2074	187.6074			P	***687.3573***	***344.1823***	***670.3307***	***335.6690***	6
4	488.2504	244.6288	471.2238	236.1155	N	**590.3045**	295.6559	***573.2780***	287.1426	5
5	**545.2718**	273.1396	528.2453	264.6263	G	**476.2616**	238.6344	459.2350	230.1212	4
6	***692.3402***	***346.6738***	675.3137	338.1605	F	**419.2401**	210.1237	402.2136	201.6104	3
7	**789.3930**	395.2001	772.3665	386.6869	P	**272.1717**	**136.5895**	255.1452	128.0762	2
8					R	**175.1190**	88.0631	158.0924	79.5498	1

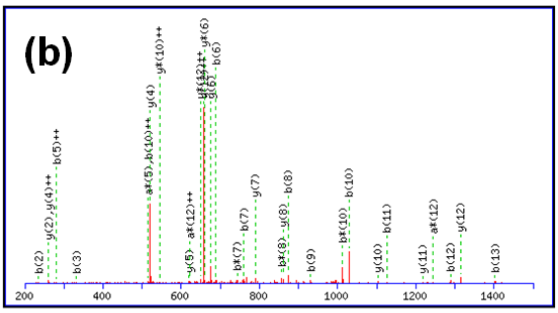

Monoisotopic mass of neutral peptide Mr(calc): 1547.7984
Ions Score: 55 **Expect:** 0.0012
Matches (Bold Red): 32/144 fragment ions using 60 most intense peaks

#	a	a^{++}	a^*	a^{*++}	b	b^{++}	b^*	b^{*++}	Seq.	y	y^{++}	y^*	y^{*++}	#
1	60.0444	30.5258			88.0393	44.5233			S					14
2	207.1128	104.0600			**235.1077**	118.0575			F	1461.7736	731.3905	1444.7471	722.8772	13
3	304.1656	152.5864			**332.1605**	166.5839			P	**1314.7052**	**657.8563**	1297.6787	**649.3430**	12
4	418.2085	209.6079	401.1819	201.0946	446.2034	223.6053	429.1769	215.0921	N	**1217.6525**	609.3299	1200.6259	600.8166	11
5	532.2514	266.6293	**515.2249**	258.1161	560.2463	**280.6268**	543.2198	272.1135	N	**1103.6095**	552.3084	1086.5830	**543.7951**	10
6	661.2940	331.1506	644.2675	322.6374	**689.2889**	345.1481	672.2624	336.6348	E	989.5666	495.2869	972.5401	486.7737	9
7	732.3311	366.6692	715.3046	358.1559	**760.3260**	380.6667	**743.2995**	372.1534	A	**860.5240**	430.7656	843.4975	422.2524	8
8	845.4152	423.2112	828.3886	414.6980	**873.4101**	437.2087	**856.3836**	428.6954	I	**789.4869**	395.2471	772.4604	386.7338	7
9	902.4367	451.7220	885.4101	443.2087	**930.4316**	465.7194	913.4050	457.2061	G	**676.4028**	338.7051	**659.3763**	330.1918	6
10	1001.5051	501.2562	984.4785	492.7429	**1029.5000**	**515.2536**	**1012.4734**	506.7404	V	**619.3814**	310.1943	602.3548	301.6811	5
11	1098.5578	549.7826	1081.5313	541.2693	**1126.5527**	563.7800	1109.5262	555.2667	P	**520.3130**	**260.6601**	503.2864	252.1468	4
12	1261.6212	631.3142	**1244.5946**	**622.8009**	**1289.6161**	645.3117	1272.5895	636.7984	Y	423.2602	212.1337	406.2336	203.6205	3
13	1374.7052	687.8563	1357.6787	679.3430	**1402.7001**	701.8537	1385.6736	693.3404	L	**260.1969**	130.6021	243.1703	122.0888	2
14									K	147.1128	74.0600	130.0863	65.5468	1

Fig. 7. Two LC-MS spectra and putative amino acid sequences Two (of the four in total) example LC-MS spectra produced by analysis of trypic digest fragments of the putative MXE protein. Each identified a different partial XTH homolog gene. The putative peptides that they encode are shown below each spectrum, positive ion fragment m/z values are highlighted in red. Spectrum and sequence (a) is shown in green, and spectrum and sequence (b) in blue, within the putative mature protein in Fig. 9.

```
A   GFYGDFQVEPVPDHVIIQSDSLLQLTMDKDSGGSVVSKSNYLFGYFNMKMKLISGNSAGT 60
C   GFYGDFQVEPVPDHVIIQSDSLLQLTMDKNSGGSVVSKSNYLFGYFNMKMKLISGNSAGT 60
F   GFYGDFQVEPVPDHVIIQSDSLLQLTMDKNSGGSVVSKSNYLFGYFNMKMKLISGNSAGT 60
G   GFYGDFQVEPVPDHVIIQSDSLLQLTMDKNSGGSVVSKSNYLFGYFNMKMKLISGNSAGT 60
Con GFYGDFQVEPVPDHVIIQSDSLLQLTMDKNSGGSVVSKSNYLFGYFNMKMKLISGNSAGT
    ****************************:******************************

A   VTTFYIFSDEANHDEIDFEFLGNYSGDPYLLHTNIFASGVGNREQQFFLWFDPTADFHDY 120
C   VTTFYIFSDEANHDEIDFEFLGDYSGDPYLLHTNIFASGVGNREQQSFLWFDPTADFHDY 120
F   VATFYIFSDEANHDEIDFEFLGNYSGDPYLLHTNIFASGVGNREQQFFLWFDPTADFHDY 120
G   VTTFYIFSDEANHDEIDFEFLGNYSGDPYLLHTNIFASGVGNREQQFFLWFDPTADFHDY 120
Con VTTFYIFSDEANHDEIDFEFLGNYSGDPYLLHTNIFASGVGNREQQFFLWFDPTADFHDY 120
    *:*******************:********************** ************

A   TIIWNPQQILFLVDGRAVRSFPNNEAIGVPYLKSQWMNVHLSLWNGETWATLGGLRRIDW 180
C   TIIWNPQQILFLVDGRAVRSFPNNEAIGVPYLKSQWMNVHLSLWNGETWATLGGLRRIDW 180
F   TIIWNPQQILFLVDGRAVRSFPNNEAIGVPYLKSQWMNVHLSLWNGETWATLGGLRRIDW 180
G   TIIWNPQQILFLVDGRAVRSFPNNEAIGVPYLKSQWMNVHLSLWNGETWATLGGLRRIDW 180
Con TIIWNPQQILFLVDGRAVRSFPNNEAIGVPYLKSQWMNVHLSLWNGETWATLGGLRRIDW 180
    ************************************************************

A   NSAPFVASYSTFVGDSCFDSADSPCMAPKWWNQAAYQSLSTSDAGSIQWVRENYLKYDYC 240
C   NSAPFVASYSTFVGDSCFDSADSPCMASKWWNQAAYQSLSTSDASSIQWVRENYLKYDYC 240
F   NSAPFVASYSTFVGDSCFDSADSPCMASKWWNQAAYQSLSTSDASSIQWVRENYLKYDYC 240
G   NSAPFVASYSTFVGDSCFDSADSPCTASKWWNQAAYQSLSTSDASSIQWVRENYLKYDYC 240
Con NSAPFVASYSTFVGDSCFDSADSPCMASKWWNQAAYQSLSTSDASSIQWVRENYLKYDYC 240
    ************************ *.****************.***************

A   YDTKLYPNGFPRECSNRGF 259
C   YDTKLYPNGFPRECSNRGF 259
F   YDTKLYPNGFPRECSNRGF 259
G   YDTKLYPNGFPRECSNRGF 259
Con YDTKLYPNGFPRECSNRGF 259
    ******************
```

Fig. 8. ClustalW alignment of the four isoforms of the putative mature MXE proteins Sequences A, C, F and G were directly amplified from *E. fluviatile* cDNA. The consensus sequence was created by site-directed mutagenesis of G. These sequences were inserted into *P. pastoris* for recombinant expression. The four peptide fragments identified from MS/MS data are highlighted in blue, red, green and by underlining.

3.1.3. Transient expression of MXE candidate

All five candidate genes were inserted into the pPICZαA pichia expression vector and the resultant vector was used to transform *P. pastoris* (SMD1168H) from which expression was induced. A high expressing line was identified by MXE reaction analysis of crude cell medium. A large batch of cell medium from this line was subjected to Nickel affinity chromatography (IMAC) and assayed for MXE and XET activity (Fig. 9). The ratio of MXE : XET (~3) is typical of that observed for the endogenous purified MXE protein (Fig. 17; Fig. 32) and distinguishes MXE from other XTHs which typically have a ratio of far less (<<0.1; e.g. Hrmova *et al.* 2007).

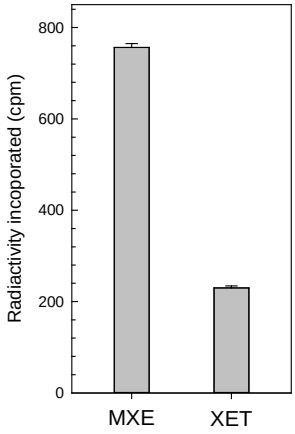

Fig. 9. MXE and XET activity in *P. pastoris* recombinantly-expressed enzyme A *P. pastoris* culture was transformed with pPICZaA vector containing the consensus putative MXE gene (Fig. 8). Following induction of gene expression, the cell medium was purified by IMAC. Reaction mixtures (13.3 µl) containing 0.75% (w/v) BMLG or tamarind xyloglucan and 25% (v/v) purified enzyme were incubated for 6 h at 25ºC. Data are the average of three reactions ± standard error.

3.1.4. Phylogenetic relationship between MXE and other, functionally related, GH16 enzymes

Homology comparison of MXE and other members of the GH16b subfamily, including three bacterial lichenases and all A. thaliana XTHs showed MXE to be a member of the XTH subfamily Group I/II (Fig. 10). This group is known otherwise to be composed of ‘standard’ XTHs and contains no enzymes with significant XEH activity (Rose et al., 2002). There is nothing from the phylogenetic tree here which suggests that MXE is in any way an unusual XTH subfamily member.

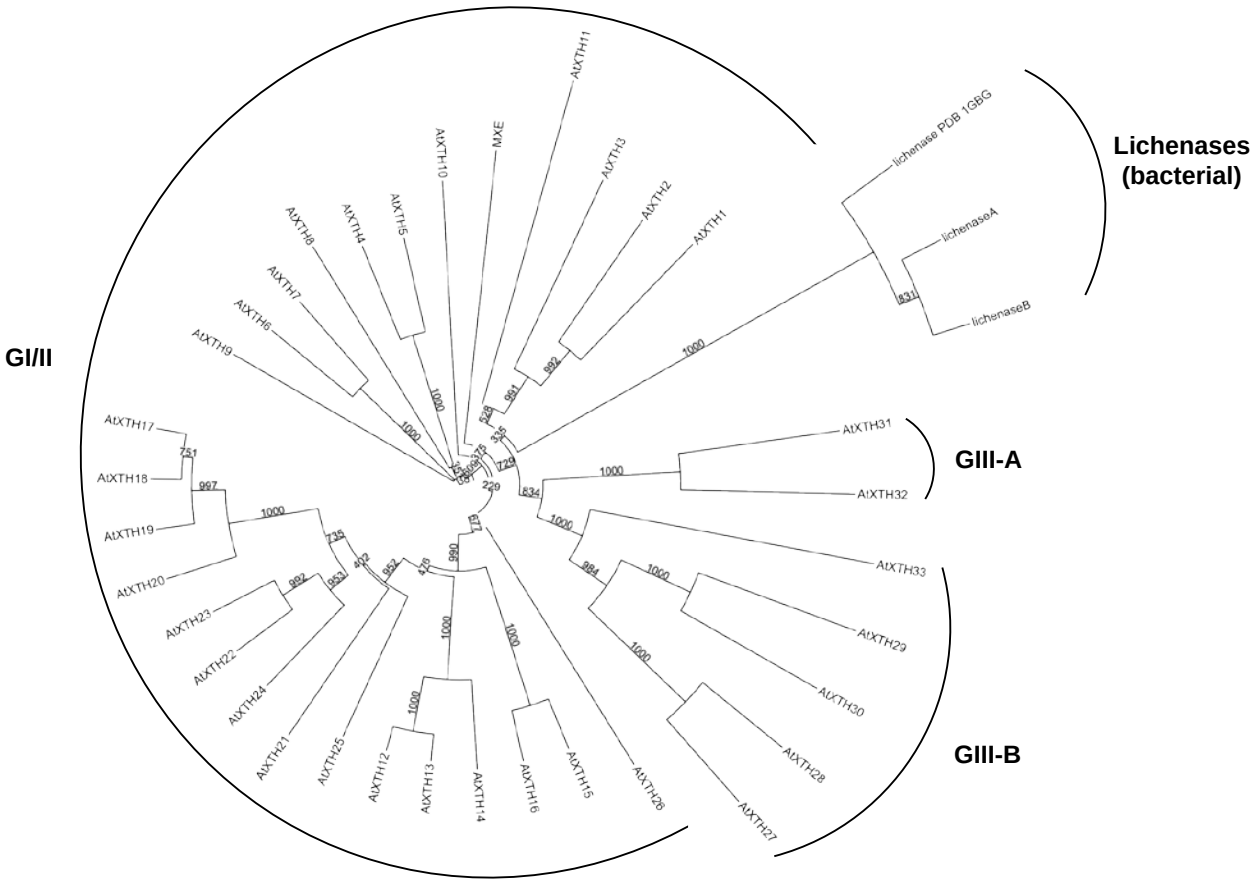

Fig. 10. Rooted cladogram showing relationship between MXE and other GH16b subfamily members Sequences aligned by use of ClustalW (http://www.bioinformatics.nl/tools/clustalw.html) with the Gonnet weight series. Bootstrap values (created using 1000 replicates) are displayed. Cladogram created using interactive tree of life (http://itol.embl.de). Clading annotation (XTH groupings I/II, III-A and III-B) according to Eklöf *et al.* (2013).

3.2. MXE substrate specificity

Elucidation of enzyme substrate specificities can hugely improve our understanding of how protein structure affect enzyme : carbohydrate interactions. This is particularly pertinent to the study of MXE, due to its already known unique substrate preferences. While the substrate specificity of MXE has been probed to some extent (Fry *et al.* 2008a), there remains much scope for further analyses. For example, it is highly likely that MXE exhibits a preference for the type of substrate native to *Equisetum*. Given that *Equisetum* MLG and xyloglucan are unique/highly unusual structures (see 1.3.1. and 1.3.2. for descriptions) these substrates were purified from *Equisetum* in order to enable deeper probing of MXE's substrate specificities.

3.2.1. Preparation of authentic *E. arvense* MXE substrates

MLG and XGOs were purified from *E. arvense* lateral shoots and the purity of the *Equisetum arvense* MLG (*Ea*MLG) sample was assessed by four hydrolytic methods: TFA, driselase, XEG and lichenase. These showed that the sample was a fraction of soluble polysaccharide material rich in *Ea*MLG with no detectable contaminating polysaccharides (Fig. 11). The sample was stored at −20°C in an aqueous solution and thoroughly boiled before further use. To demonstrate the structural distinction between MLG and xyloglucan from *E. arvense* and those from other species, three different MLGs (*E. arvense*, barley and Iceland moss) and tamarind xyloglucan was subjected to enzymic hydrolyses. These, as well as the purified *Ea*XGOs, were compared by TLC (Fig. 12). Consistent with previous reports (Fry *et al.*, 2008b) there is a decreasing tetramer content moving from *Equisetum* to barley to Iceland moss MLGs. *Ea*MLG is shown to be constructed predominantly from tetramer units, barley MLG has a slight predominance of trimer over tetramer, these two being its main constituent subunits. Finally, Iceland moss MLG is composed largely of trimer also, but has significantly more pentamer than tetramer. In addition, a band which did not match to any of the standard MLGOs was prevalent in *Ea*MLG (see 3.6.). The pattern of XGOs produced by XEG digestion of *Equisetum* xyloglucan is shown to be distinct from that of tamarind xyloglucan; this again is consistent with previous reports (Peña *et al.*, 2008). *Ea*XGOs were reductively tritiated producing [^{3}H]XGO-ols and, after purification by preparative

paper chromatography were shown on preparative TLC to contain 6 distinct bands who migrated in comparison to [^{3}H]XXXGol with what would be expected of *Equisetum* [^{3}H]XGO-ols. Each was eluted from TLC and quantified by scintillation counting and tested for purity by TLC fluorography (Fig. 13). Results (Fig. 14) suggest a high degree of purity, though because this TLC analysis was performed using the same solvent as the purification it is unable to assess the purity of co-migrating [^{3}H]*Ea*XGO-ols.

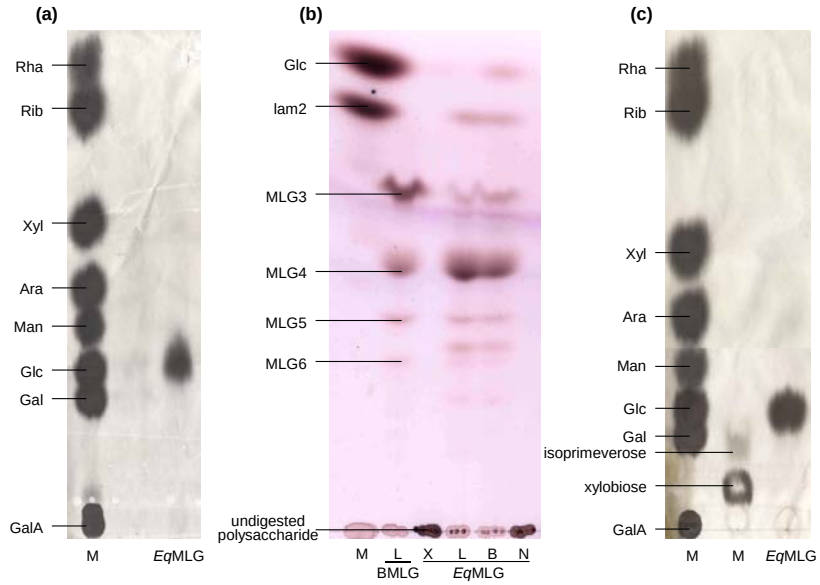

Fig. 11. Demonstration of purity of *Ea*MLG fraction TFA (a) and driselase (c) (both analysed by paper chromatography) and XEG and lichenase (b) (analysed by TLC) hydrolyses. M, marker mix; X, XEG; L, lichenase; B, XEG and lichenase sequentially; N, no enzyme; BMLG, barley MLG.

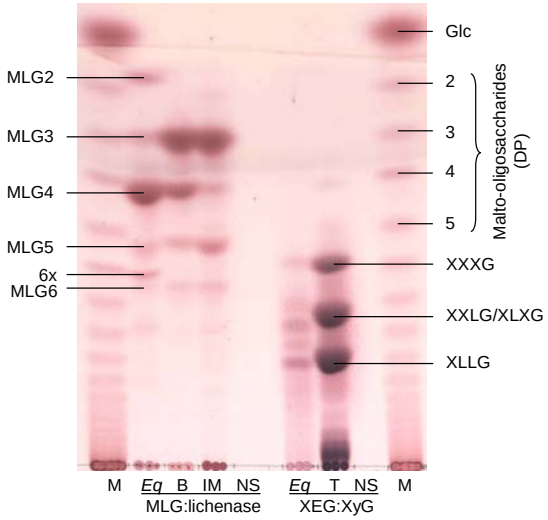

Fig. 12. Comparison of three MLGs and two xyloglucans TLC analysis of the subunit composition of three different types of MLG (post lichenase digestion; left) and two different types of xyloglucan (post XEG digestion; right). M, maltose oligosaccharide markers; polysaccharide substrate sources: *Ea*, *E. arvense*; B, barley; IM, Iceland moss; T, tamarind; NS, no substrate; xyloglucan nomenclature scheme described by Fry *et al.* (1993).

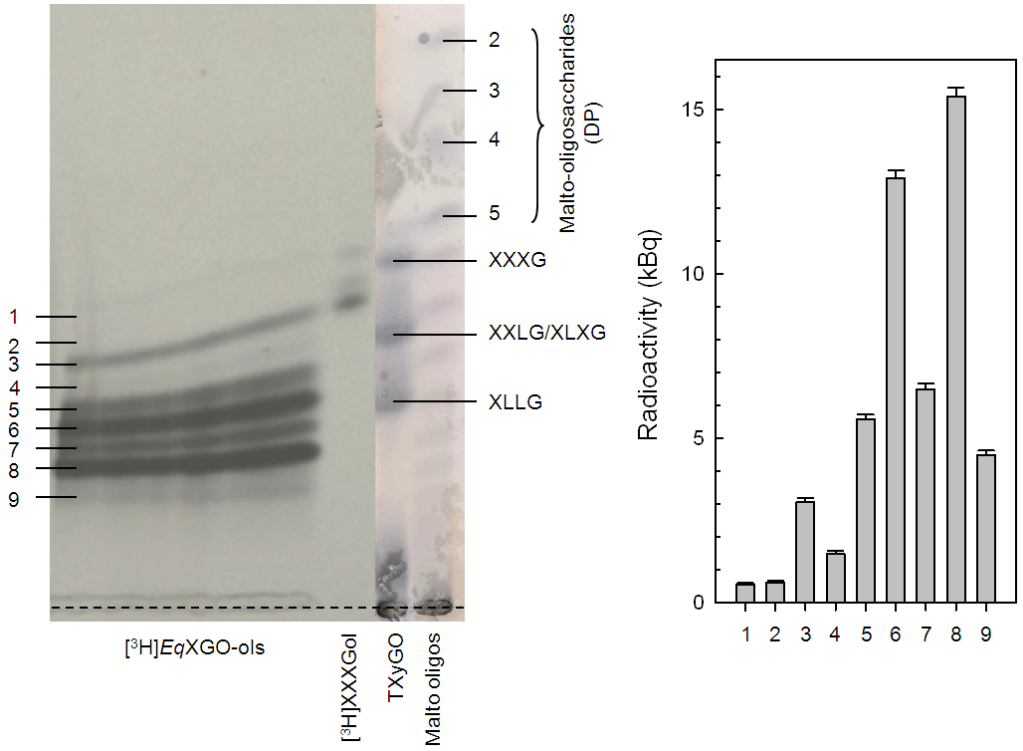

Fig. 13. [^{3}H]*Ea*XGO-ol preparative TLC-purification (a) Nine (1–9) [^{3}H]-labelled oligosaccharitol fractions resolved from each other during TLC and were detected by fluorography. Cold XGO and malto-oligosaccharide markers were thymol-stained. XGO, tamarind xyloglucan digestion products. (b) Amount of radioactivity eluted in each fraction.

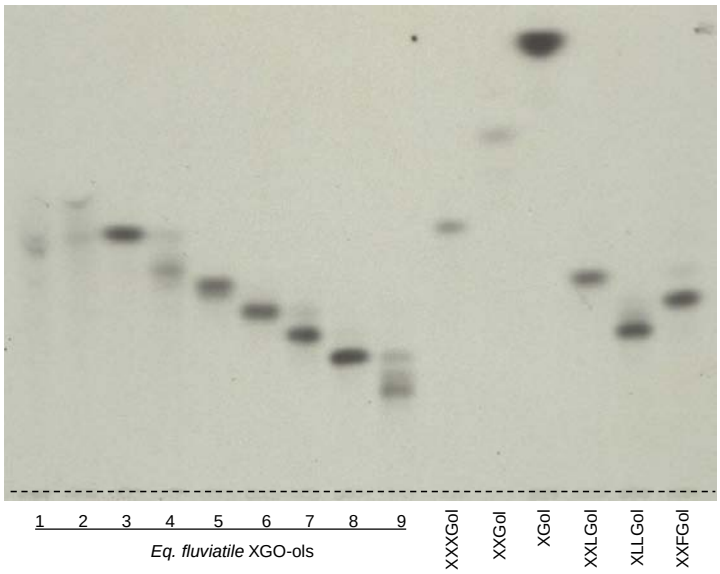

Fig. 14. Purity of [^{3}H]*Ea*XGO-ols Nine [^{3}H]*Ea*XGO-ols and six other structurally characterised [^{3}H]XGO-ols were resolved by TLC (BAW; four ascents) and detected by fluorography.

3.2.2. Preparation of non-native MXE substrate candidates

In order to thoroughly probe the substrate specificity of the MXE enzyme, other [^{3}H]-labelled oligosaccharides were produced. [^{3}H]GXXGol was created by α-xylosidase digestion of [^{3}H]XXXGol followed by preparative paper chromatography purification. [^{3}H]GGXXXGol was created by sequential MXE:lichenase treatments (see 3.3.1.). To test the purity of these candidate substrates, all resolved by TLC and detected by fluorography and thymol-staining (Fig. 15). Most oligosaccharitol samples were largely if not completely radiochemically pure. All [^{3}H]MLGO-ol samples were, as expected, composed of multiple bands. A minor amount of thymol-stainable material was present in some samples, indicating either chemical impurity or low specific activity. At the time of writing, these purified ^{3}H-labelled oligosaccharitols had yet to be tested as substrates.

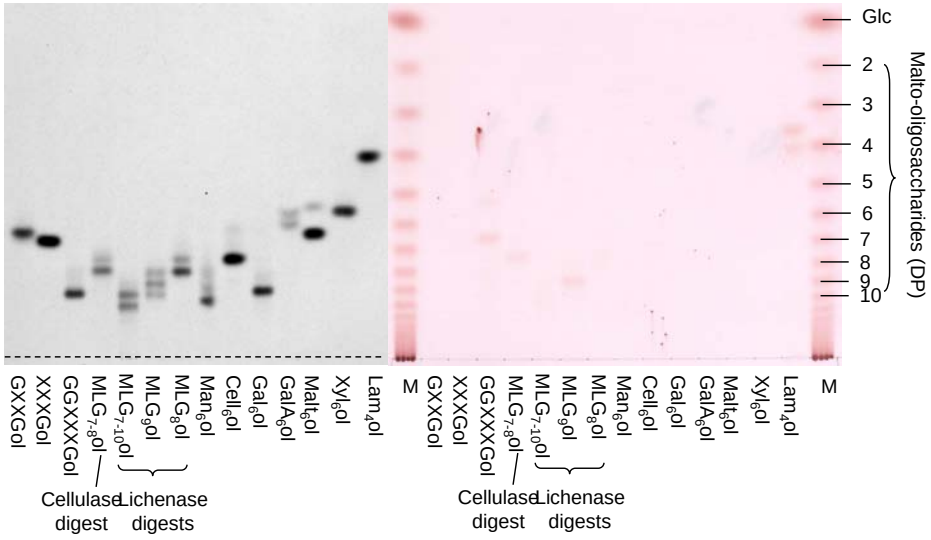

Fig. 15. Purity of other ^{3}H-labelled oligosaccharitols Moieties in solutions containing 0.5 kBq of 13 ^{3}H-labelled oligosaccharitols were resolved by TLC and detected by fluorography (a) and thymol staining (b).

3.2.3. MXE donor substrate specificity analysis

Purified *E. arvense* MLG as well as the commercial barley and Iceland moss MLGs were used to probe the donor substrate specificity of MXE from an *E. fluviatile* crude enzyme extract. With regard to maximum reaction rate, *E. arvense* MLG is clearly a far better substrate that BMLG, which was in turn far better than IMMLG. Because of the variation in tetramer content between the three MLGs (IMMLG<BMLG<*Ea*MLG), this observation is consistent with the hypothesis of Fry *et al.* (2008a) that the tetrameric MLG subunit is the target structure for MXE, although Fry *et al.* (2008a) actually reported no activity against IMMLG. The affinity of MXE for BMLG (K_m 3.1–3.4 mg ml^{-1}) is consistent with the measurement of Fry *et. al.* (2008a), and the higher affinity (K_m 2.0 mg ml^{-1}) for *Ea*MLG is again supportive of the hypothesis that the tetrameric MLG subunit is the target structure for MXE. However, the higher still affinity of MXE for IMMLG (Km 1.4 mg ml^{-1}), which has the lowest tetramer content of all three, suggests this understanding of the target structure of MXE may be too simplistic. It is possible that the low solubility of IMMLG limited the reaction rates at high substrate concentrations. The result of this would be artificially low V_{max} and K_m values. Nonetheless, because the V_{max} when IMMLG is used as the donor is so low (2.4 Bq h^{-1}, compared to 14.0 and 19.2 for

BMLG and *Ea*MLG respectively) increasing tetrameric content appears to play a positive role on MXE activity.

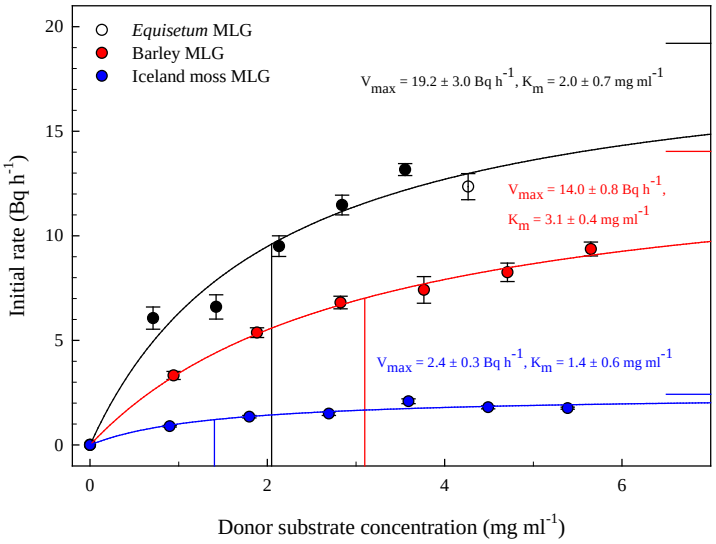

Fig. 16. Reaction profiles and enzymological constants of MXE using three structurally distinct donor substrates Duplicate reaction mixtures (12 µl) containing 25% (v/v) *E. fluviatile* crude enzyme extract, 0.52 µM (0.5 kBq) [^{3}H]XXXGol and 0–5.6 mg ml^{-1} MLG (*E. arvense*, barely or Iceland moss) were incubated at room temperature for 0 (acid added before enzyme), 1, 2 and 4 hours. Thus data points are calculated from 8 readings ± standard error. Horizontal lines at far right, V_{max} values; vertical lines from bottom, K_m values.

3.2.4. MXE acceptor substrate specificity analysis

3.2.4.1. Equisetum MXE and XET acceptor substrate specificity toward [^{3}H]*Ea*XGO-ols

In order to assess the acceptor substrate specificity of MXE toward *Equisetum*-derived XGOs and to compare this specificity to that of XTHs from *Equisetum*, preparations of *Equisetum* MXE and XTHs needed to be created. An *E. fluviatile* crude enzyme extract was subjected to fractionation by isoelectric focusing using pH 3–5 ampholytes and fractions were assayed for MXE and XET activities in addition to measuring the pH (Fig. 17). As shown previously, MXE activity was found in fractions around pH 4 while XET activity cofractionated with MXE in fractions around pH 4 but was also found alone in neutral pH fractions (enzyme fraction C). However, during this fractionation experiment two distinct MXE- (and XET-)

containing peaks resolved, one peaked at ~pH 3.7 (fraction A), the other at pH 4.2 (fraction B); I was unable to repeat the resolution of MXE activity (peaks A and B) in later experiments. Purified [^{3}H]*Ea*XGO-ols were used to probe MXE acceptor substrate specificities of fractions A and B as well as the XET acceptor substrate specificities of fractions A, B and C (Fig. 18). The acceptor substrate specificities exhibited toward [^{3}H]*Ea*XGO-ols by fractions A and B were almost identical and so results are shown cumulatively as fraction AB. MXE and XET activities have distinct patterns of substrate preference for different XGO-ols. MXE-containing fractions AB exhibited a distinct preference for those [^{3}H]*Ea*XGO-ols which migrated faster on TLC with decreasing preference to those with lower mobility. In contrast, with the exception of [^{3}H]*Ea*XGO-ol 9, fraction C, which contained XET activity alone, favoured oligosaccharides which migrated less on TLC, preferring [^{3}H]*Ea*XGO-ol 8 above all. Similar patterns were observed for the stock [^{3}H]XGO-ols where, but for [^{3}H]XXFGol, fraction C's activity was highest on the substrates which migrated slowest on TLC. Fractions A/B didn't favour these. Based on the observations of Fry *et al.* (2008a) and the presumed identity of [^{3}H]EaXGO-ol 3 as [^{3}H]XXXGol, fraction A/B was expected to be more active when using [^{3}H]XXXGol relative to others. The apparent low activity was the product of the use of a low specific activity sample of [^{3}H]XXXGol. Interestingly the acceptor substrate specificity of fractions AB varied depending on whether MLG or xyloglucan was used as the donor substrate. For example, fraction AB's preference for [^{3}H]*Ea*XGO-ol 8 doubled when xyloglucan was used as the donor. This presumably indicates that the conformation of the acceptor binding portion of MXE's active site is sensitive to the type of polysaccharide bound to MXE during the intermediate step of the two-step transglycosylase reaction.

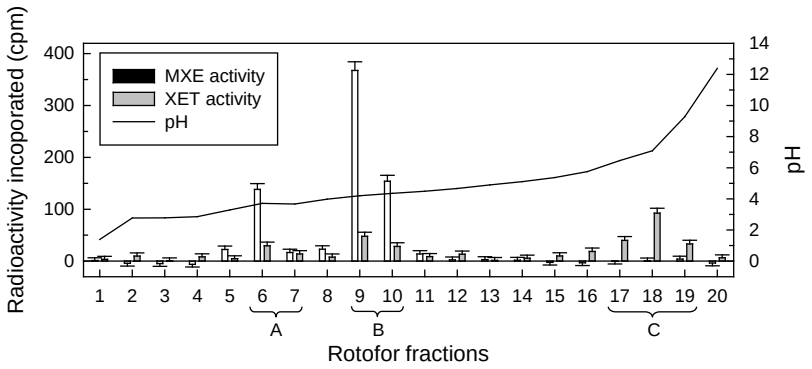

Fig. 17. Isoelectric fractionation of MXE- and XET- active enzymes from an *E. fluviatile* crude enzyme extract Reaction mixtures (12 µl) containing 17% (v/v) rotofor fraction, 0.78 µM (0.75 kBq) [^{3}H]XXXGol and 6.7 mg ml^{-1} BMLG or TXG were incubated at room temperature for 3.5 hours. Data are corrected counts from single measurements ± counting error.

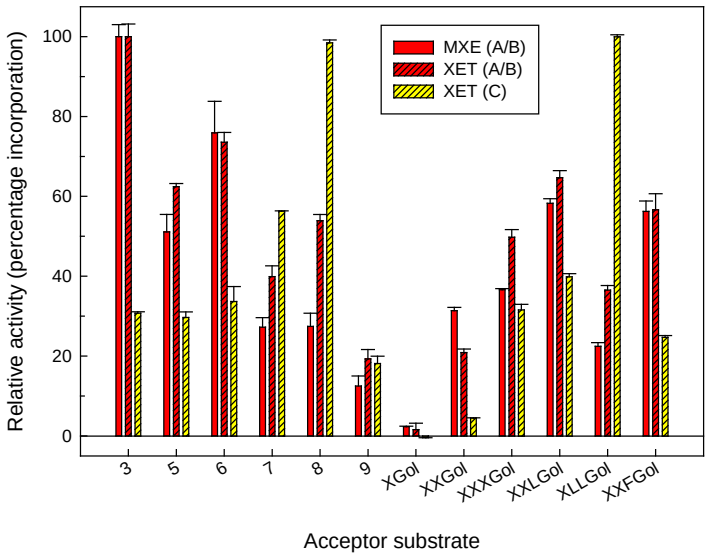

Fig. 18. Relative rate of reaction for MXE activity and for XET activity from two sources Results shown are calculated from the average of triplicate measurements ± standard deviation. 0.1 kBq [^{3}H]*Ea*XGO-ols, 0.4 kBq other [^{3}H]XGO-ols or 'no acceptor' controls were dried *in vacuo*. [^{3}H]*Ea*XGO-ols were redissolved in 32 µl 0.75% (w/v) BMLG 50% (v/v) enzyme solution. [^{3}H]XGO-ols and 'no acceptor' controls were redissolved in 6 µl 0.2% (w/v) TXG, 50% (v/v) enzyme solution. Reaction mixtures were incubated at 25ºC for 4 hours. Fraction A/B is the cumulative of the results yielded from enzymes fractions A and b in Fig. 17; Acceptor substrate 3–9 are *Equisetum* [^{3}H]XGO-ols as labelled in Fig. 13 and 14.

3.3. Identification of the nature and location of the bonds broken and formed during the MXE reaction.

A better understanding of MXE's site of attack of its substrates would further our understanding of its mode of recognition of its substrates and would allow further comparison of MXE with related enzymes (e.g. lichenases and XTHs) for with these details are understood. I sought here to investigate MXE's site of attack. Site of attack was construed here both locally (the position of the cleavage site relative to the (1→3)(1→4) bond pattern) and globally (the position of the cleavage suite relative to the termini). Both provide interesting insights into the enzymology of MXE and may prove crucial to indentifying its role *in vivo*.

3.3.1. Identification of the local site of MLG cleavage during MXE activity

MXE's site of attack on MLG, like that of other MLG-cleaving enzymes (lichenase, Planas, 2000; cellulase, Grishutin *et al.*, 2006), is likely to be sensitive to the local position of β-(1→3) bonds. However, MXE cannot be as specific to β-(1→3) bonds as lichenase is; because MXE can catalyse XET activity, it is evidently capable of accommodating β-(1→4) bonds between all subsites, lichenase, in contrast, will never cleave a β-(1→4)-D-glucan.

Because the site of attack of lichenase on MLG is known (Planas, 2000), lichenase digestion of the MXE product should yield a radioactive product whose structure is diagnostic of the site of attack of MXE on MLG. To investigate MXE's site of attack using this strategy, the MXE reaction product (created using [^{3}H]XXXGol as the acceptor substrate and washed free of unincorporated acceptor) was subjected to lichenase digestion, before a single 75% (v/v) ethanol-soluble ^{3}H-labelled product, which migrated behind [^{3}H]XXXGol, was purified by preparative TLC. Graded β-D-glucosidase treatment (Fig. 19) showed this radioactive moiety broke down via a single intermediate to [^{3}H]XXXGol. This indicates that the radioactive moiety is composed of [^{3}H]XXXGol with two β-D-Glc residues attached, most probably attached consecutively. As the exact manner in which these residues are bound was at this point still unknown, the nonasaccharide was termed [^{3}H](Glc)$_2$·XXXGol,

where '·' is an unknown bond(s) linking the two Glc residues to any residue in [^{3}H]XXXGol.

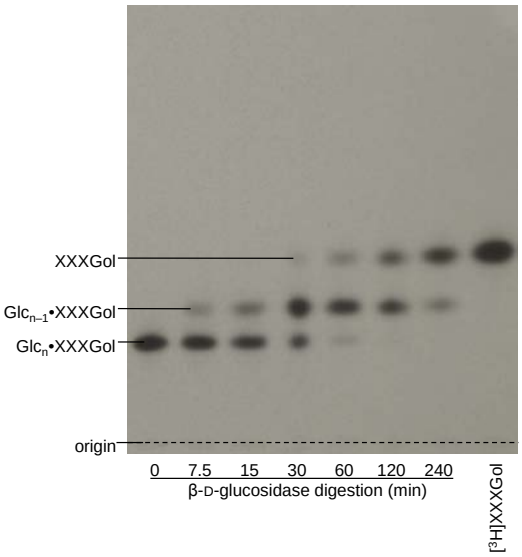

Fig. 19. Determination of glucosyl tail length in [^{3}H](Glc)$_n$·XXXGol Graded digestion of [^{3}H]Glc$_2$·XXXGol by β-D-glucosidase via a single intermediate to [^{3}H]XXXGol. Products resolved by TLC (BAW, 2 ascents) and detected by fluorography. [^{3}H]Glc$_2$·XXXGol created by incubating 0.5 μM (60 kBq) [^{3}H]XXXGol, 0.4% (w/v) BMLG, 33% (v/v) *E. fluviatile* crude extract at room temperature for 17 h, before precipitating with 75% (v/v) ethanol and washing free of unincorporated [^{3}H]XXXGol. The pellet was then redissolved and digested with lichenase and products purified by preparative TLC.

To identify the nature of the unknown bond(s), [^{3}H](Glc)$_2$·XXXGol was digested with three β-(1→4)-D-glucan endohydrolases: cellobiohydrolase and two cellulases, one capable (cell*b*) and one incapable (cell*a*) of digesting xyloglucan (Fig. 20). Both cellobiohydrolase and cell*b* were able to digest [^{3}H](Glc)$_2$·XXXGol to [^{3}H]XXXGol. Graded digestion of [^{3}H](Glc)$_2$·XXXGol with cell*b* showed breakdown of [^{3}H](Glc)$_2$·XXXGol to [^{3}H]XXXGol occurred without intermediate, confirming that the two Glc residues are removed, and thus linked, together (Fig. not shown). Because of the known substrate specificity of the three enzymes capable of degrading [^{3}H](Glc)$_2$·XXXGol to [^{3}H]XXXGol, the most fitting structure of [^{3}H](Glc)$_2$·XXXGol is:

D-Xyl-α D-Xyl-α D-Xyl-α
A **B** (1→6) (1→6) (1→6)
D-Glc-β-(1→4)-D-Glc-β-(1→4)-D-Glc-β-(1→4)-D-Glc-β-(1→4)-D-Glc-β-(1→4)-D-Glcol

hence [^{3}H]GGXXXGol. To test the hypothesised nature of the bond labelled **A**, a cell*b* digest of $(Glc)_2$·XXXGol was spiked with disaccharides and analysed by HPAEC. Spiking allowed unambiguous distinction between cellobiose and gentiobiose, indicating $(Glc)_2$·XXXGol broke down to XXXGol and cellobiose (Fig. 21). This confirmed that the bond marked **A** is indeed a β-(1→4)-bond; thus [^{3}H]$(Glc)_2$·XXXGol could be termed [^{3}H]GG·XXXGol. For this product to be yielded from sequential MXE : lichenase treatments, MXE must have cleaved its donor MLG substrate three bonds following (in reducing terminal direction from) a β-(1→3) bond and, as such, the β-(1→3) bond must have linked the residues occupying subsites -4 and -3 of MXE's active site (Fig. 22).

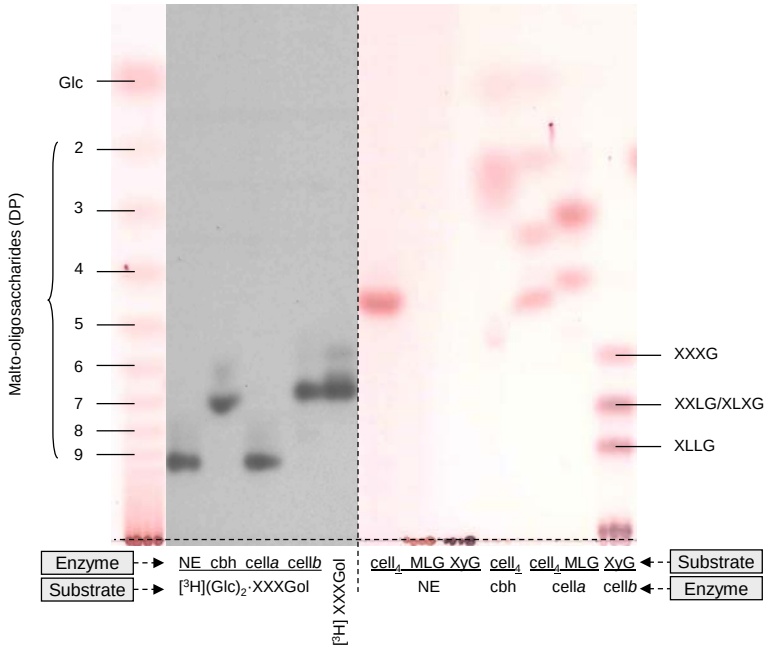

Fig. 20. Endo-cleavage of glucosyl tail from [^{3}H]$(Glc)_2$·XXXGol by the use of three β-(1→4)-D-glucan endohydrolases Endohydrolase products resolved by TLC (BAW, two ascents) and detected by fluorography and thymol staining. Abbreviations used: NE, no enzyme; cbh, a cellobiohydrolase (from *T. longibrachiatum)*; cell*a*, a cellulase incapable of digesting xyloglucan (from *A. niger*); cell*b*, a cellulase capable of digesting xyloglucan (from *T.*

longibrachiatum); $cell_4$, cellotetraose; MLG, mixed-linkage glucan; XyG, tamarind xyloglucan.

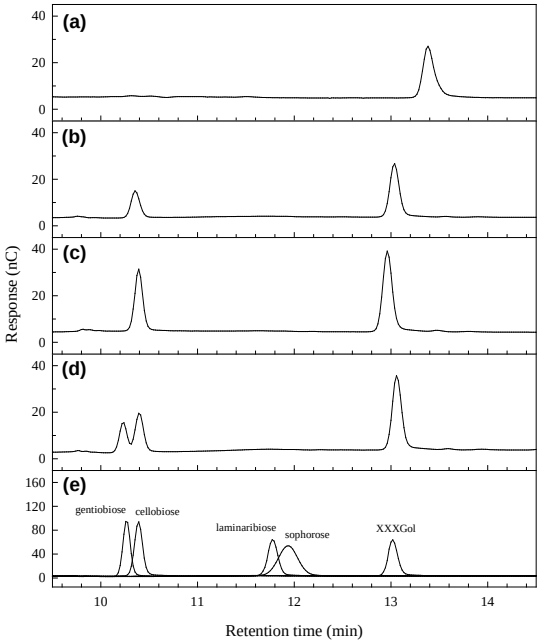

Fig. 21. HPAEC analysis of products of cell*b* digestion of $[^3H](Glc)_2$·XXXGol $[^3H](Glc)_2$·XXXGol was analysed alone (a), following cell*b* treatment (b) and following cell*b* treatment with cellobiose (c) and gentiobose (d). Five markers were also separately applied (e). Large batch MXE product was created by incubating 1.5% (w/v) BMLG, 0.25% (w/v) chlorobutanol, 50% (v/v) *E. fluviatile* crude extract, 100 µg (2 kBq) XXXGol in 7.5 ml for 6 days at 25°C with constant agitation. There was 63.5% incorporation of radioactivity into 75% (v/v) ethanol-insoluble material. After lichenase digestion of this pellet, 75% (v/v) ethanol-soluble lichenase products were purified by SEC (Biogel P-2 column 3), preparative TLC and preparative HPLC.

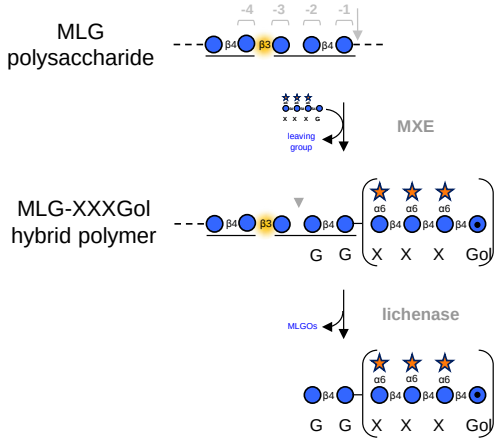

Fig. 22. Identification of the bond initially cleaved by MXE activity
Identification of the bond cleaved by MXE given that sequential MXE:lichenase treatments yield [^{3}H]GG·XXXGol. Numbers and braces in grey indicate MXE subsite occupant identities required for MXE cleavage at the specific point; arrows indicate site of cleavage.

However, it was unclear at this point whether this apparent specificity is inherent to MXE in general or a combined product of MXE's preferred site of attack and of the structure of barley MLG. To test this, MXE products were created using *E. arvense*, barley and Iceland moss MLGs and all three products were washed free of unincorporated acceptor substrate and subjected to lichenase digestion (Fig. 23). Digestion of all MXE products yielded [^{3}H]GG·XXXGol, no other radioactive moieties were detected. The sole production of [^{3}H]GG·XXXGol from MXE products using such structurally distinct MLGs indicates that it is a requirement for MXE activity that a β-(1→3) bond links residues occupying subsites -4 and -3, and β-(1→4) bonds linking residues occupying other negative subsites. This specificity distinguishes MXE from its GH16b subfamily co-member (Strohmeier *et al.*, 2004) lichenase which requires that a β-(1→3) bond links residues occupying subsites -2 and -1. If, as substrate specificity work suggests (Fig. 16), MXE targets cellotetraose units specifically, it must also require that a β-(1→3) bond links residues occupying subsites +1 and +2 Surprisingly then, MXE may, with regard to site of attack, be more similar to the cellulase characterised by Grishutin *et al.* (2006) – which requires a β-(1→3) bond between subsites +1 and +2 – than to lichenase. Finally, despite MXE's observed specificity to the linkages constituting the backbone of its glucan

substrate, because this single enzyme can catalyse both MXE and XET activity, many of its active site's subsites must also be capable of accommodating substitutions to this backbone, which MLG lacks but xyloglucan exhibits.

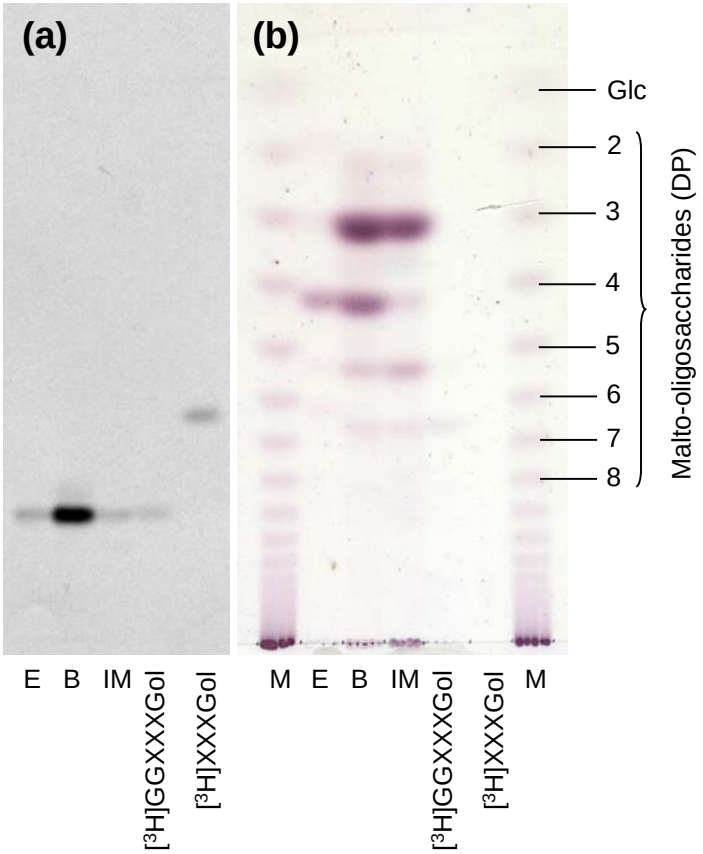

Fig. 23. Identification of the site of MXE cleavage of structurally dissimilar MLGs MXE products created by incubation of reaction mixtures (20 µl) containing 5, 10 and 15 kBq [^{3}H]XXXGol (84 MBq µmol^{-1}) with 0.3% (w/v) *E. arvense* (E), barley (B) and Iceland moss (IM) MLG respectively and 50% (v/v) *E. fluviatile* crude extract for 16 h at 25ºC. 75% (v/v) ethanol-insoluble products were then digested with lichenase; lichenase products were resolved by TLC (BAW, two ascents) and detected by fluorography (a) and thymol-staining (b).

3.3.2. Testing the nature of the bond created by MXE

To test the hypothesised nature of the bond created during the MXE reaction (bond **B**) – a β-(1→4) bond to the non-reducing terminal Glc residue in XXXGol – I exploited the fact that, regardless of the length of a xyloglucan, the only free O-4 Group is at the non-reducing terminus. To exploit this, the reductively tritiated

xyloglucan 'subunit dimer' [^{3}H]XXXGXXXGol ([^{3}H]DP14ol; specific activity 1.6 MBq µmol^{-1}) was used as an acceptor substrate for MXE activity. Polymeric MXE product was then digested by lichenase before a single radioactive product was purified by SEC (Biogel P-2 column 2). XEG digestion of both the recovered radioactive product (presumed to be [^{3}H]GG·XXXGXXXGol; [^{3}H]DP16ol) and [^{3}H]DP14ol yielded a single radioactive moiety which migrated with [^{3}H]XXXGol (Fig. 24a). This indicates that MXE attached MLG to the non-reducing terminal heptasaccharide subunit alone (Fig. 24b), which provides further support for its hypothesised β-(1→4) nature.

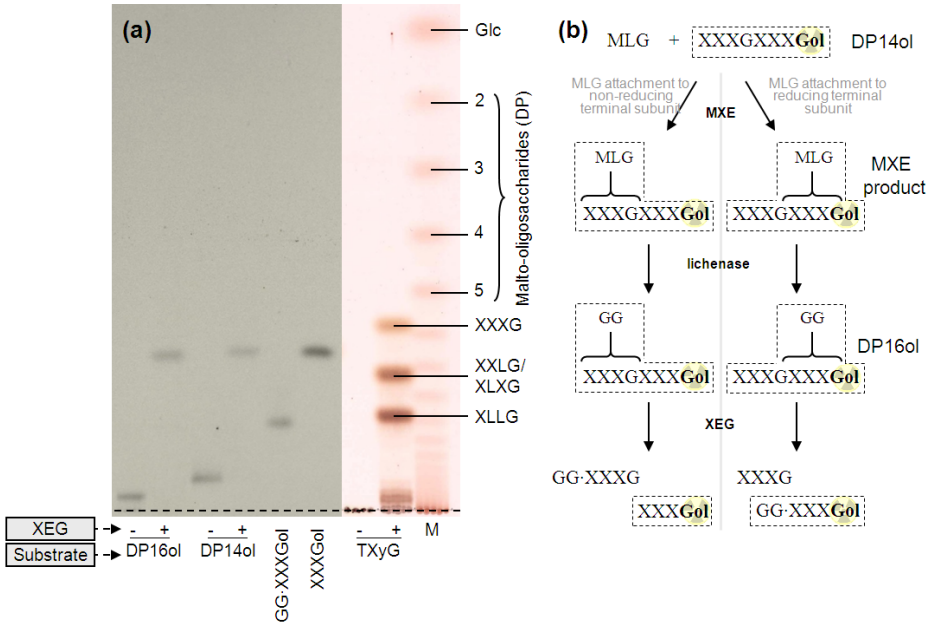

Fig. 24. Determination of which of the two subunits of XXXGXXXGol MLG is attached to during MXE activity a) [^{3}H]GG·XXXGXXXGol (DP16ol), [^{3}H]XXXGXXXGol (DP14ol) and tamarind xyloglucan (TXyG) before (-) and after (+) XEG treatment. Reaction mixtures (1 ml) containing 15 kBq [^{3}H]DP14ol, 0.75% (w/v) BMLG and 50% (v/v) *E. fluviatile* crude extract was incubated at 25ºC for 72 h after which 46% of radioactivity was shown to be incorporated into 75% (v/v) ethanol-insoluble material. This product was redissolved and digested with lichenase. The single radioactive moiety created was purified by SEC Products resolved by TLC (BAW, two ascents); the portion containing the radioactive oligosaccharides was fluorographed while the portion containing the unlabelled TXyG digestion was thymol-stained. b)

Schematic representation of the experimental strategy indicating products that would be formed during successive enzymatic treatments for attachment of MLG to either of the two subunits of XXXGXXXGol. Dashed boxes surround radioactive moieties; radioactive symbol behind radioactive residue; TXyG, tamarind xyloglucan; +/-, without and without XEG digestion; M, starch marker ladder.

3.3.3. Identification of the global site of MLG cleavage during MXE activity

As well as exhibiting specificity for the site of MLG cleavage within the local repeat unit structure of MLG subunits, it is also possible that MXE might exhibit specificity or preference for the site of MLG cleavage construed globally – i.e. MXE may prefer to cleave MLG a defined distance from either of the termini. Alternatively, MXE may cleave MLG stochastically when construed globally. Differences in MLG site of attack construed globally would have dramatic effects on the role of MXE *in vivo,* and would produce diagnostic ranges of product sizes which could be resolved by SEC (as done with XETs by Steele *et al.*, 2001) and thereby be assessed. To test this, a size-homogenous sample of barley mixed-linkage glucan (termed HBMLG) was created by SEC (CL-6B; Fig. 25) and used as a substrate for MXE activity. MXE reaction products were fractionated by SEC (CL-6B) and fractions were assayed for hexose and radioactive content (Fig. 26). The donor substrate profiles were unchanged during the incubation, indicating the absence of any contaminating endohydrolases which might otherwise complicate the discussion. As expected, the amount of radioactive product increased from 0–8 h. The fact that the size range of radioactive product encompasses sizes equal to the maximum size of the donor substrate and is a far greater range than the range of the donor substrates indicates that MXE does not exhibit a preferred site of attack at any defined distance from either MLG termini. At this point, the donor substrate profile (detected by use of the anthrone assay: total hexose) is currently a mass profile and the product profile (detected by tritium labelling, with one label per molecule) is a molar profile. To allow a direct comparison between the two, the mass profiles of the donor substrates were (converted) into molar profiles (Fig. 26) as described previously (Steele *et al.*, 2001).

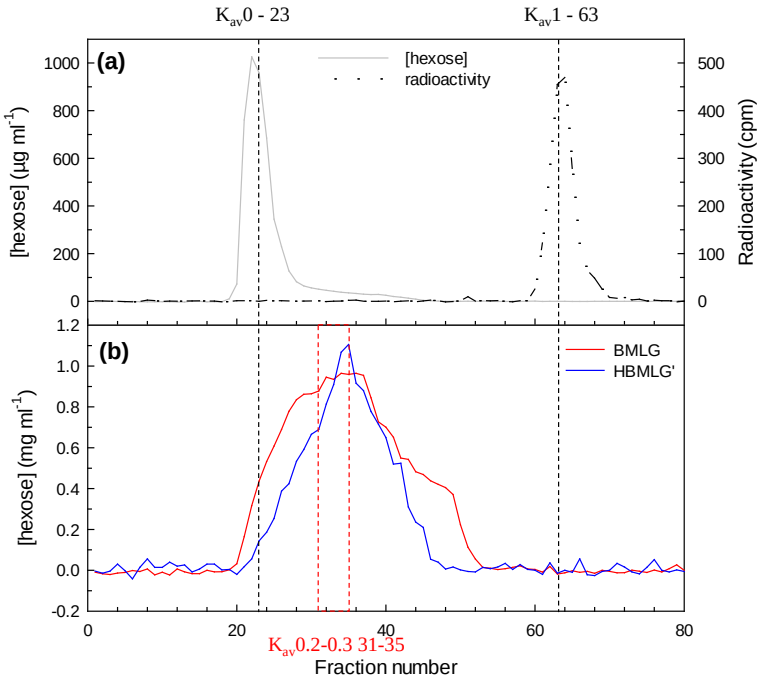

Fig. 25. Column calibration and creation of a size-homogenous BMLG fraction (HBMLG) using SEC (Sephadex CL-6B) (a) Calibration of a Sephadex CL-6B column using dextran and $^{3}H_2O$, indicating void (K_{av} 0) and total included (K_{av} 1) volumes of the column respectively. (b) Elution spectra of a commercial barley MLG sample (BMLG) and a partially size-homogenised barley MLG sample (HBMLG'). Three 10 ml 0.625% (w/v) barley MLG solutions (BMLG) were fractionated by SEC and fractions within the region K_{av} 0.2–0.3 (fractions 33-37) were pooled for all three and re-run through the column (HBMLG'). Fractions in the region K_{av} 0.2–0.3 were again pooled and were named 'size homogenous barley mixed-linkage glucan' (HBMLG, not shown here). HBMLG had an anthrone Glc equivalent hexose mass of 16.0 mg.

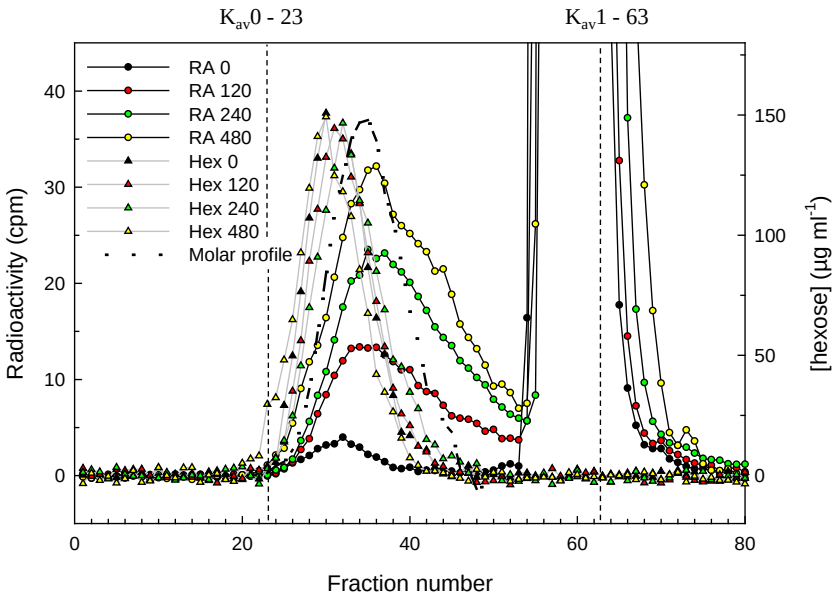

Fig. 26. Sepharose CL-6B chromatography of substrate and products of MXE using size-homogeneous mixed-linkage glucan as the donor substrate
Analysis of ^{3}H-labelled transglycosylation products formed by the action of semi-purified MXE from *E. fluviatile* on size-homogenous BMLG (HBMLG). *E. fluviatile* crude extract was fractionated in 10% (w/v) ammonium sulphate 'cuts'. Reaction mixtures (250 µl) containing 1.5 µM (37.5 kBq) [^{3}H]XXXGol, 0.8% (w/v) HBMLG and 17.6% (v/v) ammonium sulphate precipitated MXE were incubated for 0 (acid added before enzyme), 2, 4 and 8 h at 20°C. Hexose reading data (Hex 0–480, grey lines) are the average of quadruplicate measurements; radioactive data (RA 0–480, black lines) are the average of duplicate measurements. The small amount of radioactive product created at 0 h must have been catalysed during incubation after the addition of acetic acid. The molar profile of the non-radioactive, size-homogeneous BMLG (HBMLG) is shown for comparison on an arbitrary scale.

To aid analysis of the size ranges of the MXE substrates and products data were plotted cumulatively (Fig. 27). To avoid confusion of MXE products with unincorporated acceptor substrate ([^{3}H]XXXGol), only fractions 23–53 were include in this cumulation. This method shows the median substrate size to be ~200 kDa while the median product size was ~100 kDa. This, coupled with the fact that the size range of products is greater than the size range of the substrates, indicates that, when

site of cleavage is construed globally, MXE cleaves its substrate stochastically. In this respect MXE appears to operate an identical mechanism to the majority of XTHs (Nishitani & Tominaga, 1992; Steele *et al.*, 2001), though some XTHs are able to 'measure' the length of their donor substrates and discriminate accordingly (Tabuchi *et al.*, 1997).

To further investigate the mechanism of MXE attack, two hypotheses were envisaged (described in Steele *et al.*, 2001): (1) MXE selects its substrates by size (a 200 kDa MLG is twice as likely to be selected as a 100 kDa MLG, if both are equimolar); (2) MXE selects its substrates by molarity (a 200 kDa MLG is equally likely to be selected as a 100 kDa MLG, if both are equimolar). Models of expected cumulative product size distributions were computed and plotted with the observed cumulative substrate/product size distributions to enable comparison. When this methodology was performed on XTHs, Steele *et al.* (2001) showed that the profile of XET reaction products fitted best with the first model. Curiously, the profile of MXE reaction products shown here fits best with the second model; it is difficult however, to conceive of how MXE might stochastically select its substrate with regard to molarity and yet stochastically cleave its substrate with regard to size.

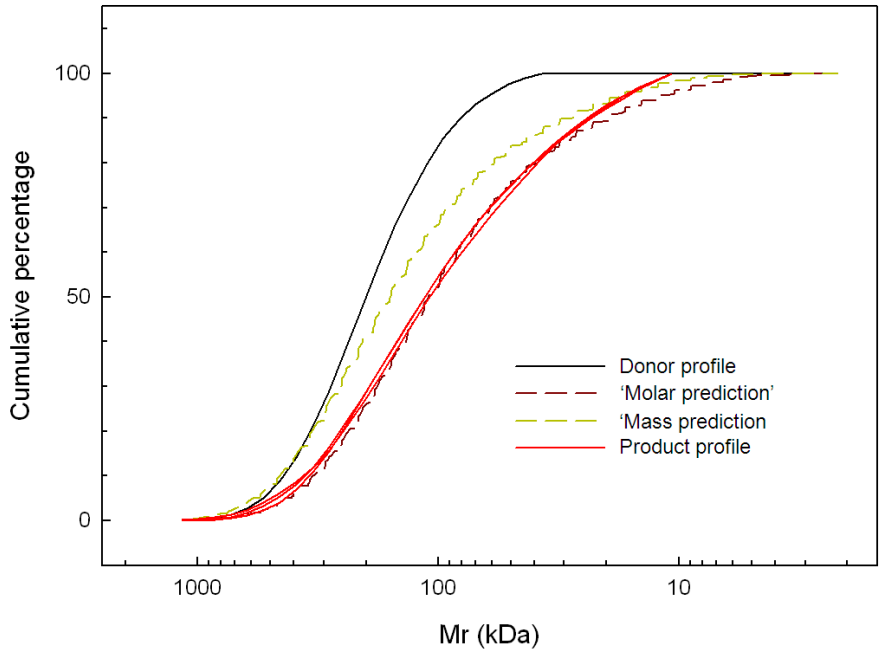

Fig. 27. M_r distribution of ^{3}H-labelled products formed by MXE The curves are calculated from the data in Fig. 26. Red lines represent the products formed

after 2, 4 and 8 h incubations (product profiles); each consists of 63 data points joined by straight lines. The black line shows the mean molar profile of the non-radioactive MLG donor substrates (donor profile). The two predicted distributions, ‘molar prediction’ and ‘mass prediction’, are M_r distribution predictions were MXE to select its substrate with regard to molarity or total mass as described in test. Data for the x-axis were calculated from the K_{av} values in Figure 25 using the calibration curve shown in Steele *et al.* (2001). Observed MXE product sizes are expected to diverge from predicted ones at lower Mr values because only fractions 23–53 from Fig. 26 were incorporated into the cumulation.

3.4. Presence of MXE in other species and tissues

While MXE has been found to appreciable extents in lateral shoot crude extracts of *Equisetum* alone, its presence in different *Equisetum* tissues had yet to be assessed. Similarly, while MXE activity is undetectable in crude extracts from athoer species, the possibility that inextractible MXE is a constituent of the cell walls of other species had also not been investigated. To assess this, crude enzyme extracts from *E. arvense* strobili were prepared for standard endotransglycosylase assays and, separately, a novel assay to assess endotransglycostylase action *in vivo* (cf. activity *in vitro*) was developed.

3.4.1. Presence of extractible MXE activity in *E. arvense* strobili crude extracts

To test whether MXE was an appreciable constituent *Equisetum* strobili (reproductive organ) tissue, crude extracts of late season *E. fluviatile* lateral shoots, *E. arvense* strobili and *E. arvense* strobili lateral stalk were assayed for MXE and XET activities (Fig. 28). Neither strobili nor strobili stalks contained appreciable MXE activity, though both contained XET activity. *E. fluviatile* lateral shoots, as expected contained both MXE and XET activities, with the latter predominating. A confounding factor in the assessment of *E. arvense* strobilus enzyme constitution is the fact that the tissue rapidly becomes dry. As such, the assessment of the enzyme constitution may be hindered by protein degradation during this drying process. Nonetheless, any such degradation would be expected to occur similarly to XET- and MXE-active enzymes and thus MXE must still be a relatively minor component of strobili.

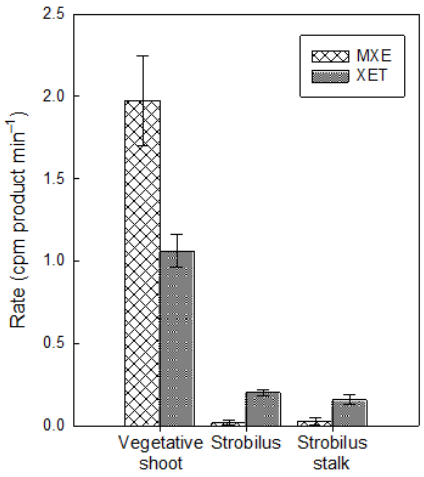

Fig. 28. Extractable endotransglucosylase activities from *E. arvense* vegetative and reproductive tissues Total extracts from mature *E. arvense* vegetative shoot, strobilus and strobilus stalk were assayed for MXE and XET activities with four time points (0–4 h).

3.4.2. Presence of MXE action in various barley tissues

To investigate the hypotheses that barley might contain inextractible MXE-active enzymes and/or enzymes which only catalyse MXE to a significant extent *in situ*, an assay which is able to assess MXE reaction in vivo – i.e. MXE action (cf. MXE activity in vitro) – was devised. Freshly cut pieces of tissue from 13 different barley organ samples (Fig. 29) were thinly sliced and incubated in aqueous [^{3}H]XXLGol before endogenous hemicelluloses were extracted and either digested with lichenase or XEG, or left undigested. 75% (v/v) ethanol-soluble products were analysed by duplicate TLCs: one was cut and assayed for radioactivity (Fig. 30), the other was thymol-stained to show total oligosaccharides produced from endogenous polysaccharides (Fig. 31). By this method, both MXE and XET action were assayed concurrently under natural conditions, and without the potential shortfalls of an *in vitro* assay, such as glycosylation differences (heterologously expressed proteins) or artificially-buffered pH. Also, because both MXE and XET actions are assayed simultaneously, they are directly comparable within an individual sample, eliminating biological variability.

While XEG was able to release ^{3}H-labelled oligosaccharides from the hemicelluloses of all barley organs tested, it released significantly more from the younger ones. This

corroborates with previous understandings that, though XET is ubiquitous throughout the plant, it is more prevalent in younger tissues (Fig. 30). As lichenase was unable to release appreciable amounts of ^{3}H-labelled oligosaccharides from any organs, MXE action was shown to be negligible (Fig. 31); this is consistent with the absence of MXE activity in barley extracts (Fry *et al.*, 2008a), and refutes the hypothesis of Hrmova *et al.* (2007) that the low amount of MXE activity catalysed by some Poaceaen XTHs *in vitro* could produce physiologically significant MXE action *in vivo*.

Lichenase released oligosaccharides from all barley organs tested, indicating the presence of endogenous MLG (Fig. 31). The highest yield was found in leaves and seedling roots, but moderate abundances were present in seedling coleoptiles and in the young leaves of 12-week-old plants. It was lowest, though nonetheless detectable, in the old leaves of the 12-week-old plants. As expected, the major MLGO in all barley organs tested was the trisaccharide, with a smaller proportion of tetrasaccharide. XEG released a range of oligosaccharides from all organs tested, demonstrating the ubiquity of xyloglucan throughout the plant. The unusual composition of Poaceaen xyloglucan (Sims *et al.*, 2000) is demonstrated by the fact that the pattern and identities of these oligosaccharides differed strongly from that obtained by similar a methodology with non-poalean plants (Xue and Fry, 2012).

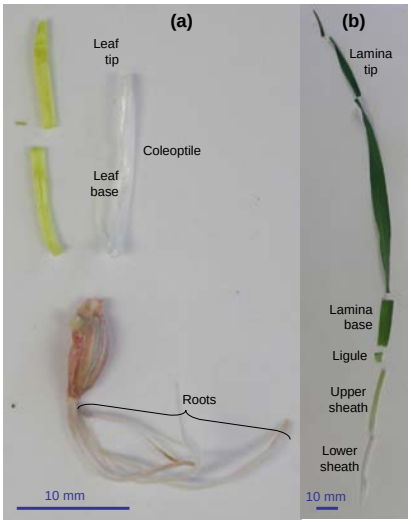

Fig. 29 Morphology of representative barley organ parts tested for MXE and XET action *in vivo* and for MLG and xyloglucan content (a) An 'older seedling', (b) 2nd leaf of a 12-week-old plant. Scale bar = 10 mm.

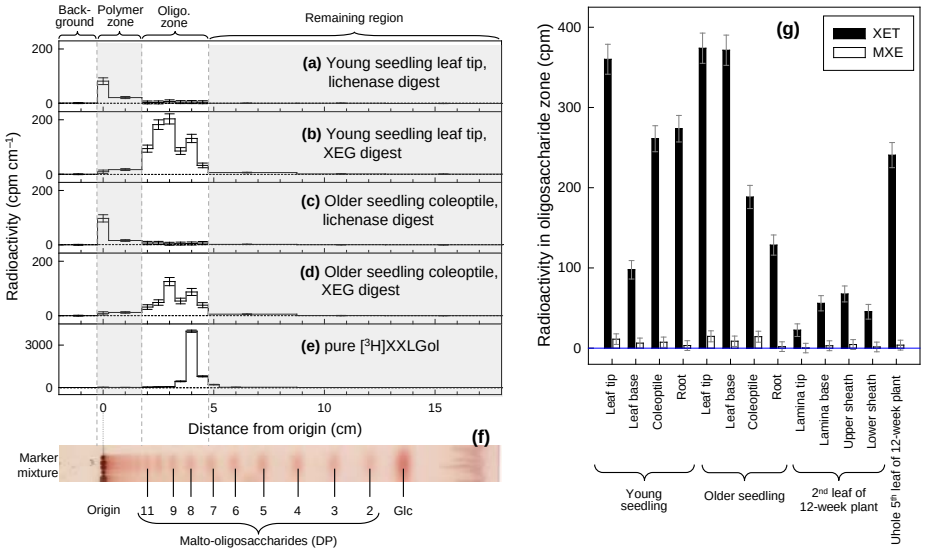

Fig. 30. *In vivo* assessment of MXE and XET action in 13 barley organs. Tissue slices from twelve barley organs (identified in Fig. 29) were incubated with [^{3}H]XXLGol before extracted hemicelluloses were digested with XEG or lichenase; low-M_r products alone were analysed by TLC, revealing [^{3}H]oligosaccharitols diagnostic of endotransglycosylase action. Four representative profiles are shown (a–d), as well as the profile of the authentic [^{3}H]XXLGol (e). A malto-oligosaccharide marker mixture was run alongside the samples (f). The oligosaccharide zone, defined as in (a-d), was quantified

for each tissue tested (g). All data are corrected for background and are given ± counting error (95% confidence limits).

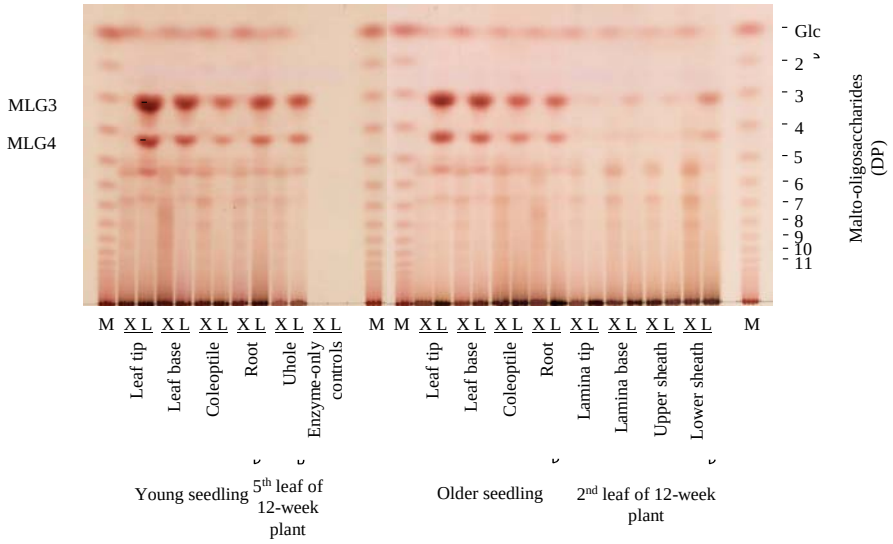

Fig. 31. Endogenous MLG and xyloglucan constitution of barley tissues. Duplicate TLCs of the samples illustrated in Fig. 30, digested with XEG ('X') or lichenase ('L'), were stained with thymol, indicating oligosaccharides originating from endogenous barley xyloglucan and MLG.

Any *in vivo* approach (or *in vitro* approach using unpurified enzymes) potentially risks being compromised by hydrolysis of acceptor substrates by exogenous glycosidases (Simmons, 2013). For example, endogenous apoplastic α-xylosidases and β-glucosidases, commonly found in plants (Koyama *et al.*, 1983; Franková & Fry, 2011), might together hydrolyse [^{3}H]XXXGol or [^{3}H]XXLGol, to products too small to serve as endotransglucosylase acceptor substrates. Any such hypothetical degradation could not be responsible for the lack of detectable MXE action in barley tissues or for the lack of detectable MXE activity in *Equisetum* strobilus extracts, because XET action and/or activity was readily detected in parallel experiments. Further, as we found detectable MLG in all barley organ samples tested (Fig. 31), the absence of detectable MXE action was also not merely the product of the absence of the donor substrate. Indeed, in most cases, lichenase-released MLG-oligosaccharides exceeded XEG-released xyloglucan-oligosaccharides, indicating that barley cell walls were richer in MLG than xyloglucan. Despite this, XET action was readily

detectable in all barley organs tested. All this provides evidence against the hypothesis of Hrmova *et al.* (2007) that the very low MXE activities of barley XTHs (e.g. *Hv*XET6), detected *in vitro*, could exert significant MXE action *in vivo*. Nonetheless, I cannot discount the possibility of extremely low levels of MXE action, similar to the rates of MXE activity observed with *Hv*XET6 (Hrmova *et al.*, 2007) and *Holcus lanatus* extracts (Fry *et al.*, 2008a), in barley tissues, but the physiological significance of this is circumspect.

3.5. Analysis of cellulose : xyloglucan endotransglucosylase (CXE) activity

Prior to this work, crude extracts of *E. fluviatile* lateral shoots had been shown to contain three related endotransglycosylase activities: MXE, XET and CXE. This section sought to test the hypothesis that the enzyme responsible for MXE, already known to catalyse XET activity as well, is also responsible for CXE.

An early season *E. fluviatile* lateral shoot crude extract was fractionated by isoelectric focusing and the fractions produced were assayed for MXE, XET and CXE activities (Fig. 32). Having already confirmed that the enzyme responsible for MXE is also able to catalyse XET activity, these two activities were expected to collocate around pH 4. Here, fractions around pH 4 were capable of catalyzing all three reactions. The co-occurrence of a peak of CXE activity at this pH is highly suggestive of a single uniquely promiscuous acidic enzyme which is capable of catalysing all three reactions. There was a further, far less prominent XET activity that was found around the neutral pH range. Fractions here were incapable of catalysing MXE or CXE activity; this is consistent with previous findings of conventional XTHs and confirms conventional XTHs are not the source of CXE.

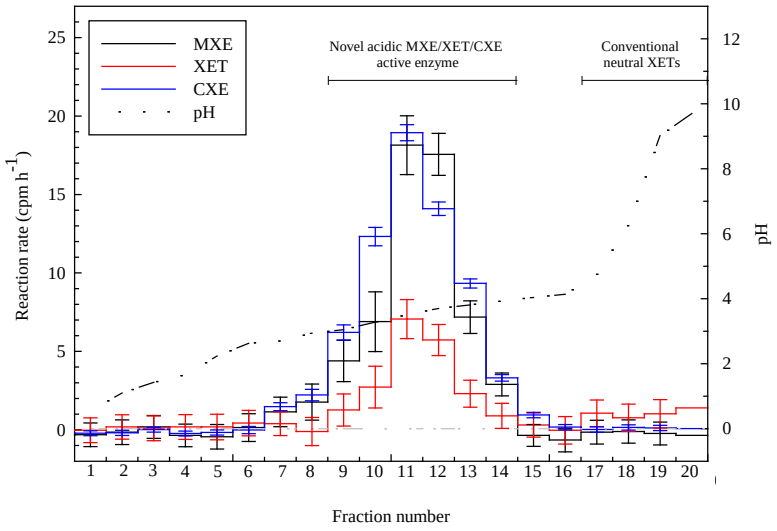

Fig. 32. MXE, XET and CXE reactions following isoelectric focusing fractionation of *E. fluviatile* crude extract MXE and XET reaction conditions: 0.75 kBq XXXGol, 2 µl rotofor enzyme fraction, 8 µl Na:citrate buffer pH 6.1 and 10 µl 1% (w/v) donor substrate, incubated for 4 hours, detected using the

standard method. Results are single reading for MXE and XET and the average of duplicate readings for CXE and are shown ± counting errors.

The actual carbohydrate structure recognised by CXE is probably those cellulose glucan chains exposed singly rather than those incorporated into the crystalline structure of a microfibril. Given this, while it is highly unusual for such promiscuity to be displayed by a single endotransglycosylase, this phenomena can be reconciled by the similarity of the three reactions (XET, MXE and CXE): all use [^{3}H]XXXGol as an acceptor substrate and a glucan-based polymer as an acceptor. Indeed, given our prior knowledge of the enzyme's ability to utilise both MLG and xyloglucan as donor substrates, it is highly conceivable that it might also be able to utilise cellulose glucan chains: MLG and xyloglucan are both variations of cellulose's β-(1→4)-D-Glc*p* backbone, the former containing backbone linkage variation without substitution, the latter containing no backbone linkage variation but significant branched substitutions (Fig. 33).

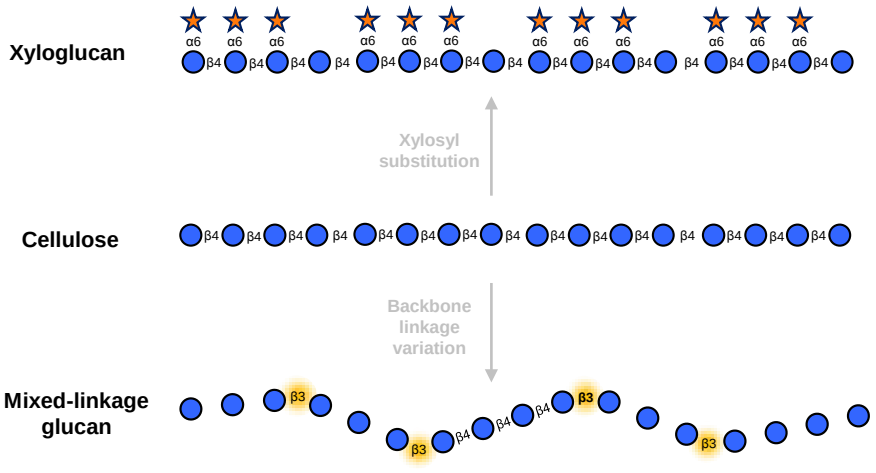

Fig. 33. Structure of three endotransglycosylase donor substrates Both xyloglucan and mixed-linkage glucan are variations of the cellulose chain, containing either xylosyl substitutions or backbone linkage variation respectively. Reducing termini on right; blue circles, D-Glc residues; orange stars, D-Xyl residues; α6, α-(1→6)-linkage, β3, β-(1→3)-linkage (highlighted in orange); β4, β-(1→4)-linkage. Following the carbohydrate symbol scheme described by Varki *et al.* (2009).

3.6. An unexpectedly lichenase-stable hexasaccharide yields new information on MLG subunit composition and distribution

MLGs are typically structurally characterised by digestion with a lichenase from *B. subtilis*, however, much of the structural information (i.e. the linkages broken) is lost during this digestion. This lichenase is a GH16b subfamily member which exhibits specificity to BMLG and cleaves (1→4) bonds following (1→3) bonds.
To further our understanding of how lichenase is able to confer specificity to BMLG and to define the site of attack as they do, and concurrently investigate whether this information can yield further knowledge about the structure of intact (i.e. non-digested) MLGs, I here characterised the products of lichenase digestion of three MLGs in detail.

3.6.1. Lichenase digestion of MLGs from three widely divergent taxa yield an unexpected oligosaccharide

Because of our current understanding of lichenase's site of attack and of MLG's structure, the oligosaccharide products of lichenase digestion were expected to be a homologous series of standard MLGOs, who differ from each other only in the length of the (1→4)-linked β-D-Glc*p* non-reducing terminal region (See 1.2.2.1.). These oligosaccharides would migrate in a regular pattern on chromatographic techniques. However, TLC analysis of digests of MLGs from *E. arvense*, barley (*Hordeum vulgare*) and Iceland moss (*Cetraria islandica*) revealed a spot (named '6x') which migrated between MLG5 and MLG6 (Fig. 34a), a characteristic inconsistent with it being a standard MLGO. After purification by preparative TLC, 6x was shown to have a retention time of ~20.5 min on HPLC (Fig. 34b–h), eluting in the zone expected of MLG9 (Wang *et al.*, 2003; Wood *et al.*, 2003; Tosh *et al.*, 2004a; Tosh *et al.*, 2004b; Fry, 2008). The divergence of 6x on HPLC relative to the other MLGOs who, relative to each other, migrate consistently in both chromatographic techniques further highlights 6x's novelty. This presence of such a novel oligosaccharide as a lichenase digestion product indicates that the substrate specificity of the enzyme is not as previously thought.

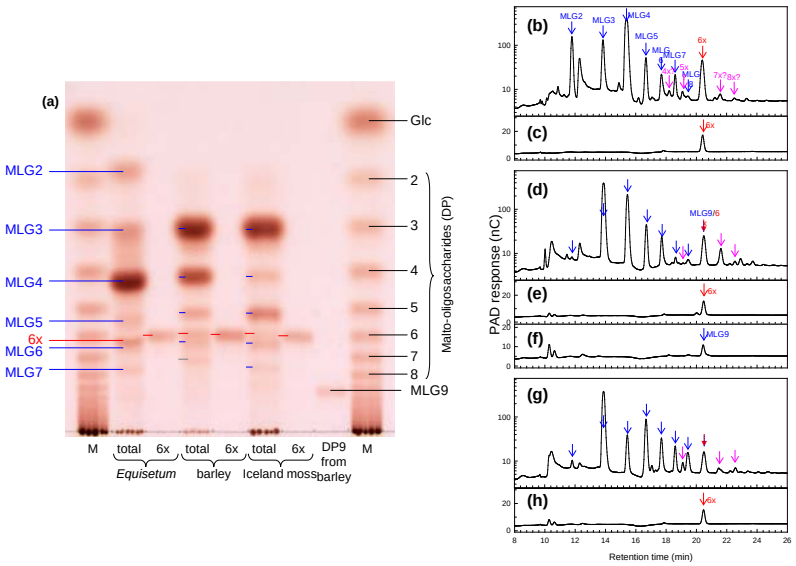

Fig. 34. Chromatographic analysis of the lichenase digestion products of three MLGs (a) TLC analysis of the crude lichenase digests of three MLGs ('total'), of their respective 6x's, and of a putative DP9 MLGO (MLG9) from barley MLG after purification by preparative HPLC and preparative TLC. Abbreviation used: M, malto-oligosaccharide marker ladder. The slight retardation of the oligosaccharides in the *Ea*MLG lane is probably a product of the large amount of tetrasaccharide there. (b–h) HPLC analysis of crude digests of *Equisetum* (b), barley (d) and Iceland moss (g) MLGs, their respective '6x's (c, e and h), and the putative barley MLG9 (f). Blue lines/arrows, standard MLGOs (DP2–9); red lines/arrows, 6x; pink arrows, candidates for other members of the x series; red/blue dotted arrows, 6x and MLG9; pink line, unknown band.

The unusual retention time of 6x on HPLC was exploited to purify it from all three MLGs. The ~20.5 min retention time peaks were purified by preparative HPLC followed by preparative TLC. While the TLC purification step showed only a single major band in the ~20.5 min peak from both *E. arvense* and Iceland moss MLGs – a result consistent with only/largely 6x eluting in this period – two distinct bands (one migrating with 6x, the other somewhat slower) were present in the same HPLC peak when purified from barley MLG. Once eluted from the preparative TLCs, all four purified oligosaccharides (6x from three MLGs and the slower migrating oligosaccharide from barley MLG alone), as well as total lichenase digests of the

polysaccharides from which they originated, were analysed both by TLC (Fig. 34a) and HPLC (Fig. 34b–h). Results show that 6x is a constituent of lichenase digests of all three types of MLG and that it and the slower migrating oligosaccharide purified from digested barley MLG both migrate at ~20.5 min retention time peak on HPAEC. Thus, in previous HPLC work, the co-eluting 6x and MLG9 would have been lumped together as MLG9.

3.6.2. Stability of 6x during prolonged lichenase digestion

To test whether 6x was merely a product of incomplete digestion or a side reaction such as transglycosylation, I digested *Ea*MLG with lichenase for various time periods (Fig. 35). The maximum yield of the standard MLGOs with DP 2–7 and of 6x, was obtained by 30 min. Following this, no breakdown, or further production, of these oligosaccharides occurred. This indicates that 6x is neither a product of incomplete lichenase activity nor a by-product of a side-reaction. In contrast, three oligosaccharides which eluted slightly later than 6x were found at their maximum yield between 2 and 5 min incubation and declined thereafter; these are deduced to be intermediary products of partial hydrolysis, e.g. G4G3G4G4G4G3G (i.e., MLG3-MLG4), G4G4G3G4G4G3G (i.e., MLG4-MLG3) and G4G4G3G4G4G4G3G (MLG4-MLG4).

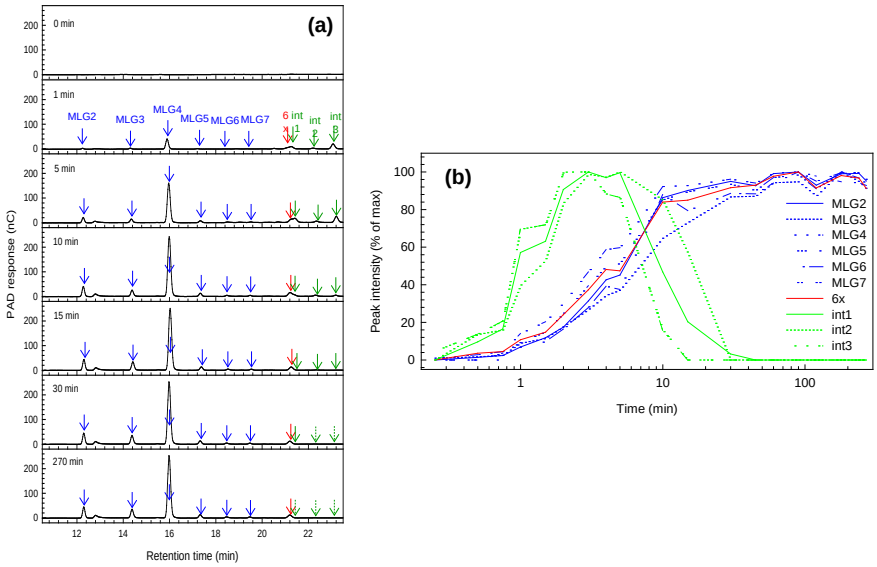

Fig. 35. Sequential lichenase digestion of *E. arvense* MLG (a) HPLC traces of lichenase digestion products at representative time-points. *Equisetum* gave no detectable conventional MLG9, which would co-elute with 6x. (b) Time-

course of relative yields of each peak seen in (a). '100%' on the y-axis represents the maximum yield of the peak in question. Blue arrows/lines, conventional MLGOs; red arrows/line, 6x; green arrows/lines, proposed intermediary digestion products.

3.6.3. Partial characterisation of 6x by acid hydrolysis and enzymic dissection

Because 6x is a non-standard MLGO, it must either be composed of residue(s) other than β-D-Glc*p*, include linkages other than (1→3) and (1→4), or comprise a different arrangement of (1→3) and (1→4)-linkages than do the standard MLGOs. Acid hydrolysis of TLC-purified 6x from *E. arvense* yielded only glucose (Fig. 36), showing it to be an oligosaccharide comprised solely of glucose. 6x was digested with β-D-glucosidase, which progressively releases β-D-Glc*p* residues, singly, from the non-reducing end(s); the intermediary products were analysed by HPLC (Fig. 37). The first products were glucose plus 'standard' MLG5 [arrows on Fig. 37(a)], indicating that 6x differs from MLG5 only in possessing a single additional β-D-Glc residue. Thereafter, MLG5 broke down as expected, via MLG4, MLG3 etc., to glucose (Fig. 37a). This indicates that 6x is G-(G4G4G4G3G), very probably with the additional G residue attached at the non-reducing end of MLG5 (i.e., as G·G4G4G4G3G, where '·' is an unknown linkage) because otherwise two potential different oligosaccharides products of β-D-glucosidase digestion would probably be formed after the removal of a single β-D-Glc residue; only one is observed. Consistent with the bond '·' in G·G4G4G4G3G being unusual, digestion kinetics indicated that cleavage of this bond (6x + H_2O → MLG5 + Glc) was rate-limiting, with the subsequent steps (e.g. MLG5 + H_2O → MLG4 + Glc) occurring very rapidly and with little accumulation of the intermediary products.

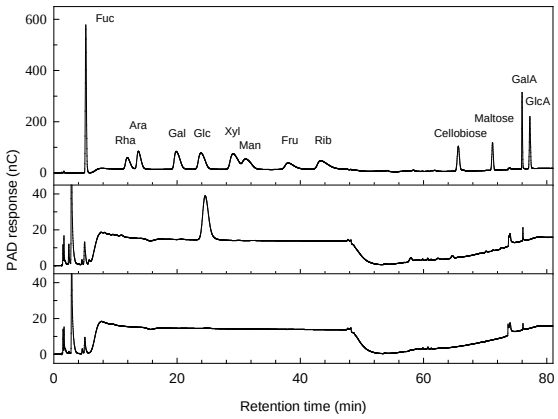

Fig. 36. Acid hydrolysis of 6x Purified 6x from *Equisetum* (b) and a 'blank' control (c) were separately subjected to TFA hydrolysis and were analysed by HPLC. Each was compared to a monosaccharide marker mixture (a).

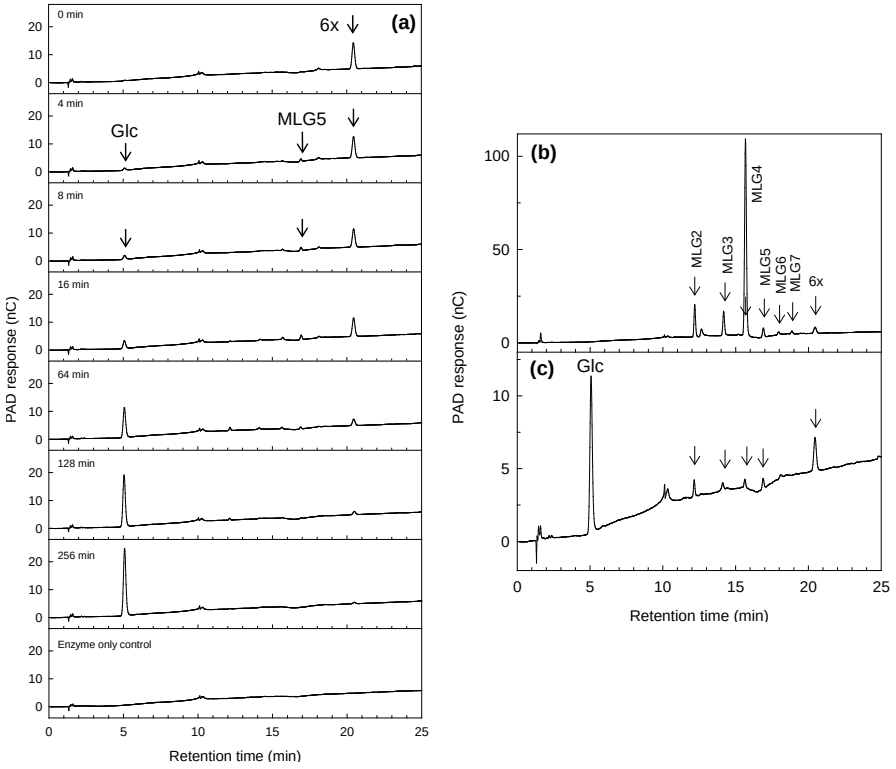

Fig. 37. Sequential β-glucosidase digestion of 6x (a) HPLC traces showing progressive β-glucosidase-mediated hydrolysis of 6x, via MLG5, to glucose; (b) MLG oligosaccharide marker mixture (a lichenase digest of *Ea*MLG); (c) focus on 64-min digestion shown of (a) highlighting intermediary breakdown products.

3.6.4. Determination of the structure of the reduced hexasaccharide, 6x-ol, by NMR spectroscopy

A bulk preparation of 6x was prepared by SEC on Bio-Gel P-2 (column 1; PyAW/CB) of a lichenase digest of *Equisetum* hemicellulose. 6x-containing fractions, identified by TLC, were reduced with $NaBH_4$, and the product (6x-ol) was purified by preparative HPLC.

The structure of 6x-ol was deduced from a series of one-dimensional (1D) and two-dimensional (2D) NMR spectra obtained at 18.4 T. The 1D proton spectrum (800 MHz) showed considerable overlap of signals. The 2D and highly selective 1D chemical-shift-selective (CSSF)–TOCSY (Robinson *et al*. 2003) spectra identified seven proton spin systems (Fig. 21/Ha). Together with the DQF–COSY spectrum and the ^{1}H–^{13}C HSQC proton–carbon correlation spectrum, it was possible to identify and to assign all the proton resonances. The corresponding carbon resonances were assigned from a 2D ^{1}H–^{13}C HSQC correlation spectrum and from a 2D ^{1}H–^{13}C HSQC–TOCSY spectrum (which, in addition to the usual HSQC cross peaks, showed signals at the same ^{13}C chemical shift for neighbouring J_{HH} coupled protons 2–3 bonds away; Table 3).

From the chemical shifts of the proton resonances and the magnitude of the proton–proton coupling constants it was clear that the sub-spectra corresponding to monosaccharides **a**–**e** arose from five glucose residues with β-anomeric linkages. Sub-spectra labelled Glcol(1–3) and Glcol(4–6) (Fig. 38a) showed no anomeric protons but a clear correlation between the protons at 3.63 ppm and 4.04 ppm in the DQF–COSY spectrum and thus these sub-spectra represented a single spin system of a terminal glucitol (Glcol) group.

The sequence of the residues and the positions of the linkages were deduced from a series of highly selective 1D ^{1}H–^{1}H CSSF–NOESY (Robinson *et al.*, 2003) spectra (Fig. 38b) and their comparison with the 1D CSSF–TOCSY spectra. Analysis of these high-resolution spectra showed that the **d**→**c**, **c**→**b** and **b**→**a** glycosidic linkages were 1→4, while the **e**→**d** linkage was 1→3 (Fig. 38c). This was further confirmed by the ^{1}H–^{13}C HMBC spectrum which showed two three-bond proton–carbon correlations across the glycosidic linkages for each residue.

The linkage between residue **a** and the glucitol group was confirmed as a 1→3 linkage by comparison of the ^{13}C chemical shifts of the glucitol group with the ^{13}C chemical shifts of three glucitol-containing disaccharides: lactitol (4-*O*-β-D-galactopyranosyl-D-glucitol), laminoaribiitol (3-*O*-β-D-glucosyl-D-glucitol) and maltitol (4-*O*-β-D-glucopyranosyl-D-glucitol) [http://sdbs.riodb.aist.go.jp/sdbs/cgi-bin/cre_index.cgi?lang=eng]. Good agreement (< 0.6 ppm) was obtained for carbons C1 to C6 with those for laminaribiitol, whereas there are differences of up to 1.8 ppm for lactitol and up to 4.4 ppm for maltitol.

Thus the deduced structure of the reduced hexasaccharide 6x-ol is β-D-Glc*p*-(1→3)-β-D-Glc*p*-(1→4)-β-D-Glc*p*-(1→4)-β-D-Glc*p*-(1→4)-β-D-Glc*p*-(1→3)-D-Glc-ol (Fig. 38c), where Glc*p* is either β-D-glucopyranose or, theoretically, α-L-glucopyranose; β-D-glucosidase digestion confirms the former. The new hexasaccharide, 6x, which can be represented as G3G4G4G4G3G, is thus a sequence of two contiguous known subunits, MLG2-MLG4.

Residue		(H-1)	H-1 [C-1]	H-2 [C-2]	H-3 [C-3]	H-4 [C-4]	H-5 [C-5]	H-6a [C-6]	H-6b
6	A		4.739 [102.7]	3.339 [73.4]	3.509 [75.5]	3.393 [69.6]	3.468 [76.0]	3.709 [60.6]	3.907
2	B		4.661 [103.0]	3.417 [73.2]	3.661 [74.1]	3.649 [78.5]	3.614 [74.6]	3.805 [60.0]	3.989
5	C		4.528 [102.3]	3.51 [73.0]	3.75 [83.8]	3.51 [75.5]	3.49 [67.9]	3.74 [60.5]	3.910
4	D		4.521 [102.3]	3.346 [72.9]	3.637 [73.9]	3.671 [78.5]	3.606 [74.8]	3.816 [59.8]	3.971
3	E		4.510 [102.3]	3.345 [72.9]	3.638 [73.9]	3.670 [78.5]	3.605 [74.8]	3.818 [59.8]	3.969
1	P+Q*	3.774	3.660 [61.9]	4.009 [72.8]	4.043 [78.4]	3.639 [70.1]	3.895 [70.7]	3.638 [62.7]	3.845

Table 3. Chemical shifts of all protons and carbons on 6x-ol Data defined by the 1D 1H, 2D and 1D 1H TOCSY, 1H DQF-COSY, and 1H-13C HSQC and HMBC (all at 800 MHz). * reduction of this residue makes distinction between H-1 & H-6, H2 & H-5 and H-3 & H-4 impossible. Data in this figure was collected and analysed by Prof. Ian Sadler, Dr. Dušan Uhrín and Dr. Lorna Murray.

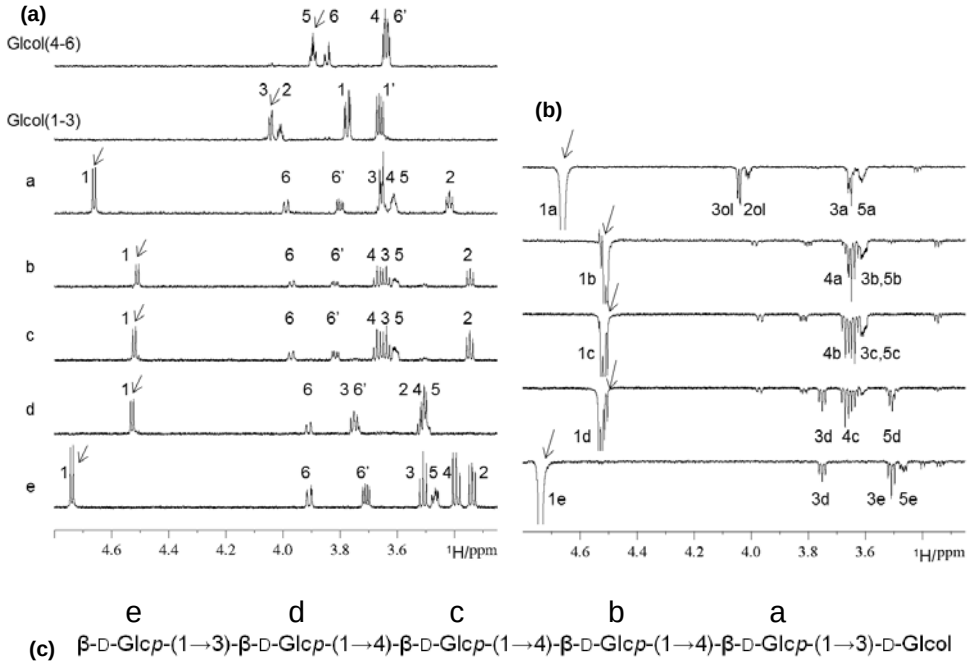

Fig. 38. Determination of the structure of the reduced novel hexasaccharide, 6x-ol, by NMR spectroscopy (a) Selective 1D CSSF-TOCSY spectra of the reduced hexasaccharide 6x-ol showing individual residue sub-spectra. Anomeric protons were selectively excited for residues a–e, while H3 and H5 were excited for the fragments Glcol(1–3) and Glcol(4–6), respectively (indicated by arrows). 160 ms mixing time was used. (b) Selective 1D CSSF-NOESY spectra (200 ms mixing time) of the reduced hexasaccharide 6x-ol, showing through space correlation of anomeric protons of rings a–e (indicated by arrows). (c) reduced hexasaccharide structure showing the residue nomenclature used. Data in this figure was collected and analysed by Prof. Ian Sadler, Dr. Dušan Uhrín and Dr. Lorna Murray.

3.6.5. Quantification of 6x (G3G4G4G4G3G) content of MLG

Lichenase digests of the three MLGs were size-fractionated by SEC (column 1; PyAW/CB), and the fractions were analysed by HPLC (Fig. 39). From barley and Iceland moss MLGs, a ~20.5-min HPLC peak was found in two distinct size-classes, judged by GPC to be a hexasaccharide (6x) and a nonasaccharide. However, from *Equisetum* MLG, the ~20.5-min peak was found only in the hexasaccharide size-class. The nonasaccharide, judged by its behaviour on TLC (Fig. 24), HPLC and SEC, is probably MLG9 (G4G4G4G4G4G4G4G3G), as labelled previously (Wang *et al.*, 2003; Wood *et al.*, 2003; Tosh *et al.*, 2004a; Tosh *et al.*, 2004b; Fry *et al.*,

2008). The yields of 6x and each of the conventional MLGOs are listed in Table 4. Further, this methodology indicated candidates for other members of the ‘x’ series (4x, 5x, 7x and 8x) based on their SEC elution volumes and HPLC retention times. It was notable that no appreciable amount of oligosaccharide eluted from SEC after the nonasaccharide.

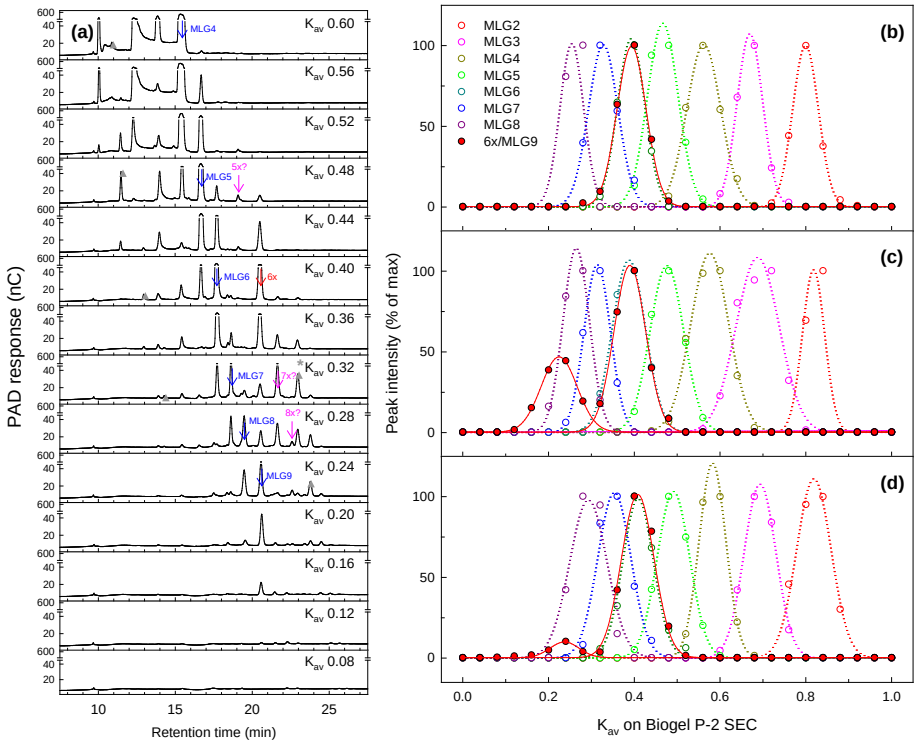

Fig. 39. Size profiles of each HPLC-resolved oligosaccharide Lichenase digests of three MLGs (a, c, barley; b, *Equisetum*; d, Iceland moss) were fractionated by SEC on Bio-Gel P-2 (column 1; PyAW/CB). Fractions were then applied to HPLC for further resolution and quantification of the oligosaccharides. (a) HPLC traces for barley MLG size fractions. Arrows indicate a given compound’s maximum peak area; solid blue arrows, standard MLGOs; red arrow, 6x; pink arrows, candidate 5x, 7x and 8x; grey arrowheads, unknown peaks; asterisk, candidate MLG2-MLG2-MLG3 peak. (b–d) Peak quantifications for MLG2–9 and 6x shown as percentage of each peak’s maximum area. Kav is defined as elution volume relative to those of dextran (Kav = 0) and glucose (Kav = 1).

MLGO	Mol-% composition of MLG without knowledge of 6x			Mol-% composition of MLG with 6x with knowledge of 6x			Mol-% composition of MLG with 6x taken as MLG2 + MLG4			Mol-% composition of MLG with 4x to 8x			Mol-% composition of MLG with 4x to 8x taken as MLG2 + MLG2 to MLG6		
	Ea	Bar	IM	*Ea*	Bar	IM	*Ea*	Bar	IM	*Ea*	Bar	IM	*Ea*	Bar	IM
MLG2	17.86	0.09	0.97	18.01	0.09	0.97	21.95	1.86	2.67	17.89	0.09	0.96	19.58	2.93	3.36
MLG3	14.64	66.16	75.11	14.76	66.35	75.32	14.05	65.17	74.03	14.66	65.59	74.75	15.55	63.74	73.35
MLG4	54.77	24.52	4.77	55.22	24.60	4.78	57.38	25.93	6.41	54.86	24.31	4.74	57.36	25.35	6.32
MLG5	4.02	3.82	9.91	4.05	3.84	9.94	3.86	3.77	9.76	4.03	3.79	9.86	4.44	4.67	9.90
MLG6	1.55	1.93	3.37	1.57	1.94	3.38	1.49	1.90	3.33	1.56	1.92	3.36	1.68	1.97	3.32
MLG7	1.26	0.16	1.99	1.27	0.16	2.00	1.21	0.16	1.96	1.26	0.16	1.98	1.32	0.15	1.93
MLG8	0.07	0.20	1.69	0.07	0.20	1.69	0.06	0.19	1.66	0.07	0.19	1.68	0.07	0.19	1.64
MLG9	5.82	3.12	2.20	<0.01	1.03	0.18	<0.01	1.01	0.18	<0.01	1.02	0.18	<0.01	0.99	0.17
4x?	-	-	-	-	-	-	-	-	-	0.18	<0.01	<0.01	-	-	-
5x?	-	-	-	-	-	-	-	-	-	0.21	0.02	0.42	-	-	-
6x	-	-	-	5.06	1.80	1.74	-	-	-	5.02	1.78	1.73	-	-	-
7x?	-	-	-	-	-	-	-	-	-	0.21	1.02	0.29	-	-	-
8x?	-	-	-	-	-	-	-	-	-	0.05	0.11	0.05	-	-	-

Table 4. Relative molarities of MLGOs from three structural dissimilar MLGs MLGO molarities were quantified from the HPLC response, which was calibrated using a range of malto-oligosaccharides. For “Relative molarities w/o knowledge of 6x” the ~20.5 min peak is assumed to be MLG9 alone; for “Relative molarities with knowledge of 6x” the 20.5 min peak was divided into 6x and MLG9 by ratios determined from Fig. 39; for “Relative Molarities with 6x as MLG2 and MLG4” the amount of 6x identified was then converted into MLG2 and MLG4. <0.01 means no peak of the correct retention time was detectable; - means n/a here.

3.6.6. Implications of 6x’s discovery for MLG subunit composition

The discovery of 6x indicates that many previous quantifications of MLG subunit composition were flawed. Specifically, the MLG9 content has been characterised too

high while the MLG4 and MLG2 content had been characterised too low. The latter case is particularly evident for poalean and Iceland moss MLG, for which no or negligible MLG2 has often been reported (Wood *et al.*, 1994; Izydorczyk *et al.*, 1998; Wood *et al.*, 2003; Lazaridou *et al.*, 2004; Tosh *et al.*, 2004; Vaikousia *et al.*, 2004; Papageorgiou *et al.*, 2005; Liu & White, 2010). The results from Fig. 39 suggest the presence of more members of the 'x series': 4x (MLG2-MLG2; G3G4G3G), 5x (MLG2-MLG3; G3G4G4G3G), 7x (MLG2-MLG5; G3G4G4G4G4G3G) and 8x (MLG2-MLG6; G3G4G4G4G4G4G3G). If correct, previous quantifications of MLG subunit compositions – particularly the MLG2 content – are further undermined.

Furthermore, our experiments (Fig. 39) indicate that there was no appreciable amount of high-M_r (DP > 9) lichenase products in the HPLC trace, contradicting some previous reports of their quantification (Izydorczyk *et al.*, 1998; Papageorgiou *et al.*, 2005). Indeed, peaks previously mis-identified as MLG10 and MLG11 are shown here to be candidates for 7x and 8x. I cannot, of course, rule out the possibility that our digests contained standard MLGOs with DP > 9 [$G(4G)_n3G$, where $n > 7$] that were insoluble in water, as suggested by Wood *et al.* (1994). One of the unidentified peaks, which eluted at K_{av} 0.32 from the digestion of barley MLG (starred grey arrowhead; Fig. 39a), might, based on GPC and HPLC retention, be MLG2-MLG2-MLG3 (G3G4G3G4G4G3G), a further novel heptasaccharide whose resistance to lichenase might be expected given 6x's resistance.

3.6.7. Implications for lichenase activity

This work disproves the previous assumption that lichenase cleaves at <u>every</u> (1→4) bond immediately following a (1→3) bond, i.e. at the (1→4) bond in the ···G3G4G··· motif. If this were the rule, lichenase would hydrolyse 6x (G3G4G4G4G3G + H_2O → G3G + G4G4G3G). The production of lichenase-resistant candidates for '4x' to '8x', i.e. $G3G(4G)_n3G$ where n is 1–5, suggests that the presence of the MLG2 subunit at the non-reducing terminus of an MLGO is the sole determinant of lichenase resistance.

The unexpected resistance of the 'x' series oligosaccharides could be rationalised if non-reducing terminal MLG2 units impart unfavourable enzyme–substrate

interactions at the negative subsites of lichenase's catalytic centre (Fig. 38). Since lichenase is only known to cleave the (1→4) bond in a ···G3G4G··· motif, catalytic activity requires a (1→4) bond between subsites +1 and –1 and a (1→3) bond between subsites –1 and –2. The resistance of 6x (MLG2-MLG4) to lichenase, despite the lability of MLG3-MLG4, implies that hydrolysis requires subsite –3 also to be occupied; and since contiguous (1→3)-bonds are unknown in MLG (Peat *et al.*, 1957; Parish *et al.*, 1960), the bond between subsites –2 and –3 will always be (1→4) (Fig. 40).

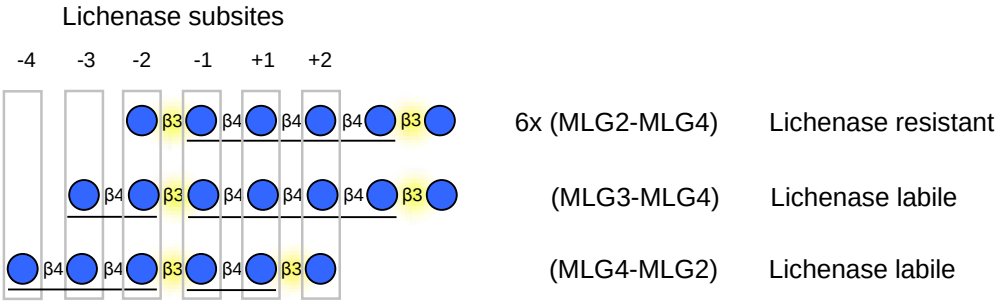

Fig. 40. Schematic representation of the residues occupying lichenase subsites during lichenase cleavage of different MLGOs The -3 and -4 subsites of GH16 lichenase are shown to be empty during the positioning that is necessary for cleavage of 6x's unexpectedly stable bond. In contrast, for cleavage of the labile bond in the heptasaccharide MLG3-MLG4, the -3 subsite is occupied. Likewise, for cleavage of the labile bond in the heptasaccharide MLG3-MLG4 both the -3 and -4 subsites are occupied. The presence of a β-(1→3) bond between subsites +1 and +2 in the latter case apparently has no limiting effect on lichenase activity. Blue circles, D-Glc; cellulosyl regions underlined.

However, any simple rule proposing that lichenase never cleaves to the reducing side of an MLG2 unit would be untenable. It is evident, especially from *Equisetum* MLG digests, that lichenase is capable of producing large amounts of MLG2 (G3G; Fig. 24 and Xue and Fry, 2012), and even barley and Iceland moss MLG yield some free MLG2. This implies that certain MLG2–MLGO bonds can be cleaved — presumably when (as in MLGO´–MLG2–MLGO) the MLG2 unit is not a non-

reducing terminus. The MLGO´–MLG2 produced would then be hydrolysable to release free MLG2 (provided MLGO´ is not itself MLG2).

3.7. The mode of recognition and site of attack of xyloglucan-cleaving enzymes

Xyloglucan-cleaving enzymes are crucial to plant development and have been the target of many biotechnological efforts. Elucidation of the site of attack of xyloglucan-cleaving enzymes might enable a better understanding of their function as well as of their enzymological properties. Here a novel strategy was employed utilising sequential treatments of XET (using a radioactive acceptor oligosaccharide) and a hydrolase. Wherever the initial acceptor substrate is regenerated from such sequential XET : hydrolase treatments, both enzymes must have cleaved the xyloglucan at the same position. In contrast, wherever larger products are yielded, the hydrolase must have cleaved the XET product tailwards (i.e. in the non-reducing terminal direction) the site of attack of the XET.

3.7.1. Identification and structural characterisation of novel ^{3}H-labelled products of XET:XEG sequential treatments

The XET acceptor substrate [^{3}H]XXLGol was allowed to permeate the cell walls of 4-day old barley seedling leaf tips and the resultant radioactive polymeric products were extracted by the use of alkali and digested with XEG. XEG products were resolved by TLC and detected by fluorography. The three detectable oligosaccharides (A, B and C; Fig. 41a) were, after elution, further purified by preparative TLC (Fig. 41b). Products A, B and C, as well as [^{3}H]XXLGol, were subjected to graded β-D-glucosidase treatment (Fig. 41c). As expected, [^{3}H]XXLGol was resistant to β-D-glucosidase. A, which migrated with [^{3}H]XXLGol, was mostly resistant to digestion, though some product of greater mobility was formed. A is probably constituted mostly of [^{3}H]XXLGol with a small amount of [^{3}H]GXLGol, probably produced by the action of endogenous barley α-D-xylosidases. B migrated slower than [^{3}H]XXLGol and was broken down directly to a product that migrated with [^{3}H]XXLGol after β-D-glucosidase treatment; B is thus most probably [^{3}H]GXXLGol. β-D-Glucosidase was likewise able to digest C to a product that migrated with [^{3}H]XXLGol, though via an intermediate that migrated with B; thus C is most probably [^{3}H]GGXXLGol. These oligosaccharides, in which the initial acceptor (here [^{3}H]XXLGol) has a β-D-glucosyl tail of differing lengths attached are collectively referred to throughout as [^{3}H]G_nXXLGols/[^{3}H]G_nXXXGols (when

[^{3}H]XXLGol and [^{3}H]XXXGol are used as the acceptor substrate respectively). The β-D-glucosyl tails must originate from the initial xyloglucan donor substrate and are therefore are most probably (1→4)-linked; hence [^{3}H]$\underline{G_n}$XXLGols. The identities of the products yielded from this experiment indicates that XET and XEG had some propensity to cleave xyloglucan at the same point (where [^{3}H]XXLGol was yielded), and yet there was some propensity for XEG to cleave before (i.e. in the non-reducing terminal direction) of XET (where [^{3}H]G_nXXLGols were yielded).

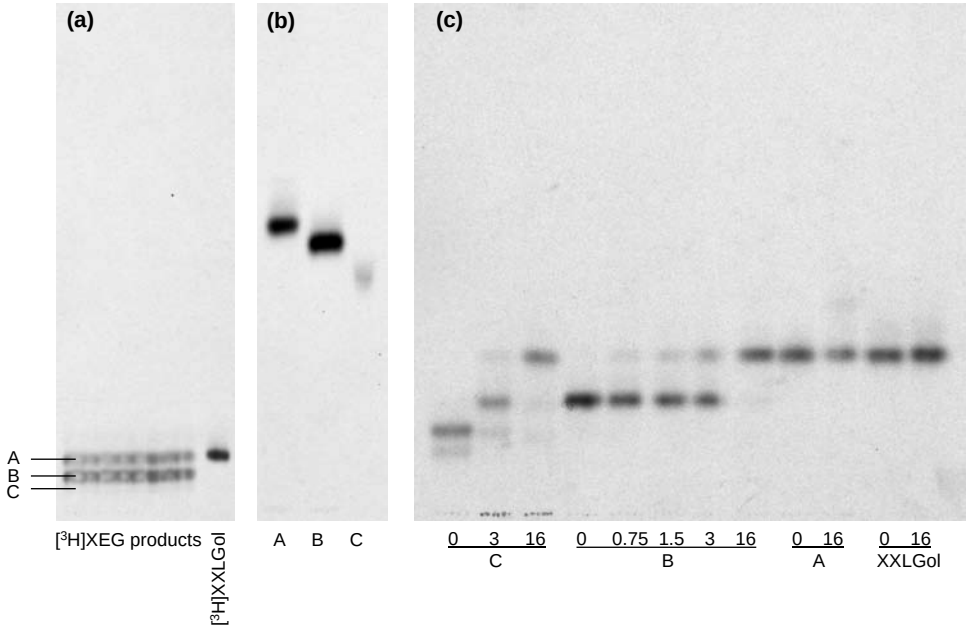

Fig. 41. Purification and characterisation of three [^{3}H]XGO-ol derivatives produced by XEG digestion of an XET product created *in vivo* from barley
In vivo XET action was performed as described in material & methods, except that 25 mg 4-day-old barley seedling leaf tips were incubated with 125 kBq (12 µM) [^{3}H]XXLGol in 125 µl; 7.75 kBq (6.2%) incorporation was achieved. Hemicelluloses were extracted using 6 M NaOH and digested with XEG; (a) three bands (A, B and C) were purified from 75% (v/v) ethanol-soluble material by preparative TLC (BAW, one ascent) with fluorography; (b) the three visible oligosaccharides (A, B and C) were, after elution, further purified by preparative TLC (PNW, one ascent) with fluorography; (c) TLC (BAW, two ascents) fluorogram showing the effect of graded β-D-glucosidase treatment on A, B, C and XXLGol.

3.7.2. [^{3}H]G_nXXLGols are formed when Poaceaen, but not when tamarind, xyloglucan is used as the XET donor substrate

To test which factors affect the production of the [^{3}H]G_nXXLGols, different enzymes and substrate combinations were tested. Maize (*Zea mays*) suspension culture sloughed extracellular polysaccharides (SEPs) – shown previously to contain maize xyloglucan (Kerr & Fry, 2003; Kerr & Fry, 2004) – were purified and one half was deacetylated by the use of alkali. On Poaceaen xyloglucan acetylation naturally occurs at the O-6 position of backbone Glc residues. These two maize xyloglucan-containing samples, as well as commercial tamarind xyloglucan, were used as donor substrates for XET activity, after which 75% (v/v) ethanol-insoluble material was subjected to endohydrolysis by XEG (GH12) or cellulase (cell*b*; GH7) (Fig. 42). The 75% (v/v) ethanol-soluble XET reaction unincorporated oligosaccharides and, following endohydrolysis, 75% (v/v) ethanol-soluble hydrolysate products were resolved by TLC, analysed by fluorography and thymol-staining (Fig. 43) and quantified by use of a radioisotope plate reader (Table 5). In addition to the initial acceptor substrate [^{3}H]XXLGol, up to three [^{3}H]G_nXXLGols, which migrated slower, were present in all reaction mixtures where either of the maize SEPs samples (containing xyloglucan composed mainly of XXGG and XXGGG 'base units') had acted as the XET donor. When tamarind xyloglucan (mainly XXXG 'base units') had been used, only [^{3}H]XXLGol was present. The absence of [^{3}H]G_nXXLGols in the unincorporated oligosaccharides from the XET incubation confirms that [^{3}H]G_nXXLGols are created by sequential XET : hydrolase treatment, and not by an unrelated (e.g. transferase) side-reaction. The fact that [^{3}H]G_nXXLGols occur whenever maize (Fig. 42; Fig. 43; Fig. 46; Fig. 47) or barley (Fig. 30; Fig. 49) xyloglucans are used, but never when tamarind xyloglucan (Fig. 43; Fig AQ) or *Equisetum* xyloglucans (Mohler *et al.*, 2013) are used, suggests that they are a product of a structural feature which distinguishes monocot xyloglucans from tamarind and *Equisetum* xyloglucans. However, because [^{3}H]XXLGol was yielded (to varying degrees) in all reactions, this structural feature must vary in Poaceaen xyloglucan, sometimes being a shared feature of all xyloglucans tested. The best candidate for this hypothesised structural feature is xyloglucan subunit length: tamarind and *Equisetum* xyloglucan are composed almost solely of Glc_4-based

subunits (XXXG), while Poaceaen xyloglucan is composed mainly of Glc_4- and Glc_5-based subunits (XXGG and XXGGG).

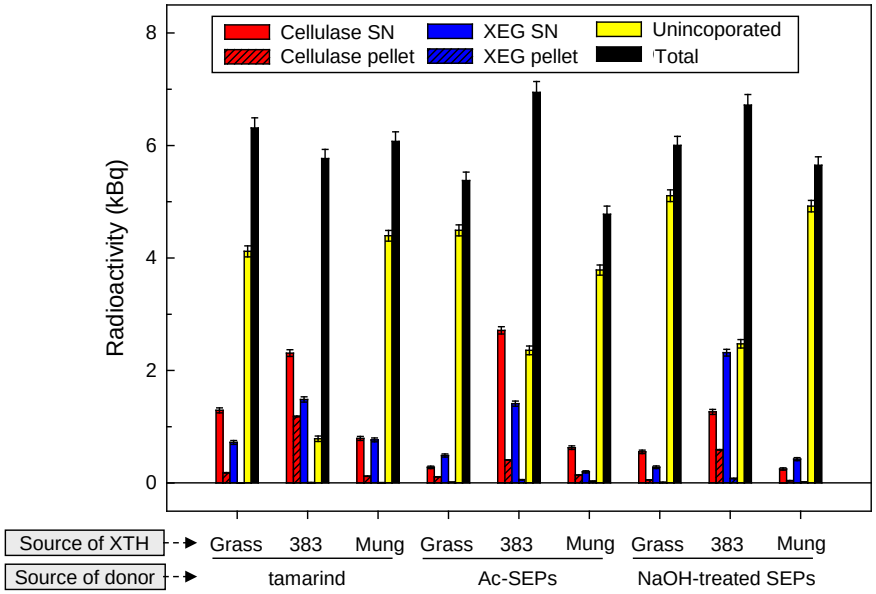

Fig. 42. Quantification of products formed during XTH-catalysed incorporation and subsequent hydrolase digestion Both sloughed-extracellular polysaccharide (SEP) samples and a 0.3% (w/v) solution of tamarind xyloglucan (20 µl) were incubated with 5 µl of three different XET-containing crude enzyme extracts and 5 kBq (0.3 µM) [^{3}H]XXLGol for 18 h at room temperature. 75% (v/v) ethanol-insoluble material was redissolved in water and split into halves; one half was subjected to XEG treatment, the other to cellulase (capable of digesting xyloglucan; cell*b*) treatment. 75% (v/v) ethanol-insoluble XET products were separated from soluble material and each was assayed for ^{3}H by scintillation counting. SN, supernatant (75% (v/v) ethanol solubilised material); grass, *Holcus lanatus* crude extract; 383, recombinantly expressed *E. fluviatile* XTH; Mung, *Vigna radiate* crude extract. The identity of the high Mr material in the unincorporated material following 383 reaction incubations is unknown.

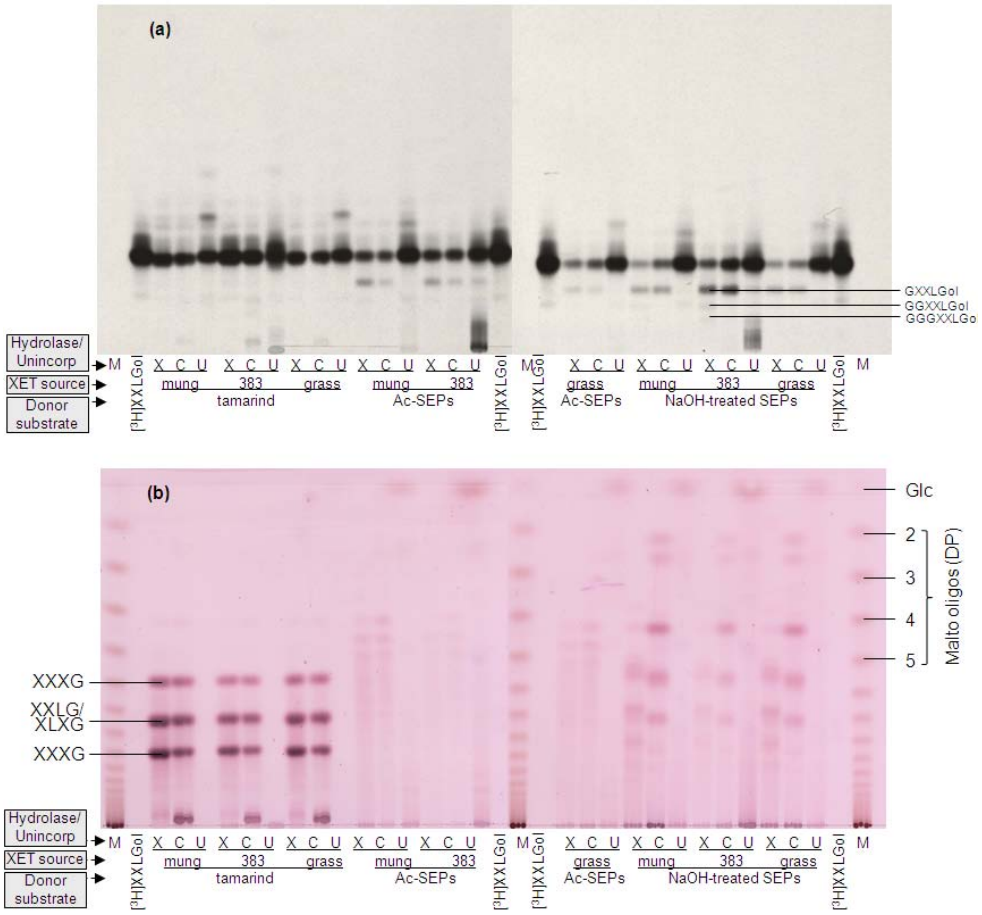

Fig. 43. Products of sequential *in vitro* XET : hydrolase treatments Products of *in vitro* XET activity (acceptor substrate was [^{3}H]XXLGol, donor substrate was one of three xyloglucan-containing samples, XET was from one of three enzyme sources) were digested by one of two hydrolases and 0.5 kBq of the products of each was resolved by TLC and detected by fluorography (a) and thymol staining (b). X, XEG; C, xyloglucan-capable cellulase; mung, *Vigna radiate* crude extract; 383, recombinant *E. fluviatile* XTH; grass, *Holcus lanatus* crude extract; tamarind, commercial tamarind xyloglucan; Ac-SEPs, (naturally) acetylated SEPs; NaOH-treated SEPs, deacetylated SEPs; U, unincorporated oligosaccharides remaining after the XET reaction period. Arrowheads indicate the [^{3}H]G_nXXLGols: GXXLGol, GGXXLGol and GGGXXLGol.

Hydrolase	[^{3}H]GXXLGol: [^{3}H]XXLGol ratio for different donor substrates		
	Tamarind xyloglucan	Ac-SEPs	NaOH-SEPs
Average	-	0.11	0.40
Post cellulase digestion	-	0.06	0.28
Post XEG digestion	-	0.17	0.52

Table 5. Quantification of [^{3}H]GXXLGol: [^{3}H]XXLGol ratios for TLCs in Fig. 43 Data obtained by quantifying the radioactivity on the TLC from Fig. 43, by use of a radioisotope plate reader. No [^{3}H]GXXLGol was detected when tamarind xyloglucan was used as a donor.

But while xyloglucan donor substrate structure was the sole qualitative determinant of [^{3}H]G$_n$XXLGol presence, other factors did affect the amount of [^{3}H]G$_n$XXLGol produced, as evidenced by variations in the [^{3}H]GXXLGol : [^{3}H]XXLGol ratio (Fig. 43a; Table 5). The ratio was highest when de-acetylated (rather than acetylated) SEPs were used and when XEG (rather than cellulase) was used. Despite the latter difference between XEG and cellulase, given that GH families 7 and 16 constitute GH clan-b, it is perhaps surprising that the mode of recognition of the XEG (GH12 family member) and cellulase (GH7) used here – with no significant relationship – appear both to differ from the mode of recognition of XET (GH16) so similarly. However, while acetylation reduced the [^{3}H]GXXLGol : [^{3}H]XXLGol ratio regardless of the hydrolase used the effect was more pronounced (the relative amount with which the [^{3}H]GXXLGol:XXLGol ratio was lowered, was greater) when cellulase was the hydrolase used. This suggests a) a distinction between the ability of these two hydrolases to accommodate acetylated Glc and thus their proclivity to be directed by acetylation, and b) that therefore the fact that xyloglucan acetylation affects the [^{3}H]GXXLGol:XXLGol ratio is a product of the direction of the hydrolases; we have no evidence here to rule out the possibility that XETs are also directed by acetylation. Nonetheless, XET source was the only variable within the experiment that had no apparent effect on the [^{3}H]GXXLGol:XXLGol ratio. This indicates that there was no significant discrepancy in regard to site of attack between the different XET sources used here, and suggests that XETs all recognise the same, or highly similar, xyloglucan motifs.

Thymol-stainable cellulase and XEG products also showed distinctions between the hydrolases and polysaccharides used (Fig. 43b). The standard products of tamarind

xyloglucan hydrolysis (XXXG, XXLG/XLXG, XLLG) were formed both by XEG and cellulase. Hydrolysis of de-acetylated SEPs yielded distinct oligosaccharides, consistent with the structural distinction between maize and tamarind xyloglucans. But, in addition, the products of XEG and cellulase hydrolysis of de-acetylated SEPs were distinct from each other, with the range of oligosaccharides produced by XEG migrating less far on TLC than those produced by cellulase. This observation mirrors the greater [^{3}H]GXXLGol : [^{3}H]XXLGol ratio produced by XEG than by the cellulase. In addition, some oligomers exhibiting disaccharide-like mobility were produced by the cellulase, suggesting intra-subunit hydrolysis which, given the fact that Poaceaen xyloglucan contains stretched of non-xylosylated glucose residues, would not be wholly unexpected for a cellulase. The thymol-stainable products of Ac-SEPs digestions were both streaked (possibly because of semi-random acetylation) and faint and were therefore difficult to assess (Fig. 43b).

3.7.3. Interpretation of the presence of [^{3}H]G$_n$XXLGols for enzymic sites of attack

Because the source of the glucosyl tails of [^{3}H]G$_n$XXLGols must be the backbone of the donor xyloglucan, the presence of the [^{3}H]G$_n$XXLGols must be explicable with reference to the sites of attack of the xyloglucan-cleaving enzymes used in this study. Of the 7 subsites present in the active sites of XTHs (-4, -3, -2, -1, +1, +2, +3), Fanutti *et al.* (1993; 1996) claimed that a β-D-glucan need only be xylosylated at positions -3 and +2 to function as a substrate, and that position -1 must be unsubstituted. This however, appeared to contradict the conclusions of Fry *et al.* (1992) and Lorences & Fry (1993) that XXG was the smallest structure capable of acting as an acceptor substrate – under the conclusions of these two papers, xylosylation in subsite +1 and +2 is a prerequisite for XET activity. The thorough probing of XTH substrate specificity by Saura-Valls *et al.* (2008) corroborated the conclusion of Fanutti *et al.* (1993; 1996) that the Glc residue at subsite -1 must be unsubstituted for activity to occur. Interestingly, they observed that where multiple unsubstituted Glc residues are found in the XET donor substrate, cleavage can occur at multiple sites. This indicates that cleavage doesn't require xylosylation at subsite +1 (xylosylation here may however still be beneficial). Despite this, Saura-Valls *et*

al. (2008) observed that donor substrate binding is dominated by the high affinity for xyloglucan structures of the positive subsites (this is consistent with observations that cello-oligosaccharides are poor XET donor or acceptors; Nishitani & Tominaga, 1992; Fry *et al.*, 1992; Fanutti *et al.*, 1993; Lorences & Fry, 1993; Mohand & Farkaš, 2006; Baumann *et al.*, 2007; Hrmova *et al.*, 2007); the negative subsites showed far less affinity for such structures and were capable of transferring unsubstituted glucans alone, provided they were at least 2 Glc in size. Consistent with the findings of Fry *et al.* (1992) and Lorences & Fry (1993) and in contrast to those of Fanutti *et al.* (1993; 1996), Saura-Valls *et al.* (2008) suggest that XXG is the minimal required structure for the acceptor binding subsites for activity to occur, with a significant affinity resulting from an X moiety in subsite +2. Xylosylation in subsite +3 and a glucose at a possible position +4 produced a moderate increase in substrate affinity. One surprising conclusion from this is that xylosylation in subsite +1 is required for acceptor substrates but not for donor substrates.

While XET activity favours substitutions of the residues in its positive subsites and is relatively promiscuous regarding the substitution of those in its negative subsites, something approaching the opposite appears true of XEG, which requires a substituted Glc in its negative subsites but can accommodate unsubstituted residues in its positive subsites. By digesting the structurally unusual xyloglucans of tomato and identifying those bonds resistant to hydrolysis and those merely slowly broken, Jia *et al.* (2003) were able to identify minimum and preferred substitution patterns for xyloglucan cleavage by the GH12 XEG. They identified an unbranched Glc residue at the –1 subsite and a side chain-bearing Glc residue at the −3 subsite as requisite for XEG cleavage. They further identify side chain-bearing Glc residues in the −4 and +2 subsites as significantly increasing the chances of productive binding and cleavage. A corollary of this is that, like XET activity, where stretches of unsubstituted Glc residues occur in a xyloglucan, XEG can cleave xyloglucan in more than one position.

Therefore, although both XTH and the XEG used can cleave at multiple positions where stretches of unsubstitutes backbone residues exist in a xyloglucan, because XTH and XEG require substituted backbone residues to occupy positive and negative

subsites respectively, as stretches of unsubstituted backbones residues increase in size, the probable sites of attack of these two enzymes diverge (Fig. 44). Tamarind xyloglucan's repeating XXXG 'base units' – which contain only a single unsubstituted Glc – guarantee each enzyme cleaves at the same point. Because the difference in subunit lengths in Poaceaen xyloglucan almost solely regard the length of stretches of unsubstituted Glc residues the [^{3}H]GXXLGol : XXLGol ratio is an indicator of the ratio of Glc_5 (e.g. XXGGG): Glc_4 (e.g. XXGG) subunits in the donor polysaccharide. The fact that the GH7 cellulase produced [^{3}H]G_nXXLGols indicates that it also differs in mode of recognition and site of attack compared to XET; it appear to exhibit a similar mode of recognition to that of XEG, with enzyme : substrate affinities being dictated more by substitutions at negative subsites than XET. However, the fact that cellulase exhibited a decreased propensity to produce [^{3}H]G_nXXLGols (as evidenced by the lower [^{3}H]GXXLGol : XXLGol ratios in Fig. 43 and Table 5), indicates that the positive subsites of cellulase exhibit a greater affinity for substituted xyloglucan background residues than those of XEG.

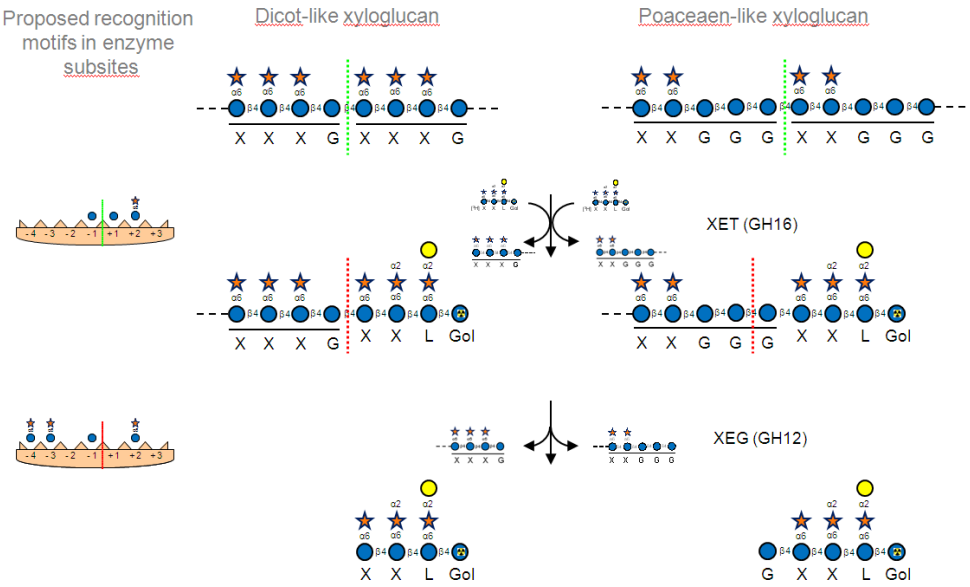

Fig. 44. Proposed model of XET and hydrolase sites of recognition and attack of xyloglucan. The left column shows models of enzymes active site subsites showing xyloglucan moieties observed to be required/highly beneficial for activity to occur; xylosylated glucose here refers to substituted glucose in general i.e. additional substitutions may be required/highly beneficial as well.

Middle and right columns show proposed preferred sights of attack of two enzyme types during sequential XET:hydrolase treatments on two dicot-type XXXG-based subunit xyloglucan (middle column) and Poaceaen-like XXGGG-based subunit xyloglucan (right column). Green dotted line indicates XET site of cleavage, red dotted line indicates hydrolase site of cleavage.

3.7.4. XEG digestion of maize xyloglucan is directed by xyloglucan acetylation

To investigate the effect of acetylation on the digestion of maize SEPs by XEG, I digested acetylated and de-acetylated SEPs using XEG and then either subjected 75% (v/v) ethanol-soluble products to alkali-treatment (which would de-acetylate acetylated products) or left them untreated. Samples were resolved by TLC and detected by thymol-staining (Fig. 45). As expected, digestion of acetylated SEP xyloglucan produced XGOs which, owing to acetylation, migrated faster than de-acetylated oligosaccharides on TLC. The profile of XGOs produced by XEG digestion of acetylated SEPs followed by NaOH-treatment differed slightly from the profile produced by XEG digestion of already de-acetylated SEPs. The most obvious example of this distinction is in the oligosaccharides that migrate between maltopentaose and maltohexaose, in which there are two major bands when de-acetylated SEPs were digested but only one when the xyloglucan was initially digested while still acetylated. As no corresponding change occurred in the NaOH treatment of the XGOs from the already deacetylated xyloglucan (lane 5, as compared with lane 4), these changes must be the product of the effect of acetylation on enzyme attack, not, for example, the presence of sodium acetate on TLC mobility.

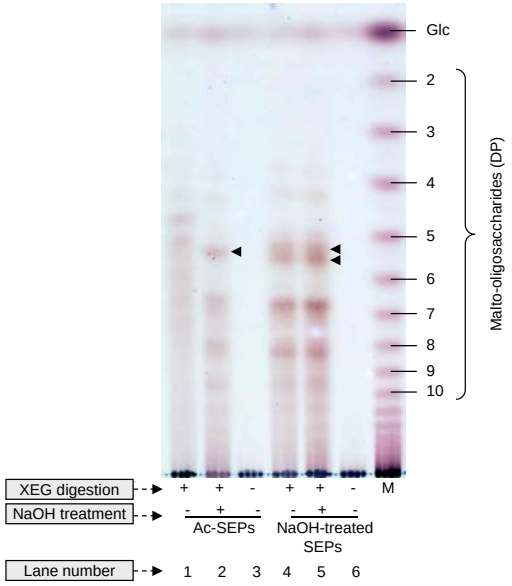

Fig. 45. Effect of maize xyloglucan acetylation on XEG-site of attack
Acetylated and de-acetylated SEPs solutions (10 µl) were digested with XEG. 75% (v/v) ethanol-soluble material was then either incubated in 3 µl 100 mM NaOH for 1 h before being slightly acidified, or left untreated. Samples were resolved by TLC (BAW, two ascents) and detected by thymol-staining. Arrowheads denote example oligosaccharides that differ between treatments and indicate discrepancies in site of attack caused by acetylation.

Jia *et al.* (2003) reported that XEG requires an unsubstituted Glc in subsite -1 and that acetylation can direct hydrolysis away from the cleavage of bonds from residues that are acetylated. Consistent with this, XEG digestion of acetylated Poaceaen xyloglucan has been shown to yield almost solely oligosaccharides with the general structure $X_n\underline{G'}_mG$, where n and m are integers and <u>G'</u> is a Glc residue which may or may not be acetylated (Gibeaut *et al.*, 2005; Hsieh & Harris 2009).

The Poaceaen xyloglucan oligosaccharides that migrate between maltopentaose and maltohexaose are, based on their mobility, probably XXGG-like structures. Where XXGG subunits are found naturally acetylated in a maize xyloglucan polysaccharide (---XX<u>G</u>GXX<u>G</u>G---, where <u>G</u> is an acetylated Glc residue), XEG would presumably produce XXGG alone, as acetylation would ensure only a single free Glc residue could be targeted for cleavage. Thus the most probable identity of the single arrowed oligosaccharide in lane 2 of Fig. 45 (XEG digestion of acetylated xyloglucan

followed by deacetylation) is XXXG. In contrast, where XXGG subunits are found in a deacetylated maize xyloglucan polysaccharide (---XXGGXXGG---), XEG would be able to cleave two bonds because of the presence of two unsubstituted Glc residues. Thus the most probable identities of the two arrowed oligosaccharides in lanes 4 and 5 (XEG digestion of de-acetylated xyloglucan) are GXXG and XXGG. The corollary of this – that deacetylation of Poaceaen xyloglucans prior to XEG treatment increases the propensity for (or perhaps even just allows) XGOs with non-reducing terminal glucosyl tails to be formed – is consistent with the increase in the [^{3}H]GXXLGol: XXLGol ratio following deacetylation observed in Fig. 43 and Table 5. This together provides further evidence that acetylation directs the site of attack of XEG.

3.7.5. Xyloglucan from maize cell culture SEPs and walls appear structurally identical

While [^{3}H]XXLGol was consistently the major product of the *in vitro* XET : hydrolase sequential treatments where maize xyloglucan acted as the substrate (Fig. 43a), [^{3}H]GXXLGol was the major product of the *in vivo* XET : XEG sequential treatments where barley xyloglucan acted as the substrate (Fig. 41). To investigate the possibility that this is the product of structural dissimilarity between cell wall-bound xyloglucan and sloughed extracellular xyloglucans, samples of maize cell culture SEPs and wall-bound hemicelluloses were used as donor substrates for XET : XEG sequential treatments. Following the production of AIR from maize cultured cells and maize culture SEPs, hemicellulose was extracted/redissolved from each by the use of alkali. Both were used as the donor substrate for XET activity and 75% (v/v) ethanol-insoluble products were digested with XEG (Fig. 46). Again, [^{3}H]G_nXXLGols (at least three) were produced when either of these xyloglucan sources acted as the XET donor substrate. The ratio [^{3}H]GXXLGol : [^{3}H]XXLGol was similar (0.44–0.55) when either xyloglucan source acted as the substrate. The range of thymol-stainable oligosaccharides produced by XEG hydrolysis of the two polysaccharides was indistinguishable. The shared [^{3}H]GXXLGol : [^{3}H]XXLGol ratio and thymol-stainable oligosaccharide range produced by digestion of SEPs and AIR xyloglucans indicates that cell wall and SEP xyloglucan exhibit no structural

distinction and further supports the contention that xyloglucan structure define the amount of [^{3}H]G_nXXLGols yielded. Further, this suggests that the difference in the [^{3}H]GXXLGol: [^{3}H]XXLGol ratios observed in the previous experiments is a manifestation of the distinct structures of the different xyloglucans and not of the distinct environments in which the reactions occurred; specifically, this suggests that maize xyloglucan has a lower XXGGG:XXGG subunit ratio than barley xyloglucan.

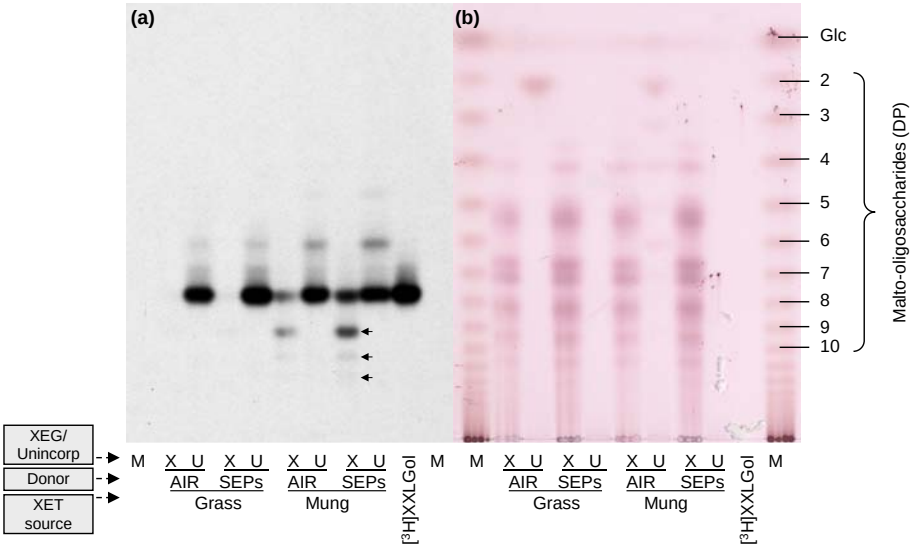

Fig. 46. TLC analysis of products of XEG digestion of XET activity products using maize cell culture xyloglucans from cell walls and from SEPs Cell wall and SEP AIRs (20 µl) were incubated with either 5 µl grass or mung bean extract and 2.5 µM XXLGol (5 kBq) at 25°C for 24 h. 75% (v/v) ethanol-insoluble XET products were digested with XEG. 75% (v/v) ethanol-soluble XEG products were resolved by TLC (BAW, two ascents) and analysed by fluorography (a) and thymol-staining (b). X, XEG digestion; U, unincorporated oligosaccharides from XET incubation; CW, cell wall-bound hemicellulose; SEPs, sloughed extracellular polysaccharide; grass, *Holcus lanatus* crude extract; mung, *Vigna radiate* crude extract. Arrows indicate [^{3}H]G_nXXLGols.

3.7.6. The XEH-active enzyme *At*XTH31 exhibits a distinct site of attack from XET activities

The difference in the site of attack of XET and the two hydrolases used thus far could be the product of the difference between transglycanase and glycanase

activities, or alternatively of the differences in substrate recognition by different GH families. To investigate this, I analysed the site of attack of *At*XTH31, a xyloglucan endohydrolase (glycanase) from GH16, the same GH family that XET activity is found in. I created XET products using a mung bean crude extract and three donor substrates (de-acetylated SEPs, maize cell culture cell wall hemicellulose and tamarind xyloglucan) and the MXE product using an *E. fluviatile* crude extract and barley MLG as the donor. In addition, I separately created all these products using [^{3}H]XXLGol and [^{3}H]XXXGol. All eight transglycanase products were then subjected to hydrolysis by XEG, cellulase and *At*XTH31. Following hydrolysis, 75% (v/v) ethanol-soluble products were resolved by TLC and analysed by fluorography (Fig. 47).

Radioactive products were essentially identical (allowing for the presence of an additional galactose group in one) regardless of acceptor substrate used, indicating that the galactosyl moiety in XXLGol played no detectable role in determining hydrolase site of attack. All hydrolases released the initial acceptor substrate alone ([^{3}H]XXLGol or [^{3}H]XXXGol) from the tamarind xyloglucan XET product. The MXE product was not digested appreciably by XEG, though a small amount of the initial acceptor substrate was produced; this is consistent with its previously observed requirement of substitutions in its negative subsites. In contrast, cellulase efficiently hydrolysed the MXE product to the initial acceptor substrate. Because of this, and cellulase's ability to produce the acceptor substrate with 3 Glc residue attached ([^{3}H]GGGXXLGol or [^{3}H]GGGXXXGol) from XET products (Fig. 43), cellulase appears capable of accommodating both substituted and non-substituted glucan backbone residues in all of its subsites. This is unsurprising given cellulase's primary celluloytic activity. However, the fact that cellulase produced the acceptor substrate alone from the MXE product but was capable of producing [^{3}H]G$_n$XXLGols from XET products (Fig. 43; Fig. 47), indicates that cellulase does more than merely accommodate substitutions in its negative subsites; substitutions at these position must produce some increased affinity. GH7 and GH16 enzymes belong to GH clan-B and thus might be expected to exhibit similar characteristics. The fact that cellulase (GH7) recognises and cleaves xyloglucan in a manner far closer to XEG (GH12) than XET (GH16) is perhaps surprising. *At*XTH31 digestion of the MXE reaction

product yielded a range of oligosaccharides of which the most predominant appeared to be the acceptor substrate with two Glc residues attached ([^{3}H]GGXXLGol or [^{3}H]GGXXXGol; this is particularly clear on 47b in which this moiety co-migrated with a structurally characterised [^{3}H]GGXXXGol marker) with decreasing amounts of oligosaccharides ranging from the acceptor substrate alone to the acceptor substrate with three Glc residues attached ([^{3}H]GGGXXLGol or [^{3}H]GGGXXXGol). The products observed following *At*XTH31 digestion of the MXE product are schematised in Fig. 48. The promiscuity regarding substrate selection that this range of products indicates is highly surprising. To produce all cleavage products shown, *At*XTH31 must: be capable of accommodating both xylosylated and non-xylosylated residues within its positive subsites; be able to accommodate a β-(1→3) bond between residues in any of its subsites except between +2/+3; and be capable of cleaving both β-(1→3) and β-(1→4) bonds. Moreover, because [^{3}H]GGXXLGol or [^{3}H]GGXXXGol was the major product of *At*XTH31 digestion of the MXE product, *At*XTH31 must favour having a β-(1→3) bond between residues in subsites -2/-1 over other possible positions. These are all surprising findings and serve to distinguish *At*XTH31 from other XTHs. XEG and cellulase digestion of SEP- and cell wall hemicellulose-XET products in Fig. 47 yielded the familiar pattern of the acceptor substrate with a ladder of [^{3}H]G$_n$XXLGols below it. *At*XTH31 digestion of these polymers yielded the acceptor substrate as the major product and the acceptor substrate with two Glc residues attached as the second most prevalent. This latter finding runs counter to the initial hypothesis that *At*XTH31 would, because of its shared GH16 family (and XTH subfamily) membership, cleave xyloglucan at the same point as XET activity did and therefore produce the initial acceptor substrate alone.

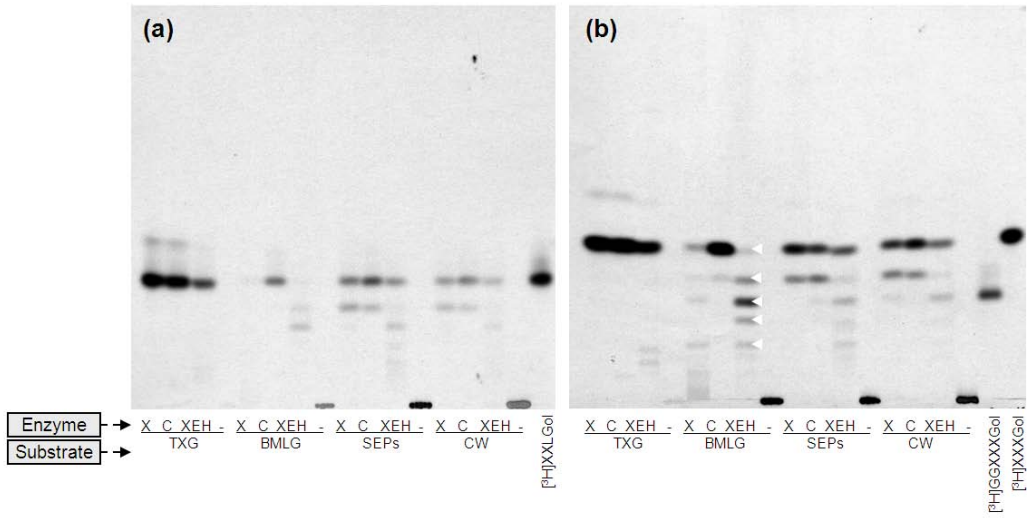

Fig. 47. Digestion of four transglycanase products using three glycanases XET products created by incubating 15 kBq [^{3}H]XXXGol (a) or [^{3}H]XXLGol (b) with 20 µl donor polysaccharide and 5 µl enzyme source. 75% (v/v) ethanol-soluble hydrolase products were resolved by TLC (BAW, two ascents) and detected by fluorography. The presence of non-mobile radioactivity at the origin indicates ethanol soluble polymeric material. X, XEG; C, cellulase; XEH, *At*XTH31

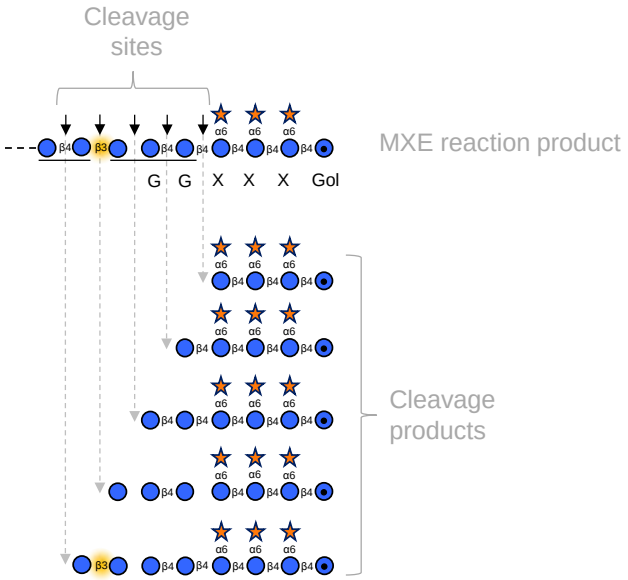

Fig. 48. Schematic showing sites of attack for cleavage of the MXE reaction product by *At*XTH31 Each oligosaccharide product created indicates a distinct site of attack. The scheme shows an MXE product created by use of XXXGol as

the acceptor substrate, but the same would apply for one created by use of XXLGol.

3.7.7. Cell wall identity dramatically influences the [^{3}H]GXXLGol : [^{3}H]XXLGol ratio when XET acts in barley *in situ*

To investigate the possibility that the products of sequential XET:XEG treatments might vary in different organs, products of *in vivo* XET action from 13 barley organs (3.4.2.) were digested with XEG and resolved by TLC (Fig. 49). Again, as well as the initial acceptor substrate [^{3}H]XXLGol, at least three [^{3}H]G_nXXLGols were formed in all barley organs tested; this again supports the contention that [^{3}H]G_nXXLGols will be formed whenever Poaceaen xyloglucan acted as the donor substrate. While the [^{3}H]GXXLGol : XXLGol ratio varied somewhat between all organs, two trends in the ratio between different organ identities were evident from the results (Fig. 49c). Firstly, the ratio was lower in older tissues, as evidenced by comparison of older seedling tissues with younger seedling tissues and 2nd mature leaf tissues with 5th mature leaf tissues. Secondly, the ratio was lower in more basal tissues, as evidenced by comparison of seedling root tissues with seedling shoot tissues and of 2nd mature leaf lamina and 5th mature leaf (which was largely lamina) with 2nd mature leaf tissues. The comparison of seedling roots with shoots was particularly stark, with a greater than two-fold excess of [^{3}H]GXXLGol in roots, despite [^{3}H]XXLGol being at least as prevalent as [^{3}H]GXXLGol in shoots. These tissue-specific patterns in the [^{3}H]GXXLGol:XXLGol ratio could feasibly be a product of differing xyloglucan structures in the different tissues, differing levels or patterns of acetylation, differences in the way that xyloglucans are accessible by XTHs within the cell walls of these different tissues (cell wall ultrastructure), or some other factor(s). As all XET sources used previously yielded identical [^{3}H]GXXLGol:XXLGol ratios (Fig. 43), it is perhaps unlikely that differences in the endogenous XTHs expressed in different tissues caused the differences observed.

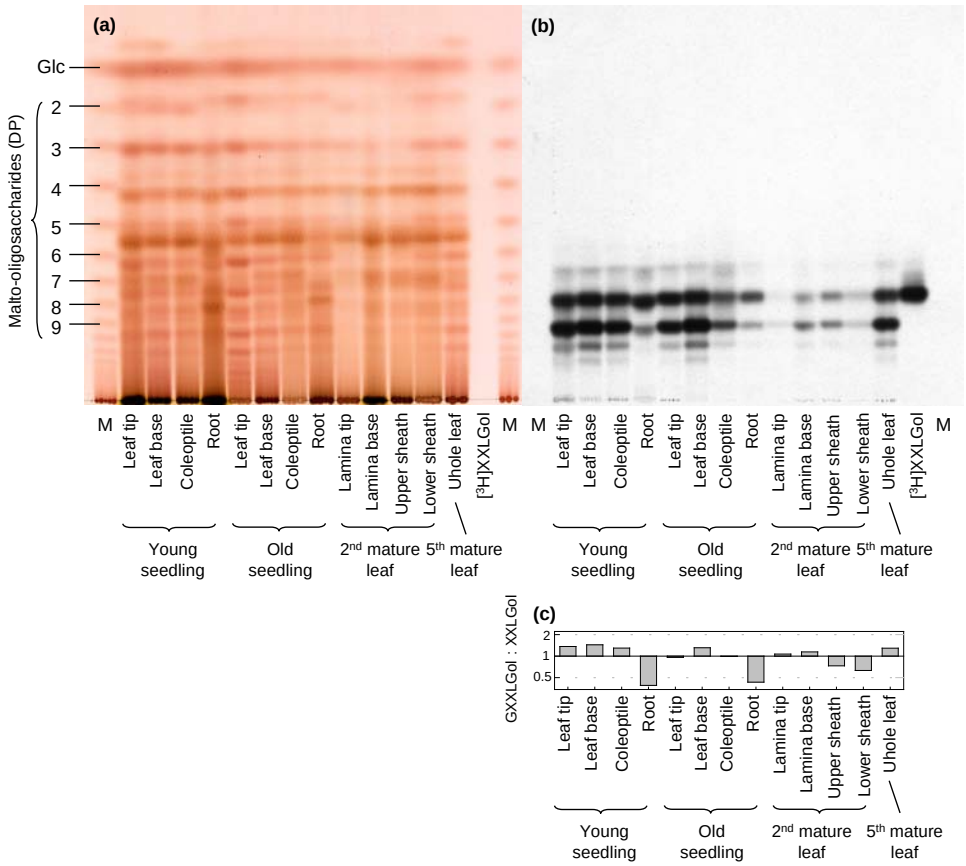

Fig. 49. XEG digestion of thirteen XET products formed in different barley organs Products of *in vivo* XET action were extracted with alkali (as in Fig. 30), digested with XEG and resolved by TLC. Oligosaccharides on that TLC were detected by thymol-staining (a) and fluorography (b). Radioactive oligosaccharides were also quantified by use of a radioisotope plate reader (c); the scale on the histogram is logarithmic.

Analysis of the thymol-stainable oligosaccharides released by XEG would aid assessment of the contribution of xyloglucan structural discrepancies to the differences in the [^{3}H]GXXLGol:XXLGol ratio. However, the unexpectedly large amount of thymol-stainable products following XEG treatment (Fig. 49a) suggests that XEG digested MLG and/or mannans in addition to xyloglucans; this confounds direct comparisons of cold xyloglucan oligosaccharides. It is evident however from Fig. 31 that the XGOs released from older seedling root xyloglucan differ from those released from other older seedling organs. Thus, it seems feasible that this difference in xyloglucan structure is a contributing factor to the differences in the

[^{3}H]GXXLGol:XXLGol ratio. The decrease in the GXXLGol : XXLGol ratio with age of barley seedlings is consistent with the report in Gibeaut *et al.* (2005) that the Glc_5(XXGGG):Glc_4(XXGG) subunit content of barley coleoptile xyloglucan decreases with seedling age. From this it can be deduced that older and more basal barley tissues have lower Glc_5:Glc_4 subunit ratios, with that of seedling shoots being particularly low. The physiological significance of this structural distinction is unknown.

4. CONCLUSION

4.1. MXE conclusion

4.1.1. MXE is a highly acidic XTH homolog

MXE's identification as an XTH homolog was unsurprising. Indeed, Fry *et al.* (2008a) speculated that MXE would probably belong to the GH16 enzyme family because of the co-occurrence of XET and lichenase activities – the reactions of which MXE is an intermediary between (for similarity between XET, MXE and lichenase see Fig. 3) – in this group. But despite MXE's identity vindicating this hypothesis, MXE exhibits characteristics which distinguish it from these orthologs. For example, though both lichenase and MXE are capable of cleaving MLG polysaccharides, they recognise MLG motifs in distinct ways (See 3.3.1.).

Further, unlike both XTHs and lichenases, MXE is highly acidic. The physiological significance of this remains, at this point, conjectural. The fact that this acidity can readily distinguish MXE from other more conventional XTHs in *E. fluviatile* crude extracts (Fig. 17) suggests that it may be related to the presumed distinct functions of MXE and XET, including MXE's proposed role in growth cessation (in contrast to the commonly perceived role of XTHs in growth promotion). Further, the acidity of the protein would cause it to be highly negatively charged at apoplastic pH ranges (typically pH 5–6). This would attract the MXE enzyme to any positively charged material in the cell wall and, perhaps more significantly, would repel the MXE protein from other negatively charged molecules, such as non-methyl-esterified pectic polysaccharides. MXE will, for example, presumably be repelled from pectin-rich regions such as the middle lamella. Consistent with this, Leroux *et al.* (2011) report that in the strengthening tissues of *E. ramosissimum* – where MLG predominates, and where the effects of growth-cessating factors (the role of MXE hypothesised by Fry et al. 2008a) might feasibly be expected to act – MLG is restricted to the inner cell wall region. Such hypotheses could be tested by the use of immunological approaches.

4.1.2. The role of MXE *in planta*

The proposed role in wall strengthening of MXE made by Fry *et al.* (2008a) was based on the correlation of MXE activity with *Equisetum* tissue age. The fact that MXE is far weaker in reproductive tissue than in vegetative ones (Fig. 28) is commensurate with this, because vegetative tissues are needed to have a greater longevity than reproductive ones which, particularly in *E. arvense*, are very short-lived. It remains conjectural whether the other novel activity of the MXE enzyme – CXE – is a physiologically significant reaction or merely an artefact/side reaction which only occurs to a significant extent *in vitro*. In light of their rarity in the plant kingdom, the co-occurrence of MLG and MXE in *Equisetum*, suggests, at the very least, that catalysing the MXE reaction is probably the main function of this enzyme.

4.1.3. Implications for the roles of XTHs and MLG in poalean cell walls

The lack of detectable MXE activity and action in barley suggests that the role played by MLG in the cell wall of *Equisetum* and cereals is, at least in some crucial respects, different, a conclusion also indicated by the different spatio-temporal localisation of the MLGs in *Equisetum* and cereal cell walls and their markedly different carbohydrate composition. In addition, the observed lack of MXE action in barley cell wall should inspire further investigation into the role of poalean XTHs. The evolution of the unique Type II wall architecture of the Poaceae – which contains a distinctively low xyloglucan complement – appears to have proceeded without a corresponding change in the number of poalean *XTH* genes; perhaps counter intuitively, enzyme extracts from young grass and cereal tissues often actually have higher XET activity than those from young dicot tissues (Fry *et al.*, 1992). While these results indicate MXE does not play an appreciable role in barley cell wall physiology, they do not rule out the possibility of other novel endotransglycosylase activities/actions in barley. The suggestion that Poaceaen XTHs might act mainly on the other, more prevalent, polysaccharides (Yokoyama *et al.*, 2004; Fincher, 2009) should now be directed toward activities other than MXE.

Such actions might have produced the endotransglucosylase product which was indigestible with XEG in the time allotted. A novel hetero-endotransglycosylase which uses xyloglucan as an acceptor but not as a donor would create a polymeric

product which would probably not be susceptible to XEG digestion. However, I was unable to produce TLC-mobile oligosaccharides by digestion with various hydrolases (lichenase, endo-β-mannanase, β-xylanase and endopolygalacturonase), and was therefore unable to provide positive evidence for such hypothetical hetero-endotransglycosylases (data not shown). An alternative explanation for the XEG-indigestible material is that it was a standard XET product which became incompletely soluble and thus partly indigestible after the drying step. This possibility is made more likely because the lower levels of xylosyl substitution on Poaceaen xyloglucan when compared to that of tamarind or *Equisetum* xyloglucan would make it less soluble; the *O*-acetylation present in native Poaceaen xyloglucan would have been lost during the NaOH extraction procedure.

4.2. Novel hexasaccharide conclusion

4.2.1. Highlighted importance of use of multiple chromatographic techniques

The discovery of 6x (G3G4G4G4G3G), a novel hexasaccharide which is the major constituent of a peak previously mis-identified in the literature as solely MLG9 (Wood *et al.*, 1994; Izydorczyk *et al.*, 1998; Wang *et al.*, 2003; Wood *et al.*, 2003; Lazaridou *et al.*, 2004; Tosh *et al.*, 2004a; Tosh *et al.*, 2004b; Fry *et al.*, 2008), highlights the importance of not relying solely on any single analytical technique. HPLC alone would have mis-identified 6x as MLG9, while GPC alone would have mis-identified it as MLG6. Their combined use as well as the use of TLC conclusively revealed 6x as a novel hexasaccharide.

The fact that 6x is resistant to lichenase has implications for our understanding of the mode of attack of lichenase and for both the subunit composition of, and subunit distribution within, the MLGs from the three phylogenetic lineages investigated here.

4.2.2. It remains conjectural whether other lichenases would produce 6x

It remains to be investigated whether the inability to cleave 6x, and potentially other members of the 'x' series, is general to lichenases or a specific feature of the GH16 *Bacillus subtilis* enzyme widely used for analytical purposes. This is particularly conjectural for plant lichenases which, owing to their GH17 family membership, are unrelated to the *B. subtilis* enzyme.

4.2.3. MLG2 units are found disproportionately at the non-reducing end of MLG4 units

Many details of the spatial distribution of MLG subunits within the intact polysaccharides are lost during lichenase digestion. Indeed, despite the stability of free 6x in the presence of lichenase, our lack of knowledge of the 6x sequence's lability when found within the intact polysaccharide means that significant aspects of any model which sought to infer subunit spatial distribution from 6x's presence would necessarily be somewhat speculative.

However, the ratios of the MLGOs produced by lichenase digestion of barley and Iceland moss MLGs (Table 4) show that MLG2 units cannot be randomly distributed in these polysaccharides. In barley for example, since MLG3 is by far the most

abundant repeat-unit, if a random distribution of subunits was assumed, MLG2s would occur mainly adjacent to MLG3s. However, the ratios of MLGOs in my digests indicate the maximum possible molar proportion of the barley polysaccharide that could be contributed by MLG2s within MLG2-MLG3 runs is 0.11%, comprising 0.09% (the proportion released as free MLG2; this could theoretically all have originated from MLG2-MLG3 sequences, if they are, to some degree, labile within the polysaccharide) plus 0.02% (the proportion of the lichenase-resistant oligosaccharide we tentatively identify as 5x: MLG2-MLG3). But the molar contribution of MLG2 within MLG2-MLG4 sequences, must have been much higher: at least 1.78% (the yield of 6x). Therefore, MLG2-MLG4 sequences outnumbered MLG2-MLG3 at least 16-fold (= 1.78 / 0.11), even though total MLG3s outnumbered total MLG4s 2.5-fold. This shows that barley MLG cannot be a randomly constructed polysaccharide, but has at least a 40-fold preference (= 16 × 2.5) for MLG2-MLG4 over MLG2-MLG3.

By similar reasoning, Iceland moss MLG has at least a 15-fold preference for MLG2-MLG4 over MLG2-MLG3. In contrast to this, *Equisetum* MLG gave a high yield of free MLG2 (18%) and a relatively low yield of MLG2-MLG4 (5%; relative to the amount of MLG2). Interpretation of this observation is more complicated, depending on assumptions about lichenase's ability to cleave 6x within the intact polysaccharide as well as the tendency of mid-chain segments of the polysaccharide to sit in the active site with an MLG2 or MLG4 in the positive and negative subsites. Any models of cereal or lichen MLG synthesis must be able to explain the non-random distribution of MLG2 subunits I have observed.

4.3. Synoptic conclusion

The GH16 family of enzymes are found in all taxonomic kingdoms where they play crucial roles in carbohydrate metabolism. The distinct research directions presented here together serve to illuminate our understanding of the interactions between GH16 enzymes and their substrates in general. Because of the focus of the work on enzymes which cleave plant hemicelluloses the findings here will be most pertinent to those interested in this field. This is especially true for identification and understanding of the enzymic features which confer xyloglucan specificity on enzymes; this will prove useful for the understanding of plant metabolism, the role/s of different XTHs, the breakdown of pant cell wall material and may prove of use to those wishing to exploit the technological characteristics of xyloglucan.

5. FUTURE WORK

5.1. Further probing of the substrate specificity of MXE

To further investigate the role(s) and enzymology of MXE different substrates should be used to probe its substrate specificity. Of particular importance is the assessment of the ability of MXE to utilise MLG oligosaccharides (MLGOs) as acceptor substrates. Given that MXE favours MLG as a donor substrate over xyloglucan it is possible that its favoured activity might be MLG : MLG endotransglycosylation. This would drastically alter our understanding of the role of MXE. Such a discovery would not have been possible prior to the purification and/or recombinant expression of MXE due to the problems that contaminating β-glucosidase enzymes would cause when using MLGOs as acceptors. It will also be important to assess substrate specificity using MLGOs yielded by digestion of MLG with different endo-hydrolases (Simmons, 2013).

5.2. Investigation of potential roles and applications of CXE/MXE *in vivo* via gain-of-function mutants

Gain-of-function mutants would provide insights into the role of MXE/CXE which would be particularly pertinent given that the expertise to enable knock-out mutants in *Equisetum* has not yet been developed. Gain of function mutants would however be thwarted by the dissimilarities between the cell wall of *Equisetum* and those of other species. To assess the role of MXE, for example, a monocot species would be the most sensible example, owing to their possession of MLG. However, in the Poaceae, the developmental timing of MLG synthesis is unlike that of *Equisetum* and the unique anatomy of *Equisetum* tissues might render comparison of the phenotype of such mutant Poaceae with *Equisetum* morphology challenging at best. To assess the role of CXE *in planta*, *A. thaliana* would be the most probable initial candidate, owing to its ease of transformation. However, the same limitations due to cell wall dissimilarities would pose a similar problem in the application of knowledge yielded from the transformant back to *Equisetum*.

Nonetheless, even if the creation of such a gain-of-function mutant proved unable to provide information about the role of MXE/CXE in *Equisetum*, it could yield useful

information about the biotechnological applications of MXE e.g. by conferring on plants improved mechanical properties (as speculated by Fry *et al.*, 2008a). For such biotech applications crop and/or tree species might prove most useful transformants.

5.3. Identification of the features of MXE which confer on it its novel substrate specificity

MXE is unique within the XTH family in exhibiting a preference for a non-xyloglucan donor substrate. As such, the active site residues which confer on MXE its substrate specificity must differ from those of other XTHs significantly. However, it is not obvious from analysing sequence information which residues are responsible. For example, because MXE is such an acidic protein (pI ~ 4), while other XTHs are commonly neutral, it also differs from other XTHs in ways presumably unrelated to its substrate specificity. Site-directed mutagenesis would enable discrimination between those residues relevant to determining MXE's substrate specificity and those unrelated. Such a study might comprise the insertion of mutations to both a common XTH and to MXE in an attempt to confer on them MLG and xyloglucan specificity respectively. The work of Baumann *et al.* (2007) which showed that the truncation of an unstructured loop was sufficient to direct a predominantly XET-active XTH toward hydrolysis, could be extended to MXE in an attempt both to test their thesis on a distantly related enzyme, but also to create an MLG-hydrolase from MXE. By catalysing MLG-cleavage, such an enzyme would provide further knowledge on the site of attack of MXE.

6. BIBLIOGRAPHY

Albersheim P. 1974. Structure and growth of walls of cells in culture. In: Street HE, eds. *Tissue culture and plant science*. London, UK: Academic Press, 379–404.

Albersheim P, Darvill A, Roberts K, Sederoff R, Staehelin A. 2011. Plant cell walls. New York, NY, USA: Garland Science.

Arnold CA. 1947. *An introduction to paleobotany*. New York: McGraw-Hill. (http://www.archive.org/stream/introductiontopa031727mbp)

Barbeyron T, Henrissat B, Kloareg B. 1994. The gene encoding the kappa-carrageenase of *Alteromonas carrageenovora* is related to beta-1,3-1,4-glucanases. *Gene* **139**: 105–109.

Barbeyron T, Gerard A, Potin P, Henrissat B, Kloareg B. 1998. The kappa-carrageenase of the marine bacterium *Cytophaga drobachiensis*. Structural and phylogenetic relationships within family-16 glycoside hydrolases. *Molecular Biology and Evolution* **15**: 528–537.

Baumann MJ, Eklöf JM, Michel G, Kallas AM, Teeri TT, Czjzek M, Brumer H III. 2007. Structural evidence for the evolution of xyloglucanase activity from xyloglucan endo-transglycosylases: biological implications for cell wall metabolism. *Plant Cell* **19**: 1947–1963.

Becnel J, Natarajan M, Kipp A, Braam J. 2006. Developmental expression patterns of Arabidopsis XTH genes reported by transgenes and Genevestigator. *Plant Molecluar Biology* **61**: 451–467.

Bell PR, Hemsley AR. 2000. *Green Plants: their Origin and Diversity*. 2nd edn, Cambridge: Cambridge University Press, pp. 349.

Bernal AJ, Yoo CM, Mutwil M, Jensen JK, Hou G, Blaukopf C, Sørensen I, Blancaflor EB, Scheller HV, Willats WG. 2008. Functional analysis of the cellulose synthase-like genes CSLD1, CSLD2, and CSLD4 in tip-growing *Arabidopsis cells*. *Plant Physiology* **148**: 1238–1253.

Bollok M, Henriksson H, Kallas Å, Jahic M, Teeri TT, Enfors SO. 2005. Production of poplar xyloglucan endotransglycosylase using the methylotrophic yeast *Pichia pastoris*. *Applied Biochemistry and Biotechnology* **126**: 61-77.

Brown JT. 1975. *Equisetum clarnoi*, a new species based on petrifactions from the Eocene of Oregon. *American Journal of Botany* **62**: 410–415.

Buckeridge MS, Vergara CE, Carpita NC. 1999. The mechanism of synthesis of a mixed-linkage (1→3), (1→4)β-D-glucan in maize. Evidence for multiple sites of glucosyl transfer in the synthase complex. *Plant Physiology* **120**: 1105–1116.

Burton RA, Wilson SM, Hrmova M, Harvey AJ, Shirley NJ, Medhurst A, Stone BA, Newbigin EJ, Bacic A, Fincher GB. 2006. Cellulose synthase-like CslF genes mediate the synthesis of cell wall (1,3;1,4)-β-D-glucans. *Science* **311:** 1940–1942.

Burton RA, Fincher GB. 2009. (1,3;1,4)-β-D-glucans in cell walls of the Poaceae, lower plants, and fungi: a tale of two linkages. *Molecular Plant* **2**: 873–82.

Burton RA, Collins HM, Kibble NA, Smith JA, Shirley NJ, Jobling SA, Henderson M, Singh RR, Pettolino F, Wilson SM, Bird AR, Topping DL, Bacic A, Fincher GB. 2011. Over-expression of specific *Hv*CslF cellulose synthase-like genes in transgenic barley increases the levels of cell wall (1,3;1,4)-β-D-glucans and alters their fine structure. *Plant Biotechnology Journal* **9**: 117–135.

Cabib E, Bowers B, Sburlati A, Silverman SJ. 1988. Fungal cell wall synthesis: the construction of a biological structure. *Microbiological Sciences* **5**: 370–375.

Cabib E, Blanco N, Grau C, Rodríguez-Peña JM, Arroyo J. 2007. Crh1p and Crh2p are required for the cross-linking of chitin to β(1-6)glucan in the *Saccharomyces cerevisiae* cell wall. *Molecular Microbiology* **63**: 921–935.

Cabib E, Farkas V, Kosík O, Blanco N, Arroyo J, McPhie P. 2008. Assembly of the yeast cell wall. Crh1p and Crh2p act as transglycosylases *in vivo* and *in vitro*. *The Journal of Biological Chemistry* **283**: 29859–29872.

Cabib E. 2009. Two novel techniques for determination of polysaccharide cross-links show that Crh1p and Crh2p attach chitin to both β(1-6)- and β(1-3)glucan in the *Saccharomyces cerevisiae* cell wall. *Eukaryotic Cell* **8**: 1626–1636.

Campbell P, Braam J. 1998. Co- and/or post-translational modifications are critical for TCH4 XET activity. *The Plant Journal* **15**: 553–561.

Campbell P, Braam J. 1999. *In vitro* activities of four xyloglucan endotransglycosylases from *Arabidopsis*. *The Plant Journal* **18**: 371–382.

Cantarel BL, Coutinho PM, Rancurel C, Bernard T, Lombard V, Henrissat B. 2009. The Carbohydrate-Active EnZymes database (CAZy): an expert resource for glycogenomics. *Nucleic Acids Research* **37**: 233–238.

Carpita NC. 2011. Update on mechanisms of plant cell wall biosynthesis: how plants make cellulose and other (1→4)-β-D-glycans. *Plant Physiology* **155**: 171–184.

Carpita NC, McCann MC. 2010. The maize mixed-linkage (1→3),(1→4)-β-D-glucan polysaccharide is synthesized at the golgi membrane. *Plant Physiology* **153**: 1362–1371.

Carroll A, Somerville C. 2009. Cellulosic biofuels. *Annual Review of Plant Biology* **60**: 165–182.

Channing A, Zamuner A, Edwards D, Guido D. 2011. *Equisetum thermale* sp. nov. (Equisetales) from the Jurassic San Agustín hot spring deposit, Patagonia: anatomy, paleoecology, and inferred paleoecophysiology. *American Journal of Botany* **98**: 680–697.

Chen C, Lewin J. 1969. Silicon as a nutrient for *Equisetum arvense*. *Canadian Journal of Botany* **47**: 125–131.

Choi JY, Seo YS, Kim SJ, Kim WT, Shin JS. 2011. Constitutive expression of CaXTH3, a hot pepper xyloglucan endotransglucosylase/hydrolase, enhanced tolerance to salt and drought stresses without phenotypic defects in tomato plants (*Solanum lycopersicum* cv. Dotaerang). *Plant Cell Reports* **30**: 867–877.

Collins HM, Burton RA, Topping DL, Liao ML, Bacic A, Fincher GB. 2010. Variability in the fine structures of non-cellulosic cell wall polysaccharides from cereal grains: potential importance in human health and nutrition. *Cereal Chemistry* **87**: 272–282.

Cosgrove DJ. 2005. Growth of the plant cell wall. *Nature Review Molecular Cell Biology* **6**: 850–861.

Creelman RA, Mullet JE. 1997. Oligosaccharins, brassinolides, and jasmonates: Nontraditional regulators of plant growth, development, and gene expression. *The Plant Cell* **9**:1211-1223.

Currie HA, Perry CC. 2007. Silica in plants: biological, biochemical and chemical studies. *Annals of Botany* **100**: 1383–1389.

Del Bem LE, Vincentz MGA. 2010. Evolution of xyloglucan-related genes in green plants. *BMC Evolutionary Biology* **10**: 341–357.

Des Marais DL, Smith AR, Britton DM, Pryer KM. 2003. Phylogenetic relationships and evolution of extant Horsetails, *Equisetum*, based on chloroplast DNA sequence data (*rbcL* and *trnL-F*). *International Journal of Plant Sciences* **164**: 737–751.

Dilbaghi N, Kaur H, Ahuja M, Kumar S. 2013. Evaluation of tropicamide-loaded tamarind seed xyloglucan nanoaggregates for ophthalmic delivery. *Carbohydrate Polymers*.**94**: 286–291.

Doblin MS, Pettolino FA, Wilson SM, Campbell R, Burton RA, Fincher GB, Newbigin E, Bacic A. 2009. A barley cellulose synthase-like *CSLH* gene mediates (1,3;1,4)-β-D-glucan synthesis in transgenic *Arabidopsis*. *Proceedings of the National Academy of Sciences USA* **106**: 5996–6001.

Duckett JG. 1973. Comparativemorphology of the gametophytes of the genus *Equisetum*, subgenus Equisetum. *Botanical Journal of the Linnean Society* **66**: 1–22.

Duckett JG. 1979. Comparative morphology of the gametophytes of *Equisetum* subgenus *Hippochaete* and the sexual behaviour of *E. ramosissimum* subsp. *debile* (Roxb.) Hauke, *E. hyemale* var. *af.ne* (Engelm.) A.A., and *E. laevigatum* A.Br. *Botanical Journal of the Linnean Society* **79**: 179–203.

Eklöf JM, Brumer H. 2010. The XTH Gene Family: An Update on Enzyme Structure, Function, and Phylogeny in Xyloglucan Remodeling. *Plant Physiology* **153**: 456-466.

Eklöf JM, Shojania S, Okon M, McIntosh LP, Brumer H. 2013. Structure-function analysis of a broad specificity *Populus trichocarpa* endo-β-glucanase reveals an evolutionary link between bacterial licheninases and plant XTH gene products. *Journal of Biological Chemistry* **288**: 15786–15799.

Epstein E. 1994. The anomaly of silicon in plant biology. *Proceedings of the National Academy of Sciences U S A* **91**: 11–17.

Espiñeira JM, Novo Uzal E, Gómez Ros LV, Carrión JS, Merino F, Ros Barceló A, Pomar F. 2011. Distribution of lignin monomers and the evolution of lignification among lower plants. *Plant Biology* **13**: 59–68.

Fanutti C, Gidley MJ, Reid JS. 1993. Action of a pure xyloglucan endo-transglycosylase (formerly called xyloglucan-specific endo-(1→4)-β-D-glucanase) from the cotyledons of germinated nasturtium seeds. *The Plant Journal* **3**: 691–700.

Fanutti C, Gidley MJ, Reid JS. 1996. Substrate subsite recognition of the xyloglucan endo-transglycosylase or xyloglucan-specific endo-(1→4)-β-D-glucanase from the cotyledons of germinated nasturtium (Tropaeolum majus L.) seeds. *Planta* **200**: 221–8.

Fincher GB. 2009. Revolutionary times in our understanding of cell wall biosynthesis and remodeling in the grasses. *Plant Physiology* **149**: 27–37.

Fry SC. 1989. The Structure and functions of xyloglucan. *Journal of Experimental Botany* **40**: 1–11.

Fry SC, Smith RC, Renwick KF, Martin DJ, Hodge SK, Matthews KJ. 1992. Xyloglucan endotransglycosylase, a new wall-loosening enzyme-activity from plants. *Biochemical Journal* **282**: 821–828.

Fry SC, York WS, Albersheim P, Darvill A, Hayashi T, Joseleau JP, Kato Y, Lorences EP, Maclachlan GA, Mcneil M, Mort AJ, Reid JSG, Seitz HU, Selvendran RR, Voragen AGJ, White AR. 1993. An unambiguous

nomenclature for xyloglucan-derived oligosaccharides. *Physiologia Plantarum* **89**: 1–3.

Fry SC. 1994. Oligosaccharins as plant growth regulators. *Biochemical Society Symposium* **60**: 5–14.

Fry SC, Mohler KE, Nesselrode BHWA, Frankova L. 2008a. Mixed-linkage beta-glucan : xyloglucan endotransglucosylase, a novel wall-remodelling enzyme from Equisetum (horsetails) and charophytic algae. *The Plant Journal* **55**: 240–252.

Fry SC, Nesselrode BHWA, Miller JG, Mewburn BR. 2008b. Mixed-linkage (1→3,1→4)-β-D-glucan is a major hemicellulose of Equisetum (horsetail) cell walls. *New Phytologist* **179**: 104–115.

Garajová S, Flodrová D, Ait-Mohand F, Farkaš V, Stratilová E. 2008. Characterization of two partially purified xyloglucan endotransglycosylases from parsley (*Petroselinum crispum*) roots. *Biologia* **63**: 313–319.

Gibeaut DM, Pauly M, Bacic A, Fincher GB. 2005. Changes in cell wall polysaccharides in developing barley (*Hordeum vulgare*) coleoptiles. *Planta* **221**: 729–738.

Gierlinger N, Sapei L, Paris O. 2008. Insights into the chemical composition of *Equisetum hyemale* by high resolution Raman imaging. *Planta* **227**: 969–980.

Geshi N, Petersen BL, Scheller HV. 2010. Toward tailored synthesis of functional polysaccharides in plants. *Annals of the New York Academy of Sciences* **1190**: 50–57.

Gilbert HJ, Stålbrand H, Brumer H. 2008. How the walls come crumbling down: recent structural biochemistry of plant polysaccharide degradation. *Current Opinion in Plant Biology* **11**: 338–348.

Gilbert HJ. 2010. The biochemistry and structural biology of plant cell wall deconstruction. *Plant Physiology* **153**: 444–455.

Gloster TM, Ibatullin FM, Macauley K, Eklöf JM, Roberts S, Turkenburg JP, Bjørnvad ME, Jørgensen PL, Danielsen S, Johansen KS, Borchert TV, Wilson KS, Brumer H, Davies GJ. 2007. Characterization and three-dimensional structures of two distinct bacterial xyloglucanases from families GH5 and GH12. *The Journal of Biological Chemistry* **282**: 19177–19189.

Golub SJ, Wetmore RH. 1948. Studies of development in the vegetative shoot apex of *Equisetum arvense* L. I. The shoot apex. *American Journal of Botany* **35**: 755–767.

Grew N. 1682. *The anatomy of plants* [WWW document] URL http://www.botanicus.org/item/31753000008869 [accessed 26 December 2012]

Grishutin SG, Gusakov AV, Dzedzyulya EI, Sinitsyn AP. 2006. A lichenase-like family 12 endo-(1→4)-β-glucanase from *Aspergillus japonicus*: study of the substrate specificity and mode of action on β-glucans in comparison with other glycoside hydrolases. *Carbohydrate Research* **341**: 218–229.

Guillon JM. 2004. Phylogeny of horsetails (*Equisetum*) based on the chloroplast rps4 gene and adjacent noncoding sequences. *Systematic Botany* **29**: 251–259.

Guillon JM. 2007. Molecular phylogeny of horsetails (*Equisetum*) including chloroplast atpB sequences. *Journal of Plant Research* **120**: 569-574.

Guo JH, Skinner GW, Harcum WW, Barnum PE. 1998. Pharmaceutical applications of naturally occurring water-soluble polymers. *Pharmaceutical Science & Technology Today* **1**: 254–261

Harada T, Torii Y, Morita S, Onodera R, Hara Y, Yokoyama R, Nishitani K, Satoh S. 2011. Cloning, characterization, and expression of xyloglucan endotransglucosylase/hydrolase and expansin genes associated with petal growth and development during carnation flower opening. *Journal of Experimental Botany* **62**: 815-823.

Hatfield RD, Nevins DJ. 1987. Hydrolytic activity and substrate-specificity of an endoglucanase from Zea mays seedling cell-walls. *Plant physiology* **83**: 203–207.

Hazen SP, Scott-Craig JS, Walton JD. 2002. Cellulose synthase-like genes of rice. *Plant Physiology* **128**: 336–340.

Henrissat B, Bairoch A. 1996. Updating the sequence-based classification of glycosyl hydrolases. *Biochemical Journal* **316**: 695–696.

Hernández-Nistal J, Martín I, Labrador E, Dopico B. 2010. The immunolocation of XTH1 in embryonic axes during chickpea germination and seedling growth confirms its function in cell elongation and vascular differentiation. *Journal of Experimental Botany* **61**: 4231–4238.

Hoffman FM & Hillson CJ. 1979. Effects of Silicon on the life cycle of *Equisetum hyemale* L. *Botanical Gazette* **140**: 127–132.

Høj PB & Fincher GB. 2003. Molecular evolution of plant β-glucan endohydrolases *The Plant Journal* **7**: 367–379.

Hrmova M, Farkaš V, Lahnstein J, Fincher GB. 2007. A barley xyloglucan xyloglucosyl transferase covalently links xyloglucan, cellulosic substrates, and (1,3;1,4)-β-D-glucans. *The Journal of Biological Chemistry* **282**:12951–12962

Hrmova M, Farkaš V, Harvey AJ, Lahnstein J, Wischmann B, Kaewthai N, Ezcurra I, Teeri TT, Fincher GB. 2009. Substrate specificity and catalytic

mechanism of a xyloglucan xyloglucosyl transferase *Hv*XET6 from barley (*Hordeum vulgare* L.). *FEBS Journal* **276**: 437–456.

Hsieh YS, Harris PJ. 2009. Xyloglucans of monocotyledons have diverse structures. *Molecular Plant* **2**: 943–965.

Hückelhoven R. 2007. Cell wall-associated mechanisms of disease resistance and susceptibility. *Annual Review of Phytopathology* **45**: 101–127.

Inouhe M., Nevins DJ. 1991. Auxin-enhanced glucan autohydrolysis in maize coleoptile cell-walls. *Plant Physiology* **96**: 285–290.

Izydorczyk MS, Macri LJ, MacGregor AW. 1998. Structure and physicochemical properties of barley non-starch polysaccharides – I. Water-extractable β-glucans and arabinoxylans. *Carbohydrate Polymers* **35**: 249–258.

Jackson CL, Dreaden TM, Theobald LK, Tran NM, Beal TL, Eid M, Gao MY, Shirley RB, Stoffel MT, Kumar MV, Mohnen D. 2007. Pectin induces apoptosis in human prostate cancer cells: correlation of apoptotic function with pectin structure. *Glycobiology* **17**: 805–819.

Jia Z, Qin Q, Darvill AG, York WS. 2003. Structure of the xyloglucan produced by suspension-cultured tomato cells. *Carbohydrate Research* **338**: 1197–208.

Johansson P, Brumer H 3rd, Baumann MJ, Kallas AM, Henriksson H, Denman SE, Teeri TT, Jones TA. 2004. Crystal structures of a poplar xyloglucan endotransglycosylase reveal details of transglycosylation acceptor binding. *Plant Cell* **16**: 874-86.

Johnston SL, Prakash R, Chen NJ, Kumagai MH, Turano HM, Cooney JM, Atkinson RG, Paull RE, Cheetamun R, Bacic A, Brummell DA, Schröder R. 2013. An enzyme activity capable of endotransglycosylation of heteroxylan polysaccharides is present in plant primary cell walls. *Planta* **237**: 173–187.

Kaewthai N, Gendre D, Eklöf JM, Ibatullin FM, Ezcurra I, Bhalerao RP, Brumer H. 2013. Group III-A XTH genes of *Arabidopsis* encode predominant xyloglucan endohydrolases that are dispensable for normal growth. *Plant Physiology* **161**: 440–454.

Kaewthai N, Harvey AJ, Hrmova M, Brumer H, Ezcurra I, Teeri1 TT, Fincher GB. 2010. Heterologous expression of diverse barley XTH genes in the yeast *Pichia pastoris*. *Plant Biotechnology* **27**: 251–258.

Kerr EM, Fry SC. 2003. Pre-formed xyloglucans and xylans increase in molecular weight in three distinct compartments of a maize cell-suspension culture. *Planta* **217**: 327–339.

Kerr EM, Fry SC. 2004. Extracellular cross-linking of xylan and xyloglucan in maize cell-suspension cultures: the role of oxidative phenolic coupling. *Planta* **219**: 73–83.

Kibbe WA. 2007. OligoCalc: an online oligonucleotide properties calculator. *Nucleic Acids Research* **35**: Web Server Issue W43-46.

Kochumalayil JJ, Zhou Q, Kasai W, Berglund LA. 2013. Regioselective modification of a xyloglucan hemicellulose for high-performance biopolymer barrier films. *Carbohydrate Polymers* **93**: 466–472.

Kosík O, Auburn RP, Russell S, Stratilová E, Garajová S, Hrmova M, Farkaš V. 2010. Polysaccharide microarrays for high-throughput screening of transglycosylase activities in plant extracts. *Glycoconjugate Journal* **27**: 79–87.

Laemmli UK. 1970. Cleavage of structural proteins during the assembly of the head of bacteriophage T4. *Nature* **227**: 680–685.

Laurienzo P. 2010. Marine Polysaccharides in Pharmaceutical Applications: An Overview**.** *Marine Drugs* **8**: 2435–2465.

Law C, Exley C. 2011. New insight into silica deposition in horsetail (*Equisetum arvense*). *BMC Plant Biology* **11**: 112.

Lazaridou A, Biliaderis CG, Micha-Screttas M, Steele BR. 2004. A comparative study on structure–function relations of mixed-linkage (1→3), (1→4) linear β-D-glucans. *Food Hydrocolloids* **18**: 837–855.

Lee H, Kwon HM, Park JW, Kurokawa K, Lee BL. 2009. N-terminal GNBP homology domain of gram-negative binding protein 3 functions as a beta-1,3-glucan binding motif in *Tenebrio molitor*. *BMB Reports* **42**: 506–510.

Lee J, Burns TH, Light G, Sun Y, Fokar M, Kasukabe Y, Fujisawa K, Maekawa Y, Allen RD. 2010. Xyloglucan endotransglycosylase/hydrolase genes in cotton and their role in fiber elongation. *Planta* **232**:1191-1205.

Leroux O, Knox JP, Masschaele B, Bagniewska-Zadworna A, Marcus SE, Claeys M, van Hoorebeke L, Viane RL. 2011. An extensin-rich matrix lines the carinal canals in *Equisetum ramosissimum*, which may function as water-conducting channels. *Annals of Botany* **108**: 307–319.

Lewin J, Reimann BEF. 1969. Silicon and plant growth. *Annual Review of Plant Physiology* **20**: 289–304

Liepman et al. (2004) Expression of cellulose synthase-like (*Csl*) genes in insect cells reveals that *CslA* family members encode mannan synthases

Liu Y, White PJ. 2010. Molecular weight and structure of water soluble (1→3), (1→4)-β-glucans affect pasting properties of oat flours. *Journal of Food Science* **76**: C68–74.

Logan KJ, Thomas BA. 1985. Distribution of lignin derivatives in plants. *New Phytologist* **99**: 571–585.

Lorences EP, Fry SC. 1993. Xyloglucan oligosaccharides with at least two α-D-xylose residues act as acceptor substrates for xyloglucan endotransglycosylase and promote the depolymerisation of xyloglucan. *Physiologia Plantarum* **88**:105–112.

Martinez-Fleites C, Guerreiro CIPD, Baumann MJ, Taylor EJ, Prates JAM, Ferreira LMA, Fontes CMGA, Brumer H, Davies GJ. 2006. Crystal structures of *Clostridium thermocellum* xyloglucanase, XGH74A, reveal the structural basis for xyloglucan recognition and degradation. *The Journal of Biological Chemistry* **34**: 24922–24933.

Marcus SE, Verhertbruggen Y, Hervé C, Ordaz-Ortiz JJ, Farkaš V, Pedersen HL, Willats WG, Knox JP. 2008. Pectic homogalacturonan masks abundant sets of xyloglucan epitopes in plant cell walls. *BMC Plant Biology* **8**: 60.

Marcus SE, Blake AW, Benians TA, Lee KJ, Poyser C, Donaldson L, Leroux O, Rogowski A, Petersen HL, Boraston A, Gilbert HJ, Willats WG, Knox JP. 2010. Restricted access of proteins to mannan polysaccharides in intact plant cell walls. *The Plant Journal* **64**: 191–203.

Maris A, Suslov D, Fry SC, Verbelen JP, Vissenberg K. 2009. Enzymic characterisation of two recombinant xyloglucan endotransglucosylase/hydrolase (XTH) proteins of *Arabidopsis* and their effect on root growth and cell wall extension. *Journal of Experimental Botany* **60**: 3959-3972.

Maris A, Kaewthai N, Eklöf JM, Miller JG, Brumer H, Fry SC, Verbelen JP, Vissenberg K. 2011. Differences in enzymic properties of five recombinant xyloglucan endotransglucosylase/hydrolase (XTH) proteins of *Arabidopsis thaliana*. *Journal of Experimental Botany* **62**: 261–271.

Mark P, Baumann MJ, Eklöf JM, Gullfot F, Michel G, Kallas AM, Teeri TT, Brumer H, Czjzek M. 2009. Analysis of nasturtium *Tm*NXG1 complexes by crystallography and molecular dynamics provides detailed insight into substrate recognition by family GH16 xyloglucan endo-transglycosylases and endo-hydrolases. *Proteins* **75**: 820–836.

McIver EE, Basinger JF. 1989. The morphology and relationships of *Equisetum fluviatoides* sp.nov. from the Paleocene Ravenscrag Formation of Saskatchewan, Canada. *Canadian Journal of Botany* **67**: 2937-2943,

Mellerowicz EJ, Immerzeel P, Hayashi T. 2008. Xyloglucan: the molecular muscle of trees. *Annals of Botany* **102**:659-665.

Mellerowicz EJ, Sundberg B. 2008. Wood cell walls: biosynthesis, developmental dynamics and their implications for wood properties. *Current Opinion in Plant Biology* **11**: 293–300.

Michel G, Chantalat L, Duee E, Barbeyron T, Henrissat B, Kloareg B, Dideberg O. 2001. The kappa-carrageenase of *P. carrageenovora* features a tunnel-shaped active site: a novel insight in the evolution of Clan-B glycoside hydrolases. *Structure* **9**: 513–525.

Miedes E, Zarra I, Hoson T, Herebers K, Sonnewald U, Lorences EP. 2011. Xyloglucan endotranglucosylase and cell wall extensibility. *Journal of Plant Physiology* **168**: 196-203.

Miedes E, Lorences EP. 2007. The implication of xyloglucan endotransglucosylase/ hydrolase (XTHs) in tomato fruit infection by *Penicillium expansum. The Journal of Agricutural Food Chemistry* **55**: 9021-9026.

Miedes E, Lorences EP. 2009. Xyloglucan endotransglucosylase/hydrolases (XTHs) during tomato fruit growth and ripening. *Journal of Plant Physiology* **166**: 489–498.

Mohand FA, Farkaš V. 2006. Screening for hetero-transglycosylating activities in extracts from nasturtium (*Tropaeolum majus*). *Carbohydrate Research* **341**: 577–581.

Mouyna I, Hartland RP, Fontaine T, Diaquin M, Simenel C, Delepierre M, Henrissat B, Latgé JP. 1998. A 1,3-β-glucanosyltransferase isolated from the cell wall of *Aspergillus* fumigatus is a homologue of the yeast Bgl2p. *Microbiology* **144**: 3171–3180.

Newbigin EJ, Bacic A, Fincher GB. 2006. Cellulose synthase-like CslF genes mediate the synthesis of cell wall (1,3;1,4)-β-D-glucans. *Science* **311**: 1940–1942.

Nishikubo N, Takahashi J, Roos AA, Derba-Macleuch M, Piens K, Brumer H, Teeri TT, Stålbrand H, Mellerowicz EJ. 2011. Xyloglucan endotransglycosylase-mediated xyloglucan rearrangements in developing wood of hybrid aspen. *Plant Physiology* **155**: 399-413.

Nishitani K. 2002. New directions to post-genomic cell wall research. *Plant Cell Physiology* **43**: 1397.

Nishitani K, Tominaga R. 1992. Endo-xyloglucan transferase, a novel class of glycosyltransferase that catalyzes transfer of a segment of xyloglucan molecule to another xyloglucan molecule. *Journal of Biological Chemistry* **267**: 21058–21064.

Nishitani K, Vissenberg K. 2006. Roles of the XTH protein family in the expanding cell. *The Expanding Cell: Plant Cell Monographs* **6**: 89–116.

Nothnagel AL, Nothnagel EA. 2007. Primary cell wall structure in the evolution of land plants. *Journal of Integrative Plant Biology* **49**: 1271–1278.

Okazawa K, Sato Y, Nakagawa T, Asada K, Kato I, Tomita E, Nishitani K. 1993. Molecular cloning and cDNA sequencing of endoxyloglucan transferase, a novel class of glycosyltransferase that mediates molecular grafting between matrix polysaccharides in plant cell walls. *Journal of Biological Chemistry* **268**: 25364–25368.

Papageorgiou M, Lakhdara N, Lazaridou A, Biliaderis CG, Izydorczyk MS. 2005. Water extractable (1/3,1/4)-β-D-glucans from barley and oats: An intervarietal study on their structural features and rheological behaviour. *Journal of Cereal Science* **42**: 213–224.

Pauly M, Andersen LN, Kauppinen S, Kofod LV, York WS, Albersheim P, Darvill A. 1998. A xyloglucan-specific *endo*-β-1,4-glucanase from *Aspergillus aculeatus:* expression cloning in yeast, purification and characterization of the recombinant enzyme. *Glycobiology* **9**: 93–100.

Peña MJ, Darvill AG, Eberhard S, York WS, O'Neill MA. 2008. Moss and liverwort xyloglucans contain galacturonic acid and are structurally distinct from the xyloglucans synthesized by hornworts and vascular plants. *Glycobiology* **18**: 891–904.

Peña MJ, Kong Y, York WS, O'Neill MA. 2012. A galacturonic acid-containing xyloglucan is involved in *Arabidopsis* root hair tip growth. *Plant Cell* **24**: 4511–4524.

Perlack RD, Wright LL, Turhollow AF, Graham RL, Stokes BJ, Erbach DC. 2005. *Biomass as feedstock for bioenergy and bioproducts industry: the technical feasibility of a billion-ton annual supply*. [WWW document] URL http://www.eere.energy.gov/biomass/publications.html. [accessed 17 October 2012].

Perry CC, Fraser MA. 1991. Silica deposition and ultrastructure in the cell wall of *Equisetum arvense*: The importance of cell wall structures and flow control in biosilicification? *Philosophical Transactions: Biological Sciences* **334**: 149–157.

Persin Z, Stana-Kleinschek K, Foster TJ, van Dam JEG, Boeriu CG, Navard P. 2011. Challenges and opportunities in polysaccharides research and technology: The EPNOE views for the next decade in the areas of materials, food and health care. *Carbohydrate Polymers* **84**: 22–32.

Piens K, Fauré R, Sundqvist G, Baumann MJ, Saura-Valls M, Teeri TT, Cottaz S, Planas A, Driguez H, Brumer H. 2008. Mechanism-based labeling defines the

free energy change for formation of the covalent glycosyl-enzyme intermediate in a xyloglucan endo-transglycosylase. *Journal of Biological Chemistry* **283**: 21864-21872.

Planas N. 2000. Bacterial 1,3-1,4-β-glucananses: structure, function and protein engineering. *Biochimica et Biophysica Acta—Protein Structure and Molecular Enzymology* **1543**: 361–382.

Popper ZA, Fry SC. 2003. Primary cell wall composition of bryophytes and charophytes. *Annals of Botany* **91**: 1–12.

Popper ZA, Fry SC. 2004. Primary cell wall composition of pteridophytes and spermatophytes. *New Phytologist* **164**: 165–174.

Popper ZA, Fry SC. 2005. Widespread occurrence of a covalent linkage between xyloglucan and acidic polysaccharides in suspension-cultured angiosperm cells. *Annals of Botany* **96**: 91–99.

Popper ZA, Fry SC. 2008. Xyloglucan-pectin linkages are formed intra-protoplasmically, contribute to wall-assembly, and remain stable in the cell wall. *Planta* **227**: 781–794.

Pryer KM, Schneider H, Smith AR, Cranfill R, Wolf PG, Hunt JS, Sipes SD. 2001. Horsetails and ferns are a monophyletic group and the closest living relatives to seed plants. *Nature* **409**: 618–622.

Purugganan MM, Braam J, Fry SC. 1997. The *Arabidopsis* TCH4 xyloglucan endotransglycosylase. Substrate specificity, pH optimum, and cold tolerance. *Plant Physiology* **115**: 181–190.

Robinson PT, Pham TN, Uhrín D. 2004. In phase selective excitation of overlapping multiplets by gradient enhanced chemical shift selective filters. *Journal of Magnetic Resonance* **170**: 97–103.

Rose JK, Braam J, Fry SC, Nishitani K. 2002. The XTH family of enzymes involved in xyloglucan endotransglucosylation and endohydrolysis: current perspectives and a new unifying nomenclature. *Plant Cell Physiology* **43**: 1421–35.

Rothwell GW. 1996. Pteridophytic evolution: An often underappreciated phytological success story. *Review of Palaeobotany and Palynology* **90**: 209–222.

Roubroeks JP, Mastromauro DI, Andersson R, Christensen BE, Aman P. 2000. Molecular weight, structure, and shape of oat (1→3),(1→4)-β-D-glucan fractions obtained by enzymatic degradation with lichenase. *Biomacromolecules* **4**: 584–591.

Sachs J von. 1887. *Lectures on the Physiology of Plants. Translated by H. Marshall Ward*. Oxford, UK: Clarendon Press.

Sapei L, Gierlinger N, Hartmann J, Nöske R, Strauch P, Paris O. 2007. Structural and analytical studies of silica accumulations in *Equisetum hyemale*. *Analytical & Bioanalytical Chemistry* **389**: 1249–1257.

Sasidharan R, Chinnappa CC, Staal M, Elzenga JTM, Yokoyama R, Nishitani K, Voesenek LACJ, Perik R. 2010 Light quality-mediated petiole elongation in Arabidopsis during shade avoidance involves cell wall modification by xyloglucan endotransglucosylase/hydrolases. *Plant Physiology* **154**: 978–990.

Saura-Valls M, Fauré R, Brumer H, Teeri TT, Cottaz S, Driguez H, Planas A. 2008. Active-site mapping of a *Populus* xyloglucan endo-transglycosylase with a library of xylogluco-oligosaccharides. *The Journal of Biological Chemistry* **283**: 21853-21863.

Scheller HV, Ulvskov P. 2010. Hemicelluloses. *Annual Review of Plant Biology* **61**: 263–289.

Schröder R, Atkinson RG, Langenkämper G, Redgwell RJ. 1998. Biochemical and molecular characterisation of xyloglucan endotransglycosylase from ripe kiwifruit. *Planta* **204**: 242–251.

Schröder R, Wegrzyn TF, Bolitho KM, Redgwell RJ. 2004. Mannan transglycosylase: a novel enzyme activity in cell walls of higher plants. *Planta* **219**: 590–600.

Schröder R, Wegrzyn TF, Sharma NN, Atkinson RG. 2006. *Le*MAN4 endo-β-mannanase from ripe tomato fruit has dual enzyme activity and can act as a mannan transglycosylase and hydrolase. *Planta* **224**: 1091–1102.

Schröder R, Atkinson RG, Redgwell RJ. 2009. Re-interpreting the role of endo-β-mannanases as mannan endotransglycosylase/hydrolases in the plant cell wall *Annals of Botany* **104**: 197–204.

Simmons TJ. 2013. Considerations in the search for mixed-linkage (1→3),(1→4)-β-D-glucan-active endotransglycosylases. *Plant Signaling & Behaviour* **8**: 4.

Singh AP, Tripathi SK, Nath P, Sane AP. 2011. Petal abscission in rose is associated with the differential expression of two ethylene-responsive xyloglucan endotransglucosylase/hydrolase genes, *RbXTH1* and *RbXTH2*. *Journal of Experimental Botany* **62**: 5091–5103.

Smelcerovic A, Knezevic-Jugovic Z, Petronijevic Z. 2008. Microbial polysaccharides and their derivatives as current and prospective pharmaceuticals. *Current Pharmaceutical Design* **14**: 3168–3195.

Smith BG, Harris PJ. 1999. The polysaccharide composition of Poales cell walls: Poaceae cell walls are not unique. *Biochemical Systematics and Ecology* **27**: 33–53.

Smith AR, Pryer KM, Schuettpelz E, Korall P, Schneider H, Wolf PG. 2006. A classification for extant ferns. *Taxon* **55**: 705–731.

de Souza CF, Lucyszyn N, Woehl MA, Riegel-Vidotti IC, Borsali R, Sierakowski MR. 2013. Property evaluations of dry-cast reconstituted bacterial cellulose/tamarind xyloglucan biocomposites. *Carbohydrate Polymers* **93**: 144–153.

Sørensen I, Pettolino FA, Wilson SM, Doblin MS, Johansen B, Bacic A, Willats WG. 2008. Mixed-linkage (1→3),(1→4)-β-D-glucan is not unique to the Poales and is an abundant component of *Equisetum arvense* cell walls. *The Plant Journal* **54**: 510–521.

Stanich NA, Rothwell GW, Stockey RA. 2009. Phylogenetic diversification of *Equisetum* (Equisetales) as inferred from Lower Cretaceous species of British Columbia, Canada. *American Journal of Botany* **96**: 1289–1299.

Steele NM, Fry SC. 1999. Purification of xyloglucan endotransglycosylases (XETs) : a generally applicable and simple method based on reversible formation of an enzyme–substrate complex. *Biochemical Journal* **340:** 207–211.

Steele NM, Sulová Z, Campbell P, Braam J, Farkaš V, Fry SC. 2001. Ten isoenzymes of xyloglucan endotransglycosylase from plant cell walls select and cleave the donor substrate stochastically. *Biochemical Journal* **355**: 671–679.

Stewart WN, Rothwell GW. 1993. *Paleobotany and the evolution of plants*, second edition. Cambridge: Cambridge University Press.

Sticklen MB. 2008. Plant genetic engineering for biofuel production: towards affordable cellulosic ethanol. *Nature Reviews Genetics* **9**: 433–443.

Stone BA, Clarke AE. 1992. Chemistry and biology of (1→3)-β-glucans. Bundoora, Victoria, Australia: La Trobe University Press.

Stratilová E, Ait-Mohand F, Rehulka P, Garajová S, Flodrová D, Rehulková H, Farkaš V. 2010. Xyloglucan endotransglycosylases (XETs) from germinating nasturtium (*Tropaeolum majus*) seeds: isolation and characterization of the major form. *Plant Physiology and Biochemistry* **48**: 207–215.

Strohmeier M, Hrmova M, Fischer M, Harvey AJ, Fincher GB, Pleiss J. 2004. Molecular modeling of family GH16 glycoside hydrolases: potential roles for xyloglucan transglucosylases/hydrolases in cell wall modification in the poaceae. *Protein Science* **13**: 3200–3213.

Sulová Z, Takácová M, Steele NM, Fry SC, Farkaš V. 1998. Xyloglucan endotransglycosylase: evidence for the existence of a relatively stable glycosyl-enzyme intermediate. *The Biochemical Journal* **330**: 1475–1480.

Sulová Z, Baran R, Farkaš V. 2001. Release of complexed xyloglucan endotransglycosylase (XET) from plant cell walls by a transglycosylation reaction with xyloglucan-derived oligosaccharides. *Plant Physiology and Biochemistry* **39**: 927–932.

Sulová Z, Farkaš V. 1999. Purification of xyloglucan endotransglycosylase based on affinity sorption of the active glycosyl-enzyme intermediate complex to cellulose. *Protein Expression and Purification* **16**: 231–235.

Taketa S, Yuo T, Tonooka T, Tsumuraya Y, Inagaki Y, Haruyama N, Larroque O, Jobling SA. 2012. Functional characterization of barley betaglucanless mutants demonstrates a unique role for CslF6 in (1,3;1,4)-β-D-glucan biosynthesis. *Journal Experimental Botany* **63**: 381–392.

Tabuchi A, Kamisaka S, Hoson T. 1997. Purification of Xyloglucan Hydrolase/Endotransferase from Cell Walls of Azuki Bean Epicotyls. *Plant Cell Physiology* **38**: 653–658.

Taylor TN, Tayler EL. 1993. *The biology and evolution of fossil plants*. Englewood Cliffs: Pentice Hall.

Taylor NG. 2008. Cellulose biosynthesis and its deposition in higher plants. *New Phytologist* **178**: 239-252.

Thompson JE, Fry SC. 2000. Evidence for a covalent linkage between xyloglucan and acidic pectins in suspension-cultured rose cells. *Planta* **211**: 275-286.

Thompson JE, Fry SC. 2001. Restructuring of wall-bound xyloglucan by transglycosylation in living plant cells. *Plant Journal* **26**: 23-34.

Thompson JE, Smith RC, Fry SC. 1997. Xyloglucan undergoes interpolymeric transglycosylation during binding to the plant cell wall *in vivo*: evidence from $^{13}C/^{3}H$ dual labelling and isopycnic centrifugsation of caesium trifluoroacetate. *Biochemical Jounral* **327**: 699—708.

Timell TE. (1964). Studies on some ancient plants. *Svensk Papperstidning-Nordisk Cellulose* **67**: 356–363.

Travan A, Marsich E, Donati I, Foulc MP, Moritz N, Aro HT, Paoletti S. 2012. Polysaccharide-coated thermosets for orthopedic applications: from material characterization to in vivo tests. *Biomacromolecules* **13**: 1564–1572.

Trethewey JAK, Campbell LM, Harris PJ. 2005. (1→3),(1→4)-β-D-Glucans in the cell walls of the Poales (*sensu lato*): an immunogold labeling study using a monoclonal antibody. *American Journal of Botany* **92**: 1660–1674.

Van Sadt VST, Suslov D, Verbelen JP, Vissenberg K. 2007. Xyloglucan endotransglucosylase activity loosens a plant cell wall. *Annals of Botany* **100**: 1467-1473.

Varki A, Cummings RD, Esko JD, Freeze HH, Stanley P, Marth JD, Bertozzi CR, Hart GW, Etzler ME. 2009. Symbol nomenclature for glycan representation. *Proteomics* **9**: 5398–5399.

Vincken JP, York WS, Beldman G, Voragen AG. 1997. Two general branching patterns of xyloglucan, XXXG and XXGG. *Plant Physiology* **114**: 9–13.

Vissenberg K, Fry SC, Pauly M, Höfte H, Verbelen J. 2005. XTH acts at the microfibril–matrix interface during cell elongation *Journal of Experimental Botany* **56**: 673–683.

Wagstaff C, Clarkson GJJ, Zhang F, Rothwell SD, Fry SC, Taylor G, Dixon MS. 2010. Modification of cell wall properties in lettuce improves shelf life. *Journal of Experimental Botany* **61**: 1239–1248.

Warner CD, Go RM, García-Salinas C, Ford C, Reilly PJ. 2011. Kinetic characterization of a glycoside hydrolase family 44 xyloglucanase/endoglucanase from *Ruminococcus flavefaciens* FD-1. *Enzyme and Microbial Technology* **48**: 27–32.

Wood PJ, Weisz J, Blackwell BA. 1994. Structural studies of (1→3),(1→4)-β-D-glucans by ^{13}C-nuclear magnetic resonance spectroscopy and by rapid analysis of cellulose-like regions using high-performance anion-exchange chromatography of oligosaccharides released by lichenase. *Cereal Chemistry* **71**: 301–307.

Xu H, Chater KF, Deng Z, Tao M. 2008. A cellulose synthase-like protein involved in hyphal tip growth and morphological differentiation in streptomyces. *Journal of Bacteriology* **190**: 4971–4978.

Xu Q, Ye X, Li L-Y, Cheng Z-M, Guo H. 2010. Structural basis for the action of xyloglucan endotransglycosylases/hydrolases: insights from homology modelling. *Interdisciplinary Sciences: Computational Life Sciences* **2**: 133–139.

Yokoyama R, Rose JK, Nishitani K. 2004. A surprising diversity and abundance of xyloglucan endotransglucosylase/hydrolases in rice. Classification and expression analysis. *Plant Physiology* **134**: 1088–1099.

Yokoyama R, Uwagaki Y, Sasaki H, Harada T, Hiwatashi Y, Hasebe M, Nishitani K. 2010. Biological implications of the occurrence of 32 members of

the XTH (xyloglucan endotransglucosylase/hydrolase) family of proteins in the bryophyte *Physcomitrella patens*. *Plant Journal* **64**: 645–656.

Zhu Y, Nam J, Carpita NC, Matthysse AG, Gelvin SB. 2003. Agrobacterium-mediated root transformation is inhibited by mutation of an *Arabidopsis* cellulose synthase-like gene. *Plant Physiology* **133**: 1000–1010.

Zhu J, Lee BH, Dellinger M, Cui X, Zhang C, Wu S, Nothnagel EA, Zhu JK. 2010. A cellulose synthase-like protein is required for osmotic stress tolerance in Arabidopsis. *The Plant Journal* **63**: 128–140.